

AALBORG UNIVERSITY

MASTER'S PROGRAMME IN CONTROL AND AUTOMATION  
MASTER'S THESIS

---

---

# **Nonlinear Optimal Control in Water Distribution Network**

---

---

Project Report  
Saruch Satishkumar Rathore  
Group. 1030

June 3, 2020







**AALBORG UNIVERSITY**  
STUDENT REPORT

**Aalborg University**  
**School of Information and**  
**Communication Technology**  
**Department of Electronic Systems**  
Frederik Bajers Vej 7  
9220 Aalborg Ø  
Tel.: 9940 9730  
Fax: 9940 9725  
<http://www.es.aau.dk>

**Title:**

Nonlinear optimal control in water distribution network

**Theme:**

Master's thesis

**Project Period:**

Spring Semester 2020

**Project Group:**

1030

**Participant(s):**

Saruch Satishkumar Rathore

**Supervisor(s):**

Carsten Skovmose Kallesøe  
Jorge Val Ledesma

**Copies:** 1

**Page Numbers:** 135

**Date of Completion:**

June 3, 2020

**Abstract:**

This project is an extension of the work presented in [22], where a MPC control was designed for a water distribution network. In this project a nonlinear optimal control system is designed for the water distribution network. The three main objectives of the project are design of nonlinear optimal control, design of consumer demand predictor and stability analysis the local flow control of the pumps by PI controller. The water network considered in this project consist of two pumping stations, two consumers and an elevated reservoir. For optimal control, a control structure is developed with NMPC as the supervisory control and a PI controller for local flow control of the pumps. The objectives of the NMPC are defined to be minimizing the operation cost and pressure variations at the consumer end. For the prediction of consumer demand a Kalman filter based predictor is developed, which predicts the future consumer demands based on pressure measurements of the elevated reservoir. The NMPC along with the predictor is implemented and tested on a simulated plant model and a laboratory setup, and performance is compared with the results of [22]. For the stability analysis, first Lyapunov stability of the delay-free nonlinear model is analysed and then the stability of linearized model with delay is analysed.

*The content of this report is freely available, but publication (with reference) may only be pursued due to agreement with the author.*



# Contents

<b>Preface</b>	<b>xi</b>
<b>1 Introduction</b>	<b>1</b>
1.1 Motivation . . . . .	1
1.2 Water distribution network . . . . .	2
1.3 Project description . . . . .	3
1.4 Report outline . . . . .	5
<b>2 System modelling</b>	<b>7</b>
2.1 Preliminaries: Basics of graph theory . . . . .	7
2.2 Component model . . . . .	9
2.2.1 Pipe model . . . . .	9
2.2.2 Valve model . . . . .	11
2.2.3 Pump model . . . . .	12
2.2.4 General two terminal component model . . . . .	12
2.2.5 Elevated reservoir model . . . . .	13
2.3 Graph theory based network model . . . . .	13
2.3.1 Simplified water network model . . . . .	14
2.3.2 Detailed water network model . . . . .	20
2.4 Modelling of the water distribution network considered in this project	25
<b>3 Control formulation</b>	<b>29</b>
3.1 Control structure and NMPC . . . . .	29
3.1.1 Nonlinear model predictive control . . . . .	30
3.2 Nonlinear MPC for water distribution network . . . . .	34
3.2.1 Constraints . . . . .	36
3.2.2 Nonlinear MPC with soft constraints . . . . .	37
3.3 Nonlinear MPC implementation and simulation test results . . . . .	38
3.3.1 NMPC control results . . . . .	39
3.4 Stability analysis . . . . .	42
3.4.1 Lyapunov stability analysis . . . . .	43

3.4.2	Stability analysis on the linearized model with delay and PI control . . . . .	53
<b>4</b>	<b>Consumer demand prediction using Kalman filter</b>	<b>61</b>
4.1	Fourier analysis . . . . .	61
4.1.1	State space representation of Fourier series model . . . . .	62
4.2	Prediction of the consumer demand curve with Kalman filter . . . . .	65
4.2.1	Kalman filter . . . . .	65
4.2.2	Kalman filter for the estimation of the consumer demand . . . . .	67
4.3	Predictor simulation test results . . . . .	69
4.3.1	Kalman filter based consumer demand predictor . . . . .	76
<b>5</b>	<b>Laboratory Setup</b>	<b>81</b>
5.1	Smart water laboratory . . . . .	81
5.1.1	Smart water laboratory modules . . . . .	82
5.1.2	Smart water laboratory communication network . . . . .	85
5.2	Water distribution network setup in the laboratory . . . . .	86
5.3	Control structure implementation for the laboratory setup . . . . .	87
<b>6</b>	<b>Results</b>	<b>91</b>
6.1	Test details, NMPC and predictor parameters . . . . .	91
6.2	Simulation test results . . . . .	94
6.2.1	NMPC with consumer demand predictor simulation test results . . . . .	94
6.2.2	On/off control simulation test results . . . . .	99
6.3	Laboratory test results . . . . .	101
6.3.1	NMPC with consumer demand predictor laboratory test results . . . . .	101
6.3.2	On/off control laboratory test results . . . . .	104
<b>7</b>	<b>Discussion</b>	<b>107</b>
7.1	Discussion on simulation test results . . . . .	107
7.2	Discussion on laboratory test results . . . . .	109
7.3	Discussion on stability analysis of the inner closed-loop system . . . . .	111
<b>8</b>	<b>Conclusion</b>	<b>113</b>
<b>9</b>	<b>Future work</b>	<b>115</b>
	<b>Bibliography</b>	<b>117</b>
<b>A</b>	<b>NMPC problem defined using multiple shooting in CasADi (MATLAB code)</b>	<b>121</b>

<b>B</b>	<b>Equilibrium point calculation and system matrices in the stability analysis of the linearised model</b>	<b>125</b>
<b>C</b>	<b>MPC simulation test results from [22]</b>	<b>129</b>
<b>D</b>	<b>PI control implementation for the laboratory setup</b>	<b>131</b>
<b>E</b>	<b>Laboratory test results with 240 minutes representing 1 day</b>	<b>133</b>



# Preface

This report was written by Saruch Satishkumar Rathore, under the guidance of Carsten Skovmose Kallesøe and Jorge Val Ledesma, as Master's thesis in 4<sup>th</sup> semester of Master's in Control and Automation at Aalborg university. The project has been executed in the period February to first week of June 2020. This report will be centered around the topic of nonlinear optimal control in water distribution network with an elevated reservoir. This is an extension of the work presented in [22].

Reader's guide In order to read and understand the report, basic knowledge of hydraulic networks, state space modelling, estimators and predictive control is a prerequisite. Throughout the report, reference to sources will be provided. These sources are available at the end of the report and are written according to the IEEE standard. A source in the text is referred by the use of [x] with x being a number. This number indicates which number in the reading list the source has. As a basis, all sources are given under the format [author, publisher, month and year of use]. If the used source is a book, the title is included; if the source is a website, a URL is included along with the last date the URL was accessed on. Figures and tables are numbered in accordance with the chapter in which they appear. For instance, the first figure in chapter 1 is named figure 1.1. A caption is provided for each illustration, as well as an explanation. All graphical elements in the report have been made by the author, otherwise a reference to the source has been assigned to the label of the figure.



# Chapter 1

## Introduction

The chapter first presents the motivation behind the project and then a briefly describes a typical water distribution network and its components. The chapter also presents the project description including the objectives of the project and also previous work in the area of the project. Lastly, outline of the report is presented.

### 1.1 Motivation

Water is imperative for existence of human life as well as economic growth and development, but unfortunately it is also scarce natural resource. Global demand of water is steadily increasing with increase in population and infrastructure development[20]. It is also predicted that with the current scenario the world might face 40% global water deficit by 2030[19]. With these conditions leakages in a water distribution cannot be afforded. High pressure in the pipelines are one of the major reason for water leakages in a water distribution network[11]. Therefore, efficient pressure management is essential in control of a water distribution network. A network should always have a sufficiently high positive pressure in the pipes such that consumer flow demands are met, nonetheless it should not be unnecessary high and thereby cause pipe bursts. So the idea is to maintain a constant sufficient minimum pressure while maintaining consumer satisfaction.

An efficient water distribution control system is also to be cost effective. Energy cost can account for up to 80% of water transportation and treatment cost[27]. This provides a great incentive for the design of a control system to potentially save on the operational cost of the water distribution network. In Europe, the average cost of electricity production from fossil fuels is expected to increase in the future, whereas production from renewable sources is expected to decrease [5]. However, the supply of electricity from renewable sources is variable and intermittent and consequently the prices are also variable, also called dynamic pricing. Dynamic pricing may also include lower prices for consumption in off-peak hours. With

this dynamic pricing model, the control system is expected to operate the pumps during these low price periods in order to save on the operating cost.

To summarise, the main motivation behind the project is to design a control system for efficient pressure management and minimization the operational cost of a water distribution network. Detailed objectives and description of the water distribution network considered in this project are presented in section 1.3.

## 1.2 Water distribution network

Water distribution network is a hydraulic network formed of different components such as pipes, pumps, valves, elevated reservoirs. The purpose of a water distribution network is to transport water from a water production facility to the end consumers.

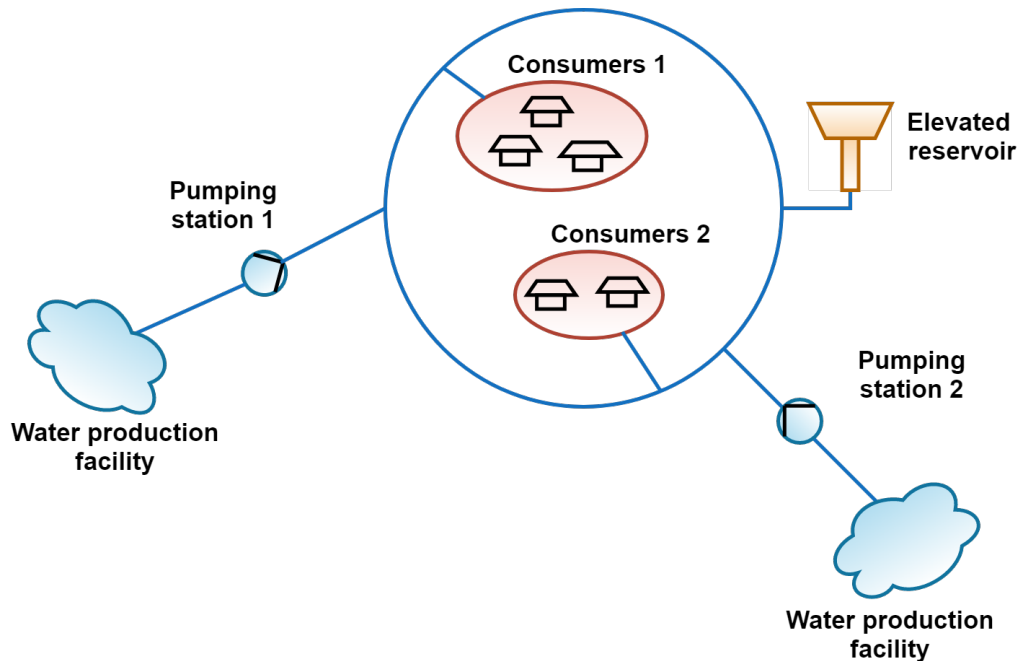


**Figure 1.1:** A typical ring-type water distribution network with two pumping stations, multiple consumers and an elevated reservoir

Figure 1.1 presents a typical ring-type water distribution network, to be found in a town with well-planned streets and roads. A water distribution network could have loops and branches similar to an electrical network. The pipes are the exoskeleton of the water network connecting different components of the network. Pipes are the elements carrying the water from one point in the network to other.

There are two pumping stations depicted in the figure 1.1. Pumping stations consist of pumps connected in parallel, supplying water from the water production

facility to the network with a positive pressure. The rotational speed of the pumps are controlled to regulate the flow and pressure in the network. Typically a water distribution network would consist of more than one pumping station, that is to ensure uninterrupted supply to consumer in case of break downs.

A water distribution network will have some consumers as well. The consumers might be divided into sets or zones. Two set of consumers are depicted in the figure 1.1. In a water network model consumers can be considered as a end valves open to atmosphere consuming water from the network. The zoning can be based on the elevation of the consumer point or how far is the consumer from the pumping station. With higher elevation the water pressure drops and similarly the farther the consumer is from the pumping station the pressure drop increases. For large water distribution network with multiple zones, booster pumps and pressure regulating valve are installed in the network to maintain desired pressure in different zones, to avoid high pressure to the low ground consumers and insufficient pressure to the high ground consumers. For a small scale water network the pressure can be maintained by the means of an elevated reservoir in the network.

In the figure 1.1, an elevated reservoir is also connected to the network. An elevated reservoir serve two purposes in a water distribution network, first as mentioned before is to maintain pressure in the network and the second is to store water for emergency usage. When the demand is low and pressure of the network is higher than the reservoir, the water flows into the reservoir. When the demand is higher, the water flows from the reservoir to the network. With this the elevated reservoir absorbs the impact on network pressure due to variation in demand. Also, a minimum water level is maintained in the reservoir for emergency usage.

### 1.3 Project description

From the motivation the first objective of the project is derived, and that is to design an nonlinear optimal control system, for a water distribution network, to minimize the operational cost and the pressure variation at the consumer node. The input in a water distribution network are the pumps and electricity cost of running the pumps is the main component in the operational cost of the network[21]. Therefore, the designed nonlinear optimal control system controls the operation of the pumps in the water network.

The water network considered in this project is a grid-type network with an elevated reservoir. The nonlinear optimal control system consist a supervisory control layer with a Nonlinear Model Predictive Control(NMPC). NMPC is designed based on a simplified water network model which is developed discarding the pipe dynamic, considering a elevated reservoir is connected to the network. MPC as a supervisory control has been previously used in [23] for control of refrigeration system. The NMPC aims to exploit the dynamics of the elevated reservoir to

achieve its objectives. Through the day the electricity prices varies, when the electricity prices are low the NMPC runs the pumps and fills the reservoir, and when the prices are high the pumps are stopped and the consumer demands are met by the reservoir. Similar work in the optimal control of water distribution network is presented in [14, 2].

This project is an extension of the work in [22], therefore the objective on the optimal control and the network considered is the same. In [22] the supervisory optimal control considered is a linear MPC, and in this work a comparison between the results of the two has also been made. The NMPC is developed on a nonlinear model of the water network, which is valid globally, whereas the linear MPC is developed on a linearized model of the water network, which is valid only close to the operating point.

For the NMPC to make optimal decision on the pump operation, it needs to consider future prices of electricity and consumer demands. In this work only the peak and off-peak hour rates are considered, i.e. the electricity prices are considered to be lower during the night hours compared to day hours, as it would in real life [15]. Prediction of consumer demands bring out the second objective of this project, which is to develop a consumer demand predictor. The consumer demand predictor developed in this project is a Kalman filter based predictor which takes in the measurement of the reservoir pressure and predicts the future consumer demand. In [22] both the electricity prices and the consumer demand were assumed to be known.

The NMPC in the supervisory control layer only gives the optimal flow commands for the pumps, a local control layer is implemented to regulate the pump speed to the control the pump flow at the desired optimal value. The local control layer consists of a PI controller. In [22], oscillatory behavior of the pump flows in the laboratory test setup was observed and it was concluded that a potential reason could be coupling of the local PI controller is the inner(local) closed-loop system. This provided the motivation for stability analysis in this project. Therefore, analysing the stability of the inner closed-loop is the third objective of this project. First Lyapunov stability of the delay-free nonlinear closed loop system is analysed and then stability of the linearised system, around an equilibrium point, with delay is analysed. The water network model used for the stability analysis takes into account the pipe dynamics as well.

The nonlinear optimal controller developed is first tested on a simulated nonlinear network model of the water distribution network. Similar water network is emulated in a smart water laboratory with different modules for pumping stations, consumer stations and elevated reservoir. The nonlinear optimal controller is then test on this laboratory setup.

## 1.4 Report outline

The rest of the report is organised as follows:

**Chapter 2** presents the water network model based on graph theory. Two types of model are presented, a simplified model for nonlinear optimal control design and a detailed model for stability analysis. This chapter also presents the water distribution network considered in the project.

**Chapter 3** presents the overall control structure of the project. It also presents the idea behind NMPC, and single and multiple shooting methods to convert NMPC problem to nonlinear programming(NLP) problem. Then the NMPC optimization problem for the project is presented. Finally, the chapter is concluded with stability analysis of the inner closed-loop system.

**Chapter 4** presents a Kalman filter based consumer demand predictor. The only available measurement to the predictor is the reservoir pressure measurement, and based on it the predictor estimates the current consumer demand and predict the future consumer demand. The chapter also presents an updated control structure with the predictor output given to the NMPC, for solving the optimization problem.

**Chapter 5** presents the smart water laboratory, its modular structure and different modules to emulate different components of a water distribution network. It also presents the water network setup in the laboratory to emulate the network considered in the simulation. Then the communication network and the control implementation in the laboratory is presented.

**Chapter 6** first presents the test details and the parameters of the NMPC, the Kalman filter based predictor and the local PI controller used for simulation and laboratory tests. Then the results for both the simulation and laboratory tests for NMPC with the predictor are presented. For comparison test results for an on/off controller are also presented.

**Chapter 7** presents a discussion on the performance of the NMPC and the predictor for simulation and laboratory test. It also presents a comparison between results of this work and [22], where a linear model was used for MPC design and the future consumer demands were assumed to be known. Finally, comments on the stability of the inner closed-loop system is also presented

**Chapter 8** presents the objectives achieved in the work and conclusion of the project.

**Chapter 9** presents the scope of improvement in the project and future work.



## Chapter 2

# System modelling

In this chapter a mathematical model for the water distribution network is presented. Foremost, some basic concept of graph theory is presented. Then, models of different components of a water distribution network are presented from previous work of [18, 22]. As mentioned in chapter 1, the water network considered in this project consists an elevated reservoir, for that network two different models developed using graph theory are presented. The first model is a simplified model, in which the network components are only pipes and a tank, and also pipe dynamics have be overlooked. This model is used in the project to developed, implement and test supervisory nonlinear optimal controller. The second model is a detailed model which includes pipe dynamics and also includes modelling all the components, including pumps and valves, of the network. This model is used for stability analysis of the system with a local PI controller. Finally, the water distribution network considered in this project is also presented.

### 2.1 Preliminaries: Basics of graph theory

In this section some basic definitions and matrices of graph theory are introduced, which would be helpful for the readers to understand graph theory as a tool for modeling of a water distribution network.

**Definition 2.1.1** *Graphs* A graph  $G = (V, E)$  consist of a set of vertices or nodes,  $V = \{v_1, \dots, v_n\}$ , and a set of edges,  $E = \{e_1, \dots, e_m\}$ , where each edge is associated to a vertex pair  $(v_i, v_j)$ ,  $i, j \in \{1, \dots, n\}$ [6].

**Definition 2.1.2** *Circuit or Loop* Circuit or loop of a graph is a closed trail with distinct vertices except the end vertices[25].

**Definition 2.1.3** *Spanning Tree* A tree is a connected graph with no loops. A tree  $T$  of a connected graph  $G = (V, E)$  is a spanning tree, if it is a sub-graph of a graph,  $G$  containing all the vertices[6].

**Definition 2.1.4 Chord** A connected sub-graph is a tree if and only if by adding one edges, exactly one loop is formed. The loop formed by adding the edges is called a fundamental loop and the edge is called chord.

**Incidence matrix,  $H$ ,** for a graph with  $n$  nodes and  $m$  edges, is a matrix with  $n$  and  $m$  columns and is defined as  $H = [h_{ij}]$ , where the element  $h_{ij}$  is defined as[25]

$$h_{ij} = \begin{cases} -1, & \text{if the } j^{\text{th}} \text{ edge is entering the } i^{\text{th}} \text{ node} \\ 0, & \text{if } j^{\text{th}} \text{ edge is not connected to the } i^{\text{th}} \text{ node} \\ 1, & \text{if } j^{\text{th}} \text{ edge is leaving the } i^{\text{th}} \text{ node} \end{cases}$$

$(n - 1)$  rows of the incidence matrix  $H$  contains all the information of  $H$  and therefore any one row can be removed[25]. Removed node is refereed as reference node and the remaining matrix is refereed as reduced incidence matrix,  $\bar{H}$ . Reduced incidence matrix can be partitioned into reduced incidence matrix for chord edges,  $\bar{H}_C$ , and reduced incidence matrix for tree edges as below.

$$\bar{H} = [\bar{H}_C \quad \bar{H}_T] \quad (2.1)$$

where,

$\bar{H}_C$  is reduced incidence matrix for the chord edges of the graph  
 $\bar{H}_T$  is reduced incidence matrix for the tree edges of the graph

**Loop matrix,  $B = [b_{ij}]$ ,** is a matrix to represent loops in a graph, with rows equal to number of loops or chords and columns equal to number of edges. The direction of the loop is defined to be same as the direction of the corresponding chord and the elements  $b_{ij}$  are defined as,

$$b_{ij} = \begin{cases} -1, & \text{if the } j^{\text{th}} \text{ edge is in the } i^{\text{th}} \text{ loop and it's direction does not agree} \\ & \text{with the loop direction} \\ 0, & \text{if the } j^{\text{th}} \text{ edge is not in the } i^{\text{th}} \text{ loop} \\ 1, & \text{if the } j^{\text{th}} \text{ edge is in the } i^{\text{th}} \text{ loop and it's direction does agree} \\ & \text{with the loop direction} \end{cases}$$

Loop matrix,  $B$ , can also be partitioned by chord edges and tree edges as below.

$$B = [B_C \quad B_T] \quad (2.2)$$

And furthermore, from known properties of graph matrices  $B$  can be represented in terms of reduced incidence matrix as[6],

$$B = [I \quad -\bar{H}_C^T \bar{H}_T^{-T}] \quad (2.3)$$

## 2.2 Component model

A water distribution network is composed of different hydraulic components such as pipes, pumps, valves and tanks. Developing a mathematical model for the water distribution network using graph theory, the two terminal components of the network are represented by edges of the graph and the connection point of the components are represented by nodes of the graph. In the mathematical model the two terminal component can be characterised by two variables, the flow through the component and the differential pressure across the component. Model for  $k^{th}$  two terminal component of the network is given as [22],

$$\begin{bmatrix} \Delta p_k \\ q_k \end{bmatrix} = \begin{bmatrix} p_i - p_j \\ q_k \end{bmatrix} \quad (2.4)$$

where,

$\Delta p_k$	is the pressure difference across the $k^{th}$ component	[bar]
$q_k$	is the flow of water through the $k^{th}$ component	[m <sup>3</sup> /h]
$p_i, p_j$	is the absolute pressure at the two end of the $k^{th}$ component	[bar]

### 2.2.1 Pipe model

Dynamic model for pipes in the water distribution network, as presented in [18], is given by,

$$\Delta p_k = \mathcal{J}_k \dot{q}_k + \lambda_k(q_k) - \Delta z_k \quad (2.5)$$

where,

$\Delta p_k$	is the drop in pressure across the $k^{th}$ pipe	[Pa]
$q_k$	is the flow of water through the $k^{th}$ pipe	[m <sup>3</sup> /s]
$\mathcal{J}_k$	is the mass inertia of water in the $k^{th}$ pipe	[kg/m <sup>4</sup> ]
$\lambda_k(q_k)$	is the drop in pressure due to friction in the $k^{th}$ pipe	[Pa]
$\Delta z_k$	is the drop in pressure due to geodesic level difference across the terminals of the $k^{th}$ pipe	[Pa]

The diameter of the pipe is assumed to be constant throughout the pipe's length and the flow is assumed to be uniform along its cross section.

The mass inertia of water in the pipe can be given by [18],

$$\mathcal{J} = \frac{L\rho}{A} \quad (2.6)$$

where,

$L$	is the pipe length	[m]
$\rho$	is the density of the water	[kg/m <sup>3</sup> ]
$A$	is the cross sectional area to the pipe	[m <sup>2</sup> ]

The pressure drop due to friction in the pipe is due to surface resistance,  $h_f$ , and the form resistance,  $h_m$ . The surface resistance is given by Darcy-Weisbach equation (2.7) [24].

$$h_f = f \frac{8Lq^2}{\pi^2 g D^5} \quad (2.7)$$

where,

$h_f$	is the surface resistance head loss	[m]
$f$	is the pipe friction factor	[·]
$D$	is the pipe diameter	[m]
$g$	is the gravitational acceleration	[m/s <sup>2</sup> ]

Considering turbulent flow, the friction factor of the pipe is given by [24],

$$f = 1.325 \left[ \ln \left( \frac{\varepsilon}{3.7D} + \frac{5.74}{R^{0.9}} \right) \right]^{-2} \quad (2.8)$$

where,

$\varepsilon$	average height of roughness projection in the pipe	[m]
$R$	is Reynolds number and for turbulent flow ( $R \geq 4000$ )	[·]

The form resistance or minor losses can be given by (2.9) [24].

$$h_m = k_f \frac{8q^2}{\pi^2 g D^4} \quad (2.9)$$

where,

$h_m$	is the form resistance head loss	[m]
$k_f$	is the coefficient of form loss	[·]

The drop in pressure due to geodesic level difference can be given by [22],

$$\Delta z_k = \rho g \Delta h_k \quad (2.10)$$

where,

$\Delta h$	is geodesic level difference across the terminals of the pipe	[m]
------------	---	-----

Substituting equations (2.6), (2.7), (2.9), (2.10) into (2.5) gives complete pipe model as,

$$\Delta p_k = \frac{L_k \rho}{A_k} \dot{q}_k + \left( f \frac{8L\rho}{\pi^2 D^5} + k_f \frac{8\rho}{\pi^2 D^4} \right) |q_k| q_k - \rho g \Delta h \quad (2.11)$$

Representing the pipe model with flow in [m<sup>3</sup>/h] and pressure in [bar], the pipe model is given as [18, 22],

$$\Delta p_k = \frac{L_k \rho}{A_k 10^5 3600^2} \dot{q}_k + \left( f \frac{8L\rho}{\pi^2 D^5 10^5 3600^2} + k_f \frac{8\rho}{\pi^2 D^4 10^5 3600^2} \right) |q_k| q_k - \frac{\rho g \Delta h}{10^5} \quad (2.12)$$

In this project the form losses are assumed to be same as the surface resistance, similar assumptions are made in [22]. Also, the water distribution network considered includes an elevated reservoir (or tank). The tank dynamics are exceedingly slow compared to the pipe dynamics and therefore are dominant in the system. In this project the dynamics of the pipes are only considered in the stability analysis and not in the supervisory nonlinear optimal control problem. Therefore for the nonlinear optimal control problem the pipe model is given by,

$$\Delta p_k = \lambda_k(q_k) - \Delta z_k \quad (2.13)$$

$$\Delta p_k = \left( f \frac{8L\rho}{\pi^2 D^5 10^5 3600^2} + k_f \frac{8\rho}{\pi^2 D^4 10^5 3600^2} \right) |q_k| q_k - \frac{\rho g \Delta h}{10^5} \quad (2.14)$$

### 2.2.2 Valve model

In this project the valves modelled in the network are valves with variable opening degree (OD). The variation in the opening degree regulates the pressure drop across the valve. As presented in [18] the model for valve can be given as,

$$\Delta p_k = \mu_k(q_k, OD_k) = \frac{1}{k_v (OD_k)^2} |q_k| q_k \quad (2.15)$$

where,

$\mu_k(q_k, OD_k)$	is a function representing pressure drop in [bar] the $k^{th}$ valve	
$k_v(OD_k)$	is the conductive function of the $k^{th}$ valve	
$OD_k$	is the opening degree of the $k^{th}$ valve	$OD_k \in [0, 100]$

Assuming a valve with a linear  $k_v$  function,  $k_v$  value can be represented in terms of  $K_{vs}$ , which is value of conductivity function at (OD=100%).

$$k_v(OD_k) = K_{vs,k} OD_k \quad (2.16)$$

Substituting linear  $k_v$  function, eq. (2.16), into valve model, eq. (2.15),

$$\Delta p_k = \mu_k(q_k, OD_k) = \frac{1}{(K_{vs} OD_k)^2} |q_k| q_k \quad (2.17)$$

### 2.2.3 Pump model

The pumps considered in this project are centrifugal pumps which deliver a positive pressure into the water distribution network. The pressure delivered by the pumps depends on two variables, the rotational speed of the pumps and the flow through the pumps. The model for the pump, as derived in [12] and also presented in [18], can be given as,

$$\Delta p_k = \alpha_k(q_k, \omega_k) = -a_{h2,k} |q_k| q_k + a_{h1,k} q_k \omega_k + a_{h0,k} \omega_k^2 \quad (2.18)$$

where,

$\alpha_k(q_k, \omega_k)$  is a function representing positive pressure delivered by the  $k^{th}$  pump [bar]  
 $a_{h2,k}, a_{h1,k}, a_{h0,k}$  are the pump constants of the  $k^{th}$  pump  
 $\omega_k$  is the rotational speed of the  $k^{th}$  pump  $\omega_k \in [0, 100]$

Discarding  $a_{h1,k} q_k \omega_k$  term also provides a good approximation of the pump curve, therefore the pump model is reduced to eq. (2.19)

$$\Delta p_k = \alpha_k(q_k, \omega_k) = -a_{h2,k} |q_k| q_k + a_{h0,k} \omega_k^2 \quad (2.19)$$

### 2.2.4 General two terminal component model

From all the different two terminal components model in a water distribution network, pipe (2.12), valve (2.17) and pump (2.19), a general two terminal components model can be given by (2.20).

$$\Delta p_k = \mathcal{J}_k \dot{q}_k + \lambda_k(q_k) + \mu_k(q_k, OD_k) - \alpha_k(q_k, \omega_k) - \Delta z_k \quad (2.20)$$

where,

$$\mathcal{J}_k = \frac{L_k \rho}{A_k 10^5 3600^2} \quad (2.21a)$$

$$\lambda_k(q_k) = \left( f \frac{8L\rho}{\pi^2 D^5 10^5 3600^2} + k_f \frac{8\rho}{\pi^2 D^4 10^5 3600^2} \right) |q_k| q_k \quad (2.21b)$$

$$\mu_k(q_k, OD_k) = \frac{1}{(K_{vs} OD_k)^2} |q_k| q_k \quad (2.21c)$$

$$\alpha_k(q_k, \omega_k) = -a_{h2,k} |q_k| q_k + a_{h0,k} \omega_k^2 \quad (2.21d)$$

$$\Delta z_k = \frac{\rho g \Delta h}{10^5} \quad (2.21e)$$

In the general two terminal component model if

$k^{th}$ component is pipe	then by default $\mu_k = 0$ and $\alpha_k = 0$
$k^{th}$ component is valve	then by default $\mathcal{J}_k = 0$ , $\lambda_k(q_k) = 0$ , $\Delta z_k = 0$ and $\alpha_k = 0$
$k^{th}$ component is pump	then by default $\mathcal{J}_k = 0$ , $\lambda_k(q_k) = 0$ , $\Delta z_k = 0$ and $\mu_k = 0$

### 2.2.5 Elevated reservoir model

Elevated reservoir (or tank) is modelled as a node in the graph. The pressure of the node connected to the tank is the pressure at the bottom of the tank. Model for the tank, assuming a constant cross sectional of the tank along the height as presented in [3, 22], can be given as,

$$\dot{p}_i = -\tau_i q_i \quad (2.22)$$

where,

$p_i$	is the node pressure where the tank is connected	[Pa]
$\tau_i$	is the tank parameter dependent on the cross sectional area, $\tau_i > 0$	[Pa/m <sup>3</sup> ]
$q_i$	is the flow in or out of the tank, with $q_i > 0$ flow is out of the tank and $q_i < 0$ flow is into the tank	[m <sup>3</sup> /s]

The tank parameter,  $\tau_i$ , can be given by eq. (2.23)

$$\tau_i = \rho g \frac{1}{A_{er,i}} \quad (2.23)$$

where,

$A_{er,i}$	is the cross sectional area to the tank	[m <sup>2</sup> ]
------------	---	-------------------

The tank model with pressure unit [bar] and flow unit [m<sup>3</sup>/h] is given by,

$$\dot{p}_i = -\frac{\tau_i}{10^5} \frac{q_i}{3600} \quad (2.24)$$

## 2.3 Graph theory based network model

A water distribution network can be represented as a directed graph in which two terminal components are represented as edges of the graph and the connection points are represented as nodes of the graph. A water distribution network with  $m$  two terminal components and  $n$  connections translates to a connected graph with  $m$  edges and  $n$  nodes. Graph theory as a tool can be used to develop a mathematical

model for a water distribution network. Graph can be represented in form of matrices, and because of known properties of graph and matrix algebra, graph theory makes a convenient tool for modelling water distribution networks. In this project the water distribution network considered is a open hydraulic network, i.e. the water can flow in and out of the network from nodes.

Further sections present two models for a water distribution network, both developed using graph theory. As mentioned before, the first model is the simplified model and the second model is the detailed model.

### 2.3.1 Simplified water network model

In this model the network is assumed to be only formed of pipe components. As a tank is connected to the water distribution network the pressure of the network would be governed by the tank. With this the pumps and consumer flows are modelled as independent flow of water in and out of the water network, this can be imagined to be equivalent to a current source in an electrical network. This model with assumption of independent flow is befitting for design of supervisory nonlinear optimal control strategy.

In the graph these independent flows are represented as nodal demands,  $d_i$ , at the nodes connected to pumps or consumer valves. The flow in and out of the tank is also represented as a nodal demand. In the case of tank flow the direction of flow depends on the difference in flow from the pumps and flow to the consumers, if the flow from the pumps is more then the water flows into the tank and conversely when the flow to the consumers is more then the water flows out of the tank.

For a water distribution network Kirchhoff's node law can be given as,

$$Hq = d \quad (2.25)$$

where,

$H \in \mathbb{R}^{n \times m}$	is incidence matrix of the graph
$q \in \mathbb{R}^m$	is the flow vector in the edges
$d \in \mathbb{R}^n$	is the vector of of forced flows at the nodes(also called nodal demands), with $d_i > 0$ when flow is into node $i$ and $d_i < 0$ when flow is out of the node

The nodal demands for the nodes connected to consumer will always be negative,  $d_i < 0$ , and nodal demands for the nodes connected to the pumps will always be positive,  $d_i > 0$ . The nodal demand at the nodes connected to the tank will be positive when the flow of water is into the network from the tank and negative when the flow of water is into the tank from the network.

In a graph with  $n$  nodes, there are only  $(n - 1)$  independent nodal demands, this is due to mass conservation of water in the network, i.e. at any given point the water out of the network must be equal to water into the network.

$$d_n = - \sum_{i=1}^{n-1} d_i \quad (2.26)$$

The mass conservation of water in the network can also be expressed in terms of the incidence matrix by following lemma [13].

**Lemma 1** *Let  $T$  be a directed tree with the incidence matrix  $H_T$  and reduced incidence matrix  $\bar{H}_T$  (without loss of generality assuming that the last row of  $H_T$  has been deleted to obtain  $\bar{H}_T$ ). The reduced incidence matrix is invertible since a tree is a connected graph with  $n-1$  edges[6]. Then the following holds,*

$$H_T \bar{H}_T^{-1} = \begin{bmatrix} I_{n-1} \\ -\mathbb{1}^T \end{bmatrix} \quad (2.27)$$

where,

$\mathbb{1}$  is a vector of ones  
 $I_{n-1}$  is an identity matrix of  $n-1$

The vector  $q \in \mathbb{R}^m$  of flows through all the edges in the water distribution network is characterised by the following lemma [13].

**Lemma 2** *Let  $q \in \mathbb{R}^m$  be the vector of flows through the edges in a flow network with underlying graph  $G$  and let  $n$  be the number of vertices in  $G$ . With  $T$  denote a particular spanning tree of  $G$  and  $q_c \in \mathbb{R}^{l=m-n+1}$  the vector of flows through the chords of  $T$  with respect to  $G$ . Finally, let  $\bar{H}_T$  be the reduced incidence matrix of  $T$  and  $\bar{d} \in \mathbb{R}^{n-1}$  the vector of demands out of the non-reference nodes. Then the following is true*

$$q = B^T q_c + \begin{bmatrix} 0_{l \times n-1} \\ \bar{H}_T^{-1} \end{bmatrix} \bar{d} \quad (2.28)$$

The nodal demands for the nodes other than nodes connected to pump, consumer valves and tank would always be zero. Therefore, the vector of all nodal demands can be represented in terms of vector for non-zero nodal demands, i.e. pump nodal demands,  $d_p$ , consumer nodal demands,  $d_c$ , and tank nodal demands,  $d_\tau$ .

$$d = F_p^T d_p + F_c^T d_c + G_\tau^T d_\tau \quad (2.29)$$

where,

$d \in \mathbb{R}^n$	$n$ is the total number of nodes in the graph
$d_p \in \mathbb{R}^{n_p}$	$n_p$ is the number of nodes connected to pumps
$d_c \in \mathbb{R}^{n_c}$	$n_c$ is the number of nodes connected to consumers
$d_\tau \in \mathbb{R}^{n_\tau}$	$n_\tau$ is the number of nodes connected to tanks
$F_p \in \mathbb{R}^{n_p \times n}$	is a matrix to extract $d_p$ from $d$ in the form $\begin{bmatrix} I_p & 0 & 0 & 0 \end{bmatrix}$
$F_c \in \mathbb{R}^{n_c \times n}$	is a matrix to extract $d_c$ from $d$ in the form $\begin{bmatrix} 0 & I_c & 0 & 0 \end{bmatrix}$
$G_\tau \in \mathbb{R}^{n_\tau \times n}$	is a matrix to extract $d_\tau$ from $d$ in the form $\begin{bmatrix} 0 & 0 & I_\tau & 0 \end{bmatrix}$

Furthermore, the vector of non-reference nodal demands can be represented in terms of vector for non-reference pump nodal demands,  $\bar{d}_p$ , consumer nodal demands,  $\bar{d}_c$ , and tank nodal demands,  $\bar{d}_\tau$ .

$$\bar{d} = \bar{F}_p^T \bar{d}_p + \bar{F}_c^T \bar{d}_c + \bar{G}_\tau^T \bar{d}_\tau \quad (2.30)$$

where,

$\bar{F}_p$	is reduced $F_p$ matrix with the reference node row removed
$\bar{F}_c$	is reduced $F_c$ matrix with the reference node row removed
$\bar{G}_\tau$	is reduced $G_\tau$ matrix with the reference node row removed

Substituting eq. (2.30) into (2.28)

$$q = B^T q_C + \begin{bmatrix} 0_{l \times n-1} \\ \bar{H}_T^{-1} \end{bmatrix} \left[ \bar{F}_p^T \bar{d}_p + \bar{F}_c^T \bar{d}_c + \bar{G}_\tau^T \bar{d}_\tau \right] \quad (2.31)$$

The flow vector can be partitioned into flow in chord edges and flow in tree edges as,

$$\begin{bmatrix} q_C \\ q_T \end{bmatrix} = B^T q_C + \begin{bmatrix} 0_{l \times n-1} \\ \bar{H}_T^{-1} \end{bmatrix} \left[ \bar{F}_p^T \bar{d}_p + \bar{F}_c^T \bar{d}_c + \bar{G}_\tau^T \bar{d}_\tau \right] \quad (2.32)$$

where,

$q_C$	is the flow vector for the chord edges of the graph
$q_T$	is the flow vector for the tree edges of the graph

Substituting eq. (2.3) into (2.32)

$$\begin{bmatrix} q_C \\ q_T \end{bmatrix} = \begin{bmatrix} I \\ -\bar{H}_T^{-1} \bar{H}_C \end{bmatrix} q_C + \begin{bmatrix} 0_{l \times n-1} \\ \bar{H}_T^{-1} \end{bmatrix} \left[ \bar{F}_p^T \bar{d}_p + \bar{F}_c^T \bar{d}_c + \bar{G}_\tau^T \bar{d}_\tau \right] \quad (2.33)$$

Consequently, expression for  $q_T$  can be given as,

$$q_T = -\bar{H}_T^{-1}\bar{H}_C q_C + \bar{H}_T^{-1}\bar{F}_p^T \bar{d}_p + \bar{H}_T^{-1}\bar{F}_c^T \bar{d}_c + \bar{H}_T^{-1}\bar{G}_\tau^T \bar{d}_\tau \quad (2.34)$$

As for this model the water distribution network only consists of pipe components, therefore the vector for pressure drop across the edges,  $\Delta p \in \mathbb{R}^m$ , can be given by eq. (2.35) using eq. (2.13)

$$\Delta p = \lambda(q) - \Delta z \quad (2.35)$$

where,

$$\begin{aligned} \lambda(q) &= [\lambda_1(q_1) \ \cdots \ \lambda_m(q_m)]^T \\ \Delta z &= [\Delta z_1 \ \cdots \ \Delta z_m]^T \end{aligned}$$

Kirchhoff's mesh law for hydraulic network can be represented by following equations,

$$B\Delta z = 0 \quad (2.36a)$$

$$B\Delta p = 0 \quad (2.36b)$$

Using equations (2.36), eq. (2.35) can be reduced to,

$$B\lambda(q) = 0 \quad (2.37)$$

$\lambda(q)$  can also be partitioned into  $\lambda_C(q_C)$   $\lambda_T(q_T)$ ,

$$B \begin{bmatrix} \lambda_C(q_C) \\ \lambda_T(q_T) \end{bmatrix} = 0 \quad (2.38)$$

Substituting  $B$  from eq. (2.3) gives,

$$\lambda_C(q_C) - \bar{H}_C^T \bar{H}_T^{-T} \lambda_T(q_T) = 0 \quad (2.39)$$

where,

$\lambda_C(q_C)$  is the vector of drop in pressure due to friction across chord edges of the graph

$\lambda_T(q_T)$  is the vector of drop in pressure due to friction across tree edges of the graph

Substituting  $q_T$  from eq. (2.34) into eq. (2.39).

$$\lambda_C(q_C) - \bar{H}_C^T \bar{H}_T^{-T} \lambda_T(q_C, d_p, d_c, d_\tau) = 0 \quad (2.40)$$

where,

$$\lambda_T(q_C, d_p, d_c, d_\tau) \equiv \lambda_T(-\bar{H}_T^{-1}\bar{H}_C q_C + \bar{H}_T^{-1}\bar{F}_p^T \bar{d}_p + \bar{H}_T^{-1}\bar{F}_c^T \bar{d}_c + \bar{H}_T^{-1}\bar{G}_\tau^T \bar{d}_\tau)$$

The differential pressure across the edges can be given as,

$$\Delta p = H^T p \quad (2.41)$$

and the level difference across the edges can be given as,

$$\Delta z = H^T z \quad (2.42)$$

The differential pressure  $\Delta p$  can also be partitioned into differential pressure across chord edges,  $\Delta p_C$ , and tree edges,  $\Delta p_T$ .

$$\begin{bmatrix} \Delta p_C \\ \Delta p_T \end{bmatrix} = \begin{bmatrix} H_C^T \\ H_T^T \end{bmatrix} p \quad (2.43)$$

where,

$\Delta p_C$  is the vector of drop in pressure across chord edges of the graph

$\Delta p_T$  is the vector of drop in pressure across tree edges of the graph

Consequently,

$$H_T^T p = \Delta p_T = \lambda_T(q_T) - \Delta z_T \quad (2.44)$$

$$\Rightarrow H_T^T p = \Delta p_T = \lambda_T(q_T) - H_T^T z \quad (2.45)$$

where,

$\Delta z_T$  is the vector of drop in pressure due to geodesic level difference across tree edges of the graph

With Lemma 1 eq. (2.45) gives,

$$\bar{H}_T^{-T} H_T^T p = \bar{p} - \mathbb{1}p_0 = \bar{H}_T^{-T} \lambda_T(q_T) - (\bar{z} - \mathbb{1}z_0) \quad (2.46)$$

where,

$\bar{p}$  is the pressure vector for the non-reference nodes

$p_0$  is the reference node pressure

$\bar{z}$  is the vector of pressure due to level at the non-reference nodes

$z_0$  is the pressure due to level at the reference node

$$\Rightarrow \bar{p} - \mathbb{1}p_0 = \bar{H}_T^{-T} \lambda_T(q_T) - (\bar{z} - \mathbb{1}z_0) \quad (2.47)$$

$$\Rightarrow \bar{p} = \bar{H}_T^{-T} \lambda_T(q_T) - (\bar{z} - \mathbb{1}z_0) + \mathbb{1}p_0 \quad (2.48)$$

With eq. (2.34), eq. (2.48) can be represented as,

$$\bar{p} = \bar{H}_T^{-T} \lambda_T(q_C, d_p, d_c, d_\tau) - (\bar{z} - \mathbb{1}z_0) + \mathbb{1}p_0 \quad (2.49)$$

where,

$$\lambda_T(q_C, d_p, d_c, d_\tau) \equiv \lambda_T(-\bar{H}_T^{-1}\bar{H}_C q_C + \bar{H}_T^{-1}\bar{F}_p^T \bar{d}_p + \bar{H}_T^{-1}\bar{F}_c^T \bar{d}_c + \bar{H}_T^{-1}\bar{G}_\tau^T \bar{d}_\tau)$$

In this project the network only consist one elevated tank and this model is to be used for designing of supervisory control, therefore it is convenient to choose tank node as the reference node , as the tank pressure can easily be measured by a sensor at the bottom of the tank. Therefore eq. (2.49) can now be written as,

$$\bar{p} = \bar{H}_T^{-T} \lambda_T(q_C, d_p, d_c, d_\tau) - (\bar{z} - \mathbb{1}z_0) + \mathbb{1}p_\tau \quad (2.50)$$

With eq. (2.22), the model for nodes connected to the tank can be given by,

$$\dot{p}_\tau = -\mathcal{T}d_\tau \quad (2.51)$$

where,

$$\begin{aligned} p_\tau & \text{ is the vector of pressure nodes connected to the tank} \\ \mathcal{T} & = \text{diag}(\tau_i) \end{aligned}$$

With Euler's method eq. (2.51) can be discretized.

$$p_\tau(k+1) = p_\tau(k) - \mathcal{T}d_\tau t_s \quad (2.52)$$

where,

$t_s$  is the sampling time of discretization

Furthermore as mentioned previously, the tank node is chosen as the reference node, the flow in the tank node can be given as,

$$d_\tau = -\left(\sum d_c(k) + \sum d_p(k)\right) \quad (2.53)$$

Therefore model equations (2.40), (2.50) and (2.52) can be written as,

$$\lambda_C(q_C) - \bar{H}_C^T \bar{H}_T^{-T} \lambda_T(q_C, d_p, d_c) = 0 \quad (2.54)$$

$$\bar{p} = \bar{H}_T^{-T} \lambda_T(q_C, d_p, d_c) - (\bar{z} - \mathbb{1}z_0) + \mathbb{1}p_\tau \quad (2.55)$$

$$p_\tau(k+1) = p_\tau(k) + \mathcal{T} \left(\sum d_c(k) + \sum d_p(k)\right) t_s \quad (2.56)$$

Equations (2.54), (2.55) and (2.56) form the simplified model for a water distribution network with an elevated tank. With this model for the water distribution network, presented in section 2.4, supervisory nonlinear optimal control is developed which is presented in chapter 3.

### 2.3.2 Detailed water network model

In the detailed network model, apart from pipes, pumps and valves are also modelled as edges. The pipe dynamics have also been considered in this model, as the model is used in the stability analysis. Derivation of this model follows model derived in [10]. In this model the nodal demands are at inlet node of the pump edge, outlet node of the consumer valves and at the node connected to the tank. Also, the nodal demands are not considered as independent flows in and out of the network, but are dependent on system states and inputs.

The nodal demand is non-zero only for the nodes open to atmosphere, i.e. pump inlets and valve outlets, and the nodes connected to the tank. Therefore, instead of the vector of all nodal demands,  $d$ , in terms of pump, consumer and tank nodes, it can directly be represented in terms of nodal demands for nodes open to atmosphere,  $d_f$ , and tank nodal demand,  $d_\tau$  only.

$$d = F_f^T d_f + G_\tau^T d_\tau \quad (2.57)$$

where,

$d \in \mathbb{R}^n$	$n$ is the total number of nodes in the graph
$d_f \in \mathbb{R}^{n_f}$	$n_f$ is the number of nodes open to atmosphere
$d_\tau \in \mathbb{R}^{n_\tau}$	$n_\tau$ is the number of nodes connected to tanks
$F_f \in \mathbb{R}^{n_f \times n}$	is a matrix to extract $d_f$ from $d$ in the form $\begin{bmatrix} I_f & 0 \end{bmatrix}$
$G_\tau \in \mathbb{R}^{n_\tau \times n}$	is a matrix to extract $d_\tau$ from $d$ in the form $\begin{bmatrix} I_\tau & 0 \end{bmatrix}$

Similar to (2.30), the vector of non-reference nodal demands can now be given as,

$$\bar{d} = \bar{F}_f^T \bar{d}_f + \bar{G}_\tau^T \bar{d}_\tau \quad (2.58)$$

where,

$\bar{F}_f$	is reduced $F_f$ matrix with row corresponding to reference node removed
$\bar{G}_\tau$	is reduced $G_\tau$ matrix with row corresponding to reference node removed

Substituting eq. (2.58) into eq. (2.28) gives,

$$q = B^T q_C + \begin{bmatrix} 0 \\ \bar{H}_T^{-1} \end{bmatrix} \left[ \bar{F}_f^T \bar{d}_f + \bar{G}_\tau^T \bar{d}_\tau \right] \quad (2.59)$$

With eq. (2.3), eq. (2.59) can also be written as,

$$q = \begin{bmatrix} I & 0 & 0 \\ -\bar{H}_T^{-1} \bar{H}_C & \bar{H}_T^{-1} \bar{F}_f^T & \bar{H}_T^{-1} \bar{G}_\tau^T \end{bmatrix} \begin{bmatrix} q_C \\ \bar{d}_f \\ \bar{d}_\tau \end{bmatrix} \quad (2.60)$$

$$\Rightarrow q = B_n^T q_n \quad (2.61)$$

where,

$$B_n = \begin{bmatrix} I & -\bar{H}_C^T \bar{H}_T^{-T} \\ 0 & \bar{F}_f \bar{H}_T^{-T} \\ 0 & \bar{G}_\tau \bar{H}_T^{-T} \end{bmatrix} \quad (2.62)$$

$$q_n = \begin{bmatrix} q_C \\ \bar{d}_f \\ \bar{d}_\tau \end{bmatrix} \quad (2.63)$$

Consequently, eq. (2.34) is now to be given as,

$$q_T = -\bar{H}_T^{-1} \bar{H}_C q_C + \bar{H}_T^{-1} \bar{F}_f^T \bar{d}_f + \bar{H}_T^{-1} \bar{G}_\tau^T \bar{d}_\tau \quad (2.64)$$

Also, using eq. (2.59), expression for  $\dot{q}$  can be given as,

$$\dot{q} = B^T \dot{q}_C + \begin{bmatrix} 0 \\ \bar{H}_T^{-1} \end{bmatrix} \left[ \bar{F}_f^T \dot{\bar{d}}_f + \bar{G}_\tau^T \dot{\bar{d}}_\tau \right] \quad (2.65)$$

And from eq. (2.64), expression for  $\dot{q}_T$  can be given as,

$$\dot{q}_T = -\bar{H}_T^{-1} \bar{H}_C \dot{q}_C + \bar{H}_T^{-1} \bar{F}_f^T \dot{\bar{d}}_f + \bar{H}_T^{-1} \bar{G}_\tau^T \dot{\bar{d}}_\tau \quad (2.66)$$

The vector for pressure drop across all the edges of the graph can given using general two terminal component model, eq. (2.20),

$$\Delta p = \mathcal{J} \dot{q} + \lambda(q) + \mu(q, OD) - \alpha(q, \omega) - \Delta z \quad (2.67)$$

where,

$$\begin{aligned} \mathcal{J} &= \text{diag}([\mathcal{J}_1 \ \cdots \ \mathcal{J}_m]) \\ \lambda(q) &= [\lambda_1(q_1) \ \cdots \ \lambda_m(q_m)]^T \\ \mu(q, OD) &= [\mu_k(q_1, OD_1) \ \cdots \ \mu_k(q_m, OD_m)]^T \\ \alpha(q, \omega) &= [\alpha_1(q_1, \omega_1) \ \cdots \ \alpha_m(q_m, \omega_m)]^T \\ \Delta z &= [\Delta z_1 \ \cdots \ \Delta z_m]^T \end{aligned}$$

Using Kirchhoff's mesh law for hydraulic network, eq. (2.36) over eq. (2.67) gives,

$$B \Delta p = B \mathcal{J} \dot{q} + B(\lambda(q) + \mu(q, OD) - \alpha(q, \omega)) - B \Delta z \quad (2.68)$$

$$\Rightarrow 0 = B \mathcal{J} \dot{q} + B(\lambda(q) + \mu(q, OD) - \alpha(q, \omega)) \quad (2.69)$$

$$\Rightarrow B\mathcal{J}\dot{q} = -B(\lambda(q) + \mu(q, OD) - \alpha(q, \omega)) \quad (2.70)$$

Substituting  $\dot{q}$  expression from eq. (2.65) into eq. (2.70).

$$B\mathcal{J}B^T\dot{q}_C + B\mathcal{J} \begin{bmatrix} 0 \\ \bar{H}_T^{-1} \end{bmatrix} \left[ \bar{F}_f^T \dot{d}_f + \bar{G}_\tau^T \dot{d}_\tau \right] = -B(\lambda(q) + \mu(q, OD) - \alpha(q, \omega)) \quad (2.71)$$

Furthermore,  $\mathcal{J}$  can also be partitioned as,

$$\begin{bmatrix} \mathcal{J}_C & 0 \\ 0 & \mathcal{J}_T \end{bmatrix} \quad (2.72)$$

where,

$\mathcal{J}_C$  is the sub-matrix of  $\mathcal{J}$  consisting chord edges of the graph

$\mathcal{J}_T$  is the sub-matrix of  $\mathcal{J}$  consisting tree edges of the graph

Also, substituting expression for  $B$ , eq. (2.3), into eq. (2.71) gives,

$$B\mathcal{J}B^T\dot{q}_C + [I \quad -\bar{H}_C^T \bar{H}_T^{-T}] \begin{bmatrix} \mathcal{J}_C & 0 \\ 0 & \mathcal{J}_T \end{bmatrix} \begin{bmatrix} 0 \\ \bar{H}_T^{-1} \end{bmatrix} \left[ \bar{F}_f^T \dot{d}_f + \bar{G}_\tau^T \dot{d}_\tau \right] = -B(\lambda(q) + \mu(q, OD) - \alpha(q, \omega)) \quad (2.73)$$

$$\Rightarrow B\mathcal{J}B^T\dot{q}_C - \bar{H}_C^T \bar{H}_T^{-T} \mathcal{J}_T \bar{H}_T^{-1} \left[ \bar{F}_f^T \dot{d}_f + \bar{G}_\tau^T \dot{d}_\tau \right] = -B(\lambda(q) + \mu(q, OD) - \alpha(q, \omega)) \quad (2.74)$$

$$\Rightarrow B\mathcal{J}B^T\dot{q}_C - \bar{H}_C^T \bar{H}_T^{-T} \mathcal{J}_T \bar{H}_T^{-1} \bar{F}_f^T \dot{d}_f - \bar{H}_C^T \bar{H}_T^{-T} \mathcal{J}_T \bar{H}_T^{-1} \bar{G}_\tau^T \dot{d}_\tau = -B(\lambda(q) + \mu(q, OD) - \alpha(q, \omega)) \quad (2.75)$$

Furthermore, with the expression of  $q_T$ , eq. (2.64), eq. (2.75) can be written as,

$$\boxed{B\mathcal{J}B^T\dot{q}_C - \bar{H}_C^T \bar{H}_T^{-T} \mathcal{J}_T \bar{H}_T^{-1} \bar{F}_f^T \dot{d}_f - \bar{H}_C^T \bar{H}_T^{-T} \mathcal{J}_T \bar{H}_T^{-1} \bar{G}_\tau^T \dot{d}_\tau = -B(\lambda(q_C, \bar{d}_f, \bar{d}_\tau) + \mu(q_C, \bar{d}_f, \bar{d}_\tau, OD) - \alpha(q_C, \bar{d}_f, \bar{d}_\tau, \omega))} \quad (2.76)$$

Similar to eq. (2.46), partitioning  $\Delta p$  and using Lemma 1 on eq. (2.67) gives,

$$\bar{H}_T^{-T} H_T^T p = \bar{p} - \mathbf{1}p_0 = \bar{H}_T^{-T} \mathcal{J}_T \dot{q}_T + \bar{H}_T^{-T} (\lambda_T(q_T) + \mu_T(q_T, \omega_T)) - (\bar{z} - \mathbf{1}z_0) \quad (2.77)$$

where,

$OD_T$  is a vector of opening degree of valves for tree edges of the graph

$\omega_T$  is a vector of angular speed of pumps for tree edges of the graph

Multiplying eq. (2.77) by  $\bar{F}_f$  gives,

$$\bar{F}_f(\bar{p} - \mathbf{1}p_0) = \bar{F}_f\bar{H}_T^{-T}\mathcal{J}_T\dot{q}_T + \bar{F}_f\bar{H}_T^{-T}(\lambda_T(q_T) + \mu_T(q_T, OD_T) - \alpha_T(q_T, \omega_T)) - \bar{F}_f(\bar{z} - \mathbf{1}z_0) \quad (2.78)$$

$\bar{F}_f$  extracts non-reference nodes which are open to atmospheric pressure from vector of all non-reference nodes. Deliberately choosing one of the nodes which are open to atmosphere as the reference node. Subtracting reference node pressure, i.e. atmospheric pressure from the pressure at the nodes open to atmosphere leads to L.H.S of eq. (2.78) being zero.

$$0 = \bar{F}_f\bar{H}_T^{-T}\mathcal{J}_T\dot{q}_T + \bar{F}_f\bar{H}_T^{-T}(\lambda_T(q_T) + \mu_T(q_T, OD_T) - \alpha_T(q_T, \omega_T)) - \bar{F}_f(\bar{z} - \mathbf{1}z_0) \quad (2.79)$$

$$\Rightarrow \bar{F}_f\bar{H}_T^{-T}\mathcal{J}_T\dot{q}_T = -\bar{F}_f\bar{H}_T^{-T}(\lambda_T(q_T) + \mu_T(q_T, OD_T) - \alpha_T(q_T, \omega_T)) + \bar{F}_f(\bar{z} - \mathbf{1}z_0) \quad (2.80)$$

Substituting expression for  $\dot{q}_T$ , eq. (2.66), into eq. (2.80).

$$-\bar{F}_f\bar{H}_T^{-T}\mathcal{J}_T\bar{H}_T^{-1}\bar{H}_C\dot{q}_C + \bar{F}_f\bar{H}_T^{-T}\mathcal{J}_T\bar{H}_T^{-1}\bar{F}_f^T\dot{\bar{d}}_f + \bar{F}_f\bar{H}_T^{-T}\mathcal{J}_T\bar{H}_T^{-1}\bar{G}_\tau^T\dot{\bar{d}}_\tau = -\bar{F}_f\bar{H}_T^{-T}(\lambda_T(q_T) + \mu_T(q_T, OD_T) - \alpha_T(q_T, \omega_T)) + \bar{F}_f(\bar{z} - \mathbf{1}z_0) \quad (2.81)$$

Again, with the expression of  $q_T$ , eq. (2.64), eq. (2.81) can be written as,

$$\boxed{-\bar{F}_f\bar{H}_T^{-T}\mathcal{J}_T\bar{H}_T^{-1}\bar{H}_C\dot{q}_C + \bar{F}_f\bar{H}_T^{-T}\mathcal{J}_T\bar{H}_T^{-1}\bar{F}_f^T\dot{\bar{d}}_f + \bar{F}_f\bar{H}_T^{-T}\mathcal{J}_T\bar{H}_T^{-1}\bar{G}_\tau^T\dot{\bar{d}}_\tau = -\bar{F}_f\bar{H}_T^{-T}(\lambda_T(q_C, \bar{d}_f, \bar{d}_\tau) + \mu_T(q_C, \bar{d}_f, \bar{d}_\tau, OD) - \alpha_T(q_C, \bar{d}_f, \bar{d}_\tau, \omega)) + \bar{F}_f(\bar{z} - \mathbf{1}z_0)} \quad (2.82)$$

Now, multiplying eq. (2.77) by  $\bar{G}_\tau$  gives,

$$\bar{G}_\tau(\bar{p} - \mathbf{1}p_0) = \bar{G}_\tau\bar{H}_T^{-T}\mathcal{J}_T\dot{q}_T + \bar{G}_\tau\bar{H}_T^{-T}(\lambda_T(q_T) + \mu_T(q_T, OD_T) - \alpha_T(q_T, \omega_T)) - \bar{G}_\tau(\bar{z} - \mathbf{1}z_0) \quad (2.83)$$

$\bar{G}_\tau$  extracts non-reference nodes which are connected to tank from vector of all non-reference nodes, therefore eq. (2.83) gives,

$$(\bar{p}_\tau - \mathbb{1}p_0) = \bar{G}_\tau \bar{H}_T^{-T} \mathcal{J}_T \dot{q}_T + \bar{G}_\tau \bar{H}_T^{-T} (\lambda_T(q_T) + \mu_T(q_T, OD_T) - \alpha_T(q_T, \omega_T)) - \bar{G}_\tau(\bar{z} - \mathbb{1}z_0) \quad (2.84)$$

$$\Rightarrow \bar{G}_\tau \bar{H}_T^{-T} \mathcal{J}_T \dot{q}_T = -\bar{G}_\tau \bar{H}_T^{-T} (\lambda_T(q_T) + \mu_T(q_T, OD_T) - \alpha_T(q_T, \omega_T)) + \bar{G}_\tau(\bar{z} - \mathbb{1}z_0) + (\bar{p}_\tau - \mathbb{1}p_0) \quad (2.85)$$

Again, substituting expression for  $\dot{q}_T$ , eq. (2.66), into eq. (2.85).

$$-\bar{G}_\tau \bar{H}_T^{-T} \mathcal{J}_T \bar{H}_T^{-1} \bar{H}_C \dot{q}_C + \bar{G}_\tau \bar{H}_T^{-T} \mathcal{J}_T \bar{H}_T^{-1} \bar{F}_f^T \dot{d}_f + \bar{G}_\tau \bar{H}_T^{-T} \mathcal{J}_T \bar{H}_T^{-1} \bar{G}_\tau^T \dot{d}_\tau = -\bar{G}_\tau \bar{H}_T^{-T} (\lambda_T(q_T) + \mu_T(q_T, OD_T) - \alpha_T(q_T, \omega_T)) + \bar{G}_\tau(\bar{z} - \mathbb{1}z_0) + (\bar{p}_\tau - \mathbb{1}p_0) \quad (2.86)$$

Again, with the expression of  $q_T$ , eq. (2.64), eq. (2.86) can be written as,

$$\boxed{-\bar{G}_\tau \bar{H}_T^{-T} \mathcal{J}_T \bar{H}_T^{-1} \bar{H}_C \dot{q}_C + \bar{G}_\tau \bar{H}_T^{-T} \mathcal{J}_T \bar{H}_T^{-1} \bar{F}_f^T \dot{d}_f + \bar{G}_\tau \bar{H}_T^{-T} \mathcal{J}_T \bar{H}_T^{-1} \bar{G}_\tau^T \dot{d}_\tau = -\bar{G}_\tau \bar{H}_T^{-T} (\lambda_T(q_C, \bar{d}_f, \bar{d}_\tau) + \mu_T(q_C, \bar{d}_f, \bar{d}_\tau, OD) - \alpha_T(q_C, \bar{d}_f, \bar{d}_\tau, \omega)) + \bar{G}_\tau(\bar{z} - \mathbb{1}z_0) + (\bar{p}_\tau - \mathbb{1}p_0)} \quad (2.87)$$

Tank model can again be given by eq. (2.51) as,

$$\boxed{\dot{p}_\tau = -\mathcal{T}d_\tau} \quad (2.88)$$

where,

$p_\tau$  is the pressure vector at the nodes connected to the tank  
 $\mathcal{T} = \text{diag}(\tau_i)$

With equations (2.76), (2.82), (2.87) and (2.88), model for the water distribution network is given. This model can also be presented in a shorthand notation as[10],

$$B_n \mathcal{J} B_n^T \dot{q}_n = -B_n (\lambda(q_C, \bar{d}_f, \bar{d}_\tau) + \mu(q_C, \bar{d}_f, \bar{d}_\tau, OD) - \alpha(q_C, \bar{d}_f, \bar{d}_\tau, \omega)) + \mathcal{N}(\bar{z} - \mathbb{1}z_0) + \mathcal{I}(p_\tau - \mathbb{1}p_0) \quad (2.89a)$$

$$\dot{p}_\tau = -\mathcal{T}d_\tau \quad (2.89b)$$

where,

$$\mathcal{N} = \begin{bmatrix} 0 \\ \bar{F}_f \\ \bar{G}_\tau \end{bmatrix} \quad (2.90a)$$

$$\mathcal{I} = \begin{bmatrix} 0 \\ 0 \\ I \end{bmatrix} \quad (2.90b)$$

Stability analysis on this model with a local PI control is presented in section 3.4.

## 2.4 Modelling of the water distribution network considered in this project

In this section the water distribution network considered in this project is presented. Along with the network, equivalent graphs as per network models presented in sections 2.3.2 and 2.3.1 are also given.

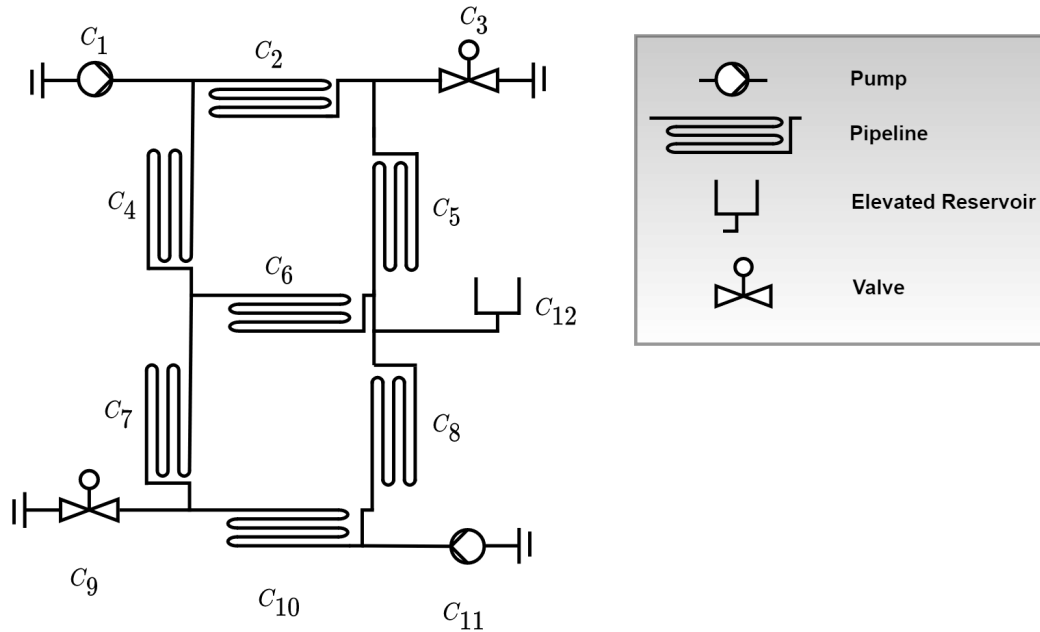


**Figure 2.1:** Grid topology water distribution network with an elevated reservoir

The water distribution network considered in this project is presented by figure 2.1. The network is a grid type water network composed of pipes,  $C_2$ ,  $C_4$ ,  $C_5$ ,  $C_6$ ,

$C_7$ ,  $C_8$  and  $C_{10}$ . Two pumps,  $C_1$  and  $C_{11}$ , are connected to the network, supplying water to the network. There are two consumers, represented by valves,  $C_3$  and  $C_9$ , are at an elevation of 0.9m. An elevated tank,  $C_{12}$ , is also connected to the network which is at an elevation of 3m. The inlet of pump is assumed to be an infinite reservoir of water at atmospheric pressure. The outlet of the valves are considered to be open to atmosphere. The network parameters are presented in tables 2.2, 2.1, 2.3 and 2.4.

**Table 2.1:** Pump parameters

Pump	$a_{h2}$	$a_{h0}$
$C_1$	0.0367	$7.335 \cdot 10^{-05}$
$C_{11}$	0.0367	$7.335 \cdot 10^{-05}$

**Table 2.2:** Pipe parameters

Pipe	Length [m]	Diameter [mm]	Roughness height [mm]
$C_2$	10	25	0.05
$C_4$	20	25	0.05
$C_5$	20	20	0.05
$C_6$	15	15	0.05
$C_7$	10	25	0.05
$C_8$	10	20	0.05
$C_{10}$	25	25	0.05

**Table 2.3:** Valve parameters

Valve	$K_{vs}$
$C_3$	1
$C_9$	1

**Table 2.4:** Parameters of the elevated tank

Tank	Diameter [m]	Height [m]	Cross sectional area [m <sup>2</sup> ]	Capacity [m <sup>3</sup> ]
$C_{12}$	0.6	0.706	0.283	0.2 (200 l)

Figure 2.2 presents a graphical representation of the water distribution network presented in figure 2.1. In this graph, as per modelling method presented in section 2.3.1, only pipes in the network are modelled as edges. The pump flows are represented by independent nodal demands  $d_1$  and  $d_6$ . Similarly consumer demands are

represented by  $d_2$  and  $d_5$ . Based on this graph, network model is developed and used to design and test the supervisory control, and the test results are presented in chapter 6.

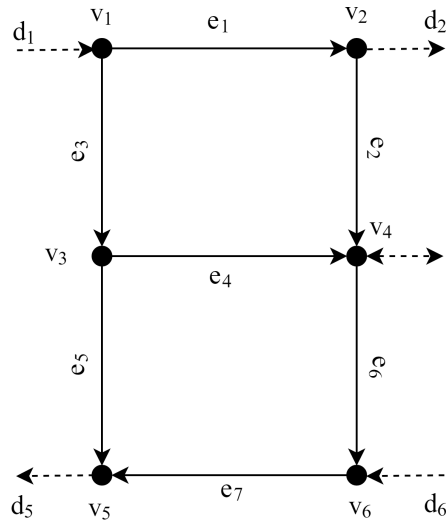


Figure 2.2: Graphical representation of network in figure 2.1 as per modelling method presented in section 2.3.1

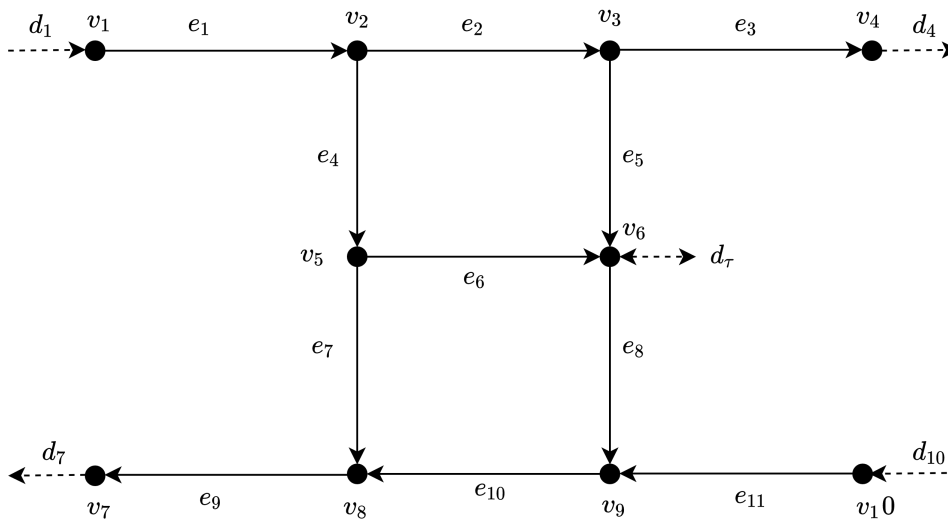


Figure 2.3: Graphical representation of network in figure 2.1 as per modelling method presented in section 2.3.2

Figure 2.3 presents a graphical representation of network in figure 2.1 as per modelling method presented in section 2.3.2. In this graph all the two terminal components are present in the network are modelled as edges. The nodal demands are at inlet nodes of pump,  $d_1$  and  $d_{10}$ , and outlet nodes of valves,  $d_4$  and  $d_7$ . These nodal demands are not independent but depends on state of network and input. Using this graph, network model is developed to study the stability of the system which is presented in section 3.4.

## Chapter 3

# Control formulation

In this chapter first the control structure developed in this project is presented which consist of a NMPC. The idea behind NMPC, it's objective, constraints and implementation is also presented in this chapter. The chapter then presents stability analysis of the inner closed-loop system, which includes Lyapunov stability of delay-free system and stability analysis of linearised system with output delay.

### 3.1 Control structure and NMPC

The control problem for the project is defined to be nonlinear optimal control of pumps in a water distribution network, with a elevated reservoir, and the proposed solution is presented in fig 3.1, i.e. the control structure exercised in this project. The water distribution network control is divided into two layers, the outer supervisory control layer and the inner local control layer, a similar structure is presented in [22]. The supervisory control layer consists of a Nonlinear Model Predictive Control (NMPC), whose task is to provide optimal control commands. NMPC takes the future price of electricity ( $P_e$ ), future consumer demands ( $d_c$ ) and the feedback of tank pressure ( $p_\tau$ ) as an input and solves an optimization problem to provide with optimal pump flow ( $d_p^*$ ) commands. An optimization problem defined as minimizing certain objectives subject to some constraints. The objectives and constraints for this projects are,

Objectives:

- Minimizing the cost of operation
- Minimizing the pressure variations at the consumer node

Constraints:

- System (or network) model and dynamics

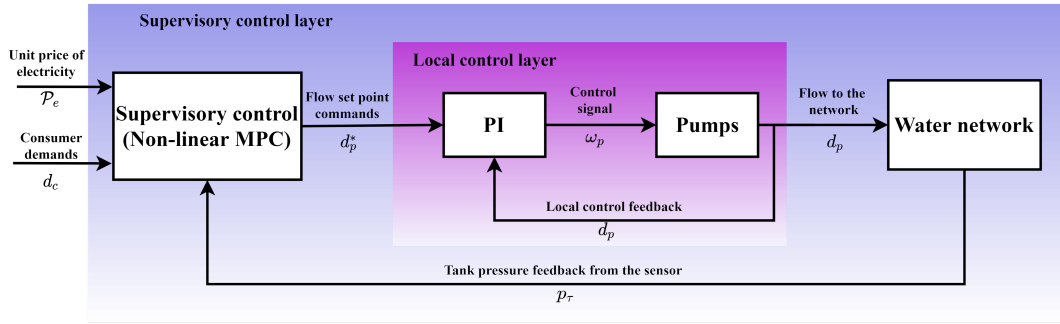


Figure 3.1: The control structure exercised in this project [22]

- Operational constraints of the actuators
- Physical constraints of the tank

The knowledge of the the future price of electricity and the future consumer demand is imperative for the optimization problem. In this project the future price of electricity is assumed to be known, whereas the consumer demand is predicted using a Kalman filter, which is presented in section 4.2. Also, the tank pressure measurements and pump flow measurements are assumed to be available from sensors.

The local control layer consists of PI (Proportional Integral) controller, whose task is to regulate the flow from the pumps at desired optimal flow set-points, provided by the NMPC. The PI control takes feedback of the pump flows and manipulates the pump flows accordingly.

The supervisory control layer operates at a sampling time 60 sec, whereas the local control layer operates at a sampling time of 1 sec. The NMPC is provided with an average of the consumer demand and the price of electricity over 60 sec as a constant for those 60 sec, based on that it computes optimal pump flow set-points for the next 60 sec. The PI control aims to control the pump flows at the provided set-point for next 60 sec, and after that NMPC provides new optimal flow set-points for next 60 sec.

For the simulation tests there is only supervisory control layer, as the nonlinear model for simulation test directly has pump flows as an input and therefore there is no need for a PI control. On the other hand in the laboratory setup, the pump flow are to be controlled by manipulating the pump speed and therefore the local control layer is implemented for laboratory testing, presented in section 6.3.

### 3.1.1 Nonlinear model predictive control

In this project the requirement is to satisfy more than one objective in control of a system with multi-variable interactions. Model predictive control (MPC) is a

advance process control method capable of handling control of such multi-input multi-output (MIMO) systems [17].

The basic idea in MPC is at time instance  $k$  solve an optimization problem to compute a sequence of optimal control input,  $u^*$ , for the period  $[k, k + H_p]$ , where  $H_p$  is prediction horizon. From this sequence of control input only the first input,  $u^*(k)$ , is applied to the system. At next time instance,  $k + 1$ , the horizon is moved by one step and again the optimization problem is solved to compute new a sequence of optimal control inputs. A nonlinear MPC is a variant of MPC, where the system model is nonlinear or the objective function is nonlinear, or both are nonlinear. In a NMPC the optimization problem is defined as,

$$\min_{\mathcal{U}^k} \mathcal{V}_{mpc}(\mathcal{X}^k, \mathcal{U}^k) = \min_{\mathcal{U}^k} \sum_{i=0}^{H_p-1} \mathcal{J}(u^{(k+i|k)}, x^{(k+i|k)}) \quad (3.1)$$

subject to,

$$x^{(k+i+1|k)} = f(x^{(k+i|k)}, u^{(k+i|k)}) \quad (3.2a)$$

$$g_{mpc}(x^{(k+i|k)}, u^{(k+i|k)}) \leq 0 \quad (3.2b)$$

for a dynamical system defined by difference equation,

$$x^{(k+1)} = f(x^{(k)}, u^{(k)}) \quad (3.3)$$

where,

$\mathcal{V}_{mpc}(\cdot)$	is the objective function over the prediction horizon of the NMPC
$u$	is the input vector
$x$	is the state vector
$\mathcal{U}^k$	is stacked vector of $u$ from time $k$ to $k + H_p - 1$
$\mathcal{X}^k$	is stacked vector of $x$ from time $k$ to $k + H_p$
$g_{mpc}(\cdot)$	is a function defining inequality constraints of the MPC problem
$f(\cdot)$	is state transition function

The constraints, (3.2), are over the entire prediction horizon, therefore there would be  $H_p$  dynamic constraints and  $H_p$  inequality constraints. The objective function over the prediction horizon  $\mathcal{V}_{mpc}(\cdot)$  is minimized with respect to  $\mathcal{U}^k$ . The optimization is subjected to the system dynamics and constraints which can be actuator limits or physical limits of the system.  $k$  represents the current time instance, and  $i$  represents the index increment (future time). The notation  $(k + i|k)$  represents predicted value at  $k + i$  time instance based on available knowledge at current time instance,  $k$ .

A nonlinear programming (NLP) problem is a optimization problem where the objective function and/or the constraints are nonlinear and in general form represented as,

$$\min_w \Theta(w) \quad (3.4)$$

subject to,

$$g_1(w) \leq 0 \quad (3.5a)$$

$$g_2(w) = 0 \quad (3.5b)$$

where,

$w$  is the optimization variable of the NLP

$\Theta(\cdot)$  is the objective function of the NLP

$g_1(\cdot)$  is a function defining equality constraints of the NLP

$g_2(\cdot)$  is a function defining inequality constraints of the NLP

To solve the NMPC optimization problem, using solvers (software programs) available for NLP, the optimization problem, (3.1) and (3.2), needs to be converted to a NLP problem. This can be accomplished by two methods, viz. single shooting or multiple shooting. In single shooting method the objective function and constraints are reduced to functions of just the optimization variable and the (known) initial value of the states. For the NMPC problem this reduction is done using the system dynamic equation,(3.3).

$$\min_{\mathcal{U}^k} \mathcal{V}_{mpc}(\mathcal{X}^k, \mathcal{U}^k) \xrightarrow{x^{(k+1)}=f(x^{(k)}, u^{(k)})} \min_{\mathcal{U}^k} \mathcal{V}_{nlp}(x^k, \mathcal{U}^k) \quad (3.6a)$$

$$g(x^{(k+i|k)}, u^{(k+i|k)}) \leq 0 \xrightarrow{x^{(k+1)}=f(x^{(k)}, u^{(k)})} g_{nlp}(x^k, \mathcal{U}^k) \leq 0 \quad (3.6b)$$

The NMPC optimization problem, presented by eq. (3.1) and (3.2), in form of NLP problem using single shooting, can be defined as,

$$\min_{\mathcal{U}^k} \mathcal{V}_{nlp}(x^k, \mathcal{U}^k) \quad (3.7)$$

subject to

$$g_{nlp}(x^k, \mathcal{U}^k) \leq 0 \quad (3.8)$$

where,

$\mathcal{U}^k$  is stacked vector of  $u$ , which is the optimization variable

$x^k$  is the initial condition of the states at the start of the optimization problem

$g_{nlp}(\cdot)$  is a function of  $\mathcal{U}^k$  and  $x^k$ , defining inequality constraints of the NMPC optimization problem

In multiple shooting, the states along with the inputs are considered as the optimization variables. Accordingly the objective function of the NMPC problem is

minimized with respect to  $\mathcal{X}^k$  and  $\mathcal{U}^k$  both, and that is the main difference between single shooting and multiple shooting. The system dynamics over the prediction horizon, eq. (3.2a), are considered to be equality constraints for the NLP problem as,

$$x^{(k+i+1|k)} = f(x^{(k+i|k)}, u^{(k+i|k)}) \quad (3.9a)$$

$$\Rightarrow x^{(k+i+1|k)} - f(x^{(k+i|k)}, u^{(k+i|k)}) = 0 \quad (3.9b)$$

$$\Rightarrow g_{2nlp}(\mathcal{X}^k, \mathcal{U}^k) = 0 \quad (3.9c)$$

the inequality constraints, (3.2b), and the objective function, (3.1), remains the same but can be represented in form,

$$g_{mpc}(x^{(k+i|k)}, u^{(k+i|k)}) \leq 0 \quad (3.10a)$$

$$\Rightarrow g_{1nlp}(\mathcal{X}^k, \mathcal{U}^k) \leq 0 \quad (3.10b)$$

$$\mathcal{V}_{nlp}(\mathcal{X}^k, \mathcal{U}^k) = \mathcal{V}_{mpc}(\mathcal{X}^k, \mathcal{U}^k) \quad (3.11)$$

The NMPC optimization problem in form of NLP problem, using multiple shooting, can now be defined as,

$$\min_{\mathcal{X}^k, \mathcal{U}^k} \mathcal{V}_{nlp}(\mathcal{X}^k, \mathcal{U}^k) \quad (3.12)$$

subject to

$$g_{1nlp}(\mathcal{X}^k, \mathcal{U}^k) \leq 0 \quad (3.13a)$$

$$g_{2nlp}(\mathcal{X}^k, \mathcal{U}^k) = 0 \quad (3.13b)$$

where,

$g_{1nlp}(\cdot)$  is a function of  $\mathcal{U}^k$  and  $\mathcal{X}^k$ , defining inequality constraints

$g_{2nlp}(\cdot)$  is a function of  $\mathcal{U}^k$  and  $\mathcal{X}^k$ , defining equality constraints

The main drawback of single shooting is nonlinearity propagation, for NMPC problems with long prediction horizon the NLP optimization problem becomes highly nonlinear. This high nonlinearity may result into poor performance of NLP solvers. Whereas, with multiple shooting the number of optimization variables increases but the degree of nonlinearity does not increase. In this project multiple shooting method is used to convert the NMPC optimization problem to NLP problem and implement as a controller.

### 3.2 Nonlinear MPC for water distribution network

The control problem or the NMPC problem in this project is multi-objective. The objective being minimizing the cost of operation and minimizing the pressure variations at the consumer end. The cost of operation can be quantified using energy consumption of the pumps and can be given as [22],

$$\begin{aligned} P_m &= \frac{d_i p_i}{\eta_p \eta_m 10^3 10^5 3600} \\ &= d_i p_i k_\eta \end{aligned} \quad (3.14)$$

where,

$$k_\eta = \frac{1}{\eta_p \eta_m 10^3 10^5 3600} \quad (3.15)$$

where,

$P_m$	is the $i^{th}$ pumping station's power consumption	[kW]
$d_i$	is the $i^{th}$ pumping station's flow	[m <sup>3</sup> /h]
$p_i$	is the $i^{th}$ pumping station's pressure developed	[bar]
$\eta_p$	is the pump's efficiency	[.]
$\eta_m$	is the motor's efficiency	[.]

The efficiency of pumps and motors at all the pumping stations is assumed to be same and constant. In reality, the efficiency is dependent of flow and pressure being delivered by the pump [22].

Now the cost of pumps operation can be give as,

$$\begin{aligned} \mathcal{E} &= P_m T_s \mathcal{P}_e \\ &= d_i p_i k_\eta T_s \mathcal{P}_e \end{aligned} \quad (3.16)$$

where,

$\mathcal{E}$	is the pumping station operational cost	[DKK]
$T_s$	is the sampling time	[minute]
$\mathcal{P}_e$	is the unit price of electricity	[DKK/kW minute]

Now the part of objective function with respect to operational cost can be defined as,

$$\mathcal{J}_1 = d_p^T \mathcal{P} p_p k_\eta T_s \quad (3.17)$$

where,

$d_p$	is the vector of flows from the pumping station nodes	[m <sup>3</sup> /h]
$p_p$	is the vector of pressures at pumping station nodes	[bar]
$\mathcal{P}$	is a 2 × 2 diagonal matrix of unit price of electricity	[DKK/kW minute]

The pump flow is the input to the system, therefore here after  $d_p$  will be represented as  $u$ . Also,  $p_p$  is represented in form of  $\bar{p}$ .

$$\mathcal{J}_1 = u^T \mathcal{P} (\bar{F}_p \bar{p}) k_\eta T_s \quad (3.18)$$

The second objective in the NMPC problem is to minimize the pressure variation at the consumer end, and that can be quantified using variance of the pressure at the consumer end.

$$\mathcal{J}_2 = (p_c - \mu_{p,c})^T (p_c - \mu_{p,c}) \quad (3.19)$$

where,

$p_c$	is vector of pressure at consumer nodes	[bar]
$\mu_{p,c}$	is vector of arithmetic mean pressure at consumer nodes	[bar]

Equation (3.19) can be further written as,

$$\mathcal{J}_2 = (\bar{F}_c (\bar{p} - \mu_{\bar{p}}))^T (\bar{F}_c (\bar{p} - \mu_{\bar{p}})) \quad (3.20)$$

With equations (3.18) and (3.20), the complete objective function for the NMPC problem can be given as,

$$\begin{aligned} \mathcal{J} &= \mathcal{J}_1 + \mathcal{J}_2 \\ &= u^T \mathcal{P} (\bar{F}_p \bar{p}) k_\eta T_s + (\bar{F}_c (\bar{p} - \mu_{\bar{p}}))^T (\bar{F}_c (\bar{p} - \mu_{\bar{p}})) \end{aligned} \quad (3.21)$$

The objective function over the prediction horizon can now be given as,

$$\begin{aligned} \mathcal{V}^k &= \sum_{i=0}^{H_p-1} \mathcal{J} \\ &= \sum_{i=0}^{H_p-1} \left( (u^{(k+i|k)})^T \mathcal{Q} \mathcal{P}^{(k+i|k)} (\bar{F}_p \bar{p}^{(k+i|k)}) k_\eta T_s \right. \\ &\quad \left. + \left( \bar{F}_c (\bar{p}^{(k+i|k)} - \frac{1}{H_p} \sum_{j=0}^{H_p-1} \bar{p}^{(k+j|k)}) \right)^T \mathcal{R} \left( \bar{F}_c (\bar{p}^{(k+i|k)} - \frac{1}{H_p} \sum_{j=0}^{H_p-1} \bar{p}^{(k+j|k)}) \right) \right) \end{aligned} \quad (3.22)$$

where,

$\mathcal{Q}$  is weight on the operational cost minimization with  $\mathcal{Q} \geq 0$   
 $\mathcal{R}$  is weight on the pressure variation minimization with  $\mathcal{R} \geq 0$

The weights  $\mathcal{Q}$  and  $\mathcal{R}$  are to penalise respective objectives in the objective function.

### 3.2.1 Constraints

#### Actuator constraints

The pumps can only deliver water with certain maximum limit in pressure and flow, this introduces inequality constraints into the NMPC optimization problem.

$$0 \leq \bar{F}_p \bar{p}^k \leq p_p^{max} \quad (3.23)$$

$$0 \leq u^k \leq d_p^{max} \quad (3.24)$$

#### Physical limits of the tank

The dimensions of the tank are fixed and therefore the water in the tank can only be filled up to a certain maximum limit. Also, for emergency purposes the water level in the tank needs to be maintained above a certain threshold. This maximum and minimum limits introduces an inequality constraint into the NMPC optimization problem.

$$p_\tau^{min} \leq p_\tau^k \leq p_\tau^{max} \quad (3.25)$$

With the objection function, (3.22), system model, eq. (2.54), (2.55) and (2.56), and the inequality constraints, (3.23), (3.24) and (3.25), the complete NMPC optimization problem can be defined as,

$$\begin{aligned} \min_{\mathcal{U}^k} \mathcal{V}^k = & \min_{\mathcal{U}^k} \sum_{i=0}^{H_p-1} \left( (u^{(k+i|k)})^T \mathcal{Q} \mathcal{P}^{(k+i|k)} (\bar{F}_p \bar{p}^{(k+i|k)}) k_\eta T_s \right. \\ & \left. + \left( \bar{F}_c (\bar{p}^{(k+i|k)} - \frac{1}{H_p} \sum_{j=0}^{H_p-1} \bar{p}^{(k+j|k)}) \right)^T \mathcal{R} \left( \bar{F}_c (\bar{p}^{(k+i|k)} - \frac{1}{H_p} \sum_{j=0}^{H_p-1} \bar{p}^{(k+j|k)}) \right) \right) \end{aligned} \quad (3.26)$$

subject to

$$\lambda_C(q_C^k) - \bar{H}_C^T \bar{H}_T^{-T} \lambda_T(q_C^k, u^k, d_c^k) = 0 \quad (3.27a)$$

$$\bar{p}^k = \bar{H}_T^{-T} \lambda_T(q_C^k, u^k, d_c^k) - (\bar{z} - \mathbb{1}z_0) + \mathbb{1}p_\tau^k \quad (3.27b)$$

$$p_{\tau}^{k+1} = p_{\tau}^k + \mathcal{T} \left( \sum d_c^k + \sum u^k \right) T_s \quad (3.27c)$$

$$0 \leq \bar{F}_p \bar{p}^k \leq p_p^{max} \quad (3.28a)$$

$$0 \leq u \leq d_p^{max} \quad (3.28b)$$

$$p_{\tau}^{min} \leq p_{\tau}^k \leq p_{\tau}^{max} \quad (3.28c)$$

Similar MPC optimization problem with linear system model is presented in [22], whereas in this project nonlinear system model is considered. This NMPC optimization problem can be converted into NLP problem with optimization variables being  $\mathcal{U}^k$ ,  $q_C$ ,  $\bar{p}$  and  $p_{\tau}$ , i.e. the objective function of the NMPC problem is to be minimized with respect to all these variables. The system model equations, (3.27), are presented as equality constraints and the inequality constraints, in eq. (3.28) remains the same in the NLP problem.

Solving the NLP problem yields a optimal set of control inputs,  $\mathcal{U}^*$ , and corresponding values of  $q_C^*$ ,  $\bar{p}^*$  and  $p_{\tau}^*$  over the prediction horizon.

$$\mathcal{U}^{*k} = \begin{bmatrix} u^{(k|k)} \\ \cdot \\ \cdot \\ \cdot \\ u^{(k+H_p-1|k)} \end{bmatrix} \quad (3.29)$$

As presented in section 3.1.1, only the first input value,  $u^{(k|k)}$  is used for the control. After that the horizon moves one time instance and the optimization problem is solved again over the prediction horizon.

### 3.2.2 Nonlinear MPC with soft constraints

In real life implementation of the NMPC the system might cross the constraints, due to large disturbances or plant-model mismatch. In such cases with hard constraints will lead to NMPC optimization (or NLP) problem being infeasible. To avoid such situations the hard constraints are 'softened', and these constraints are allowed to be violated only when required[17].

The constraint on the pressure in the tank,  $p_{\tau}$ , can be softened. A slack variable,  $\epsilon$ , is used for this and it is defined such that it is non-zero only if the constraints are violated and when it is non-zero it is heavily penalised in the cost function[17]. To soften the constraint,  $\epsilon$ , in constraint eq. (3.32d) is subtracted from the lower limit and added to the upper limit of pressure in the tank. NMPC optimization problem with soft constraint can be given as,

$$\begin{aligned}
\min_{\mathcal{U}^k, \epsilon} \mathcal{V}^k &= \min_{\mathcal{U}^k, \epsilon} \sum_{i=0}^{H_p-1} \left( (u^{(k+i|k)})^T \mathcal{Q} \mathcal{P}^{(k+i|k)} (\bar{F}_p \bar{p}^{(k+i|k)}) k_\eta T_s \right. \\
&+ \left. \left( \bar{F}_c (\bar{p}^{(k+i|k)} - \frac{1}{H_p} \sum_{j=0}^{H_p-1} \bar{p}^{(k+j|k)}) \right)^T \mathcal{R} \left( \bar{F}_c (\bar{p}^{(k+i|k)} - \frac{1}{H_p} \sum_{j=0}^{H_p-1} \bar{p}^{(k+j|k)}) \right) \right) \\
&+ \varrho \epsilon
\end{aligned} \tag{3.30}$$

subject to

$$\lambda_C(q_C^k) - \bar{H}_C^T \bar{H}_T^{-T} \lambda_T(q_C^k, u^k, d_c^k) = 0 \tag{3.31a}$$

$$\bar{p}^k = \bar{H}_T^{-T} \lambda_T(q_C^k, u^k, d_c^k) - (\bar{z} - \mathbb{1}z_0) + \mathbb{1}p_\tau^k \tag{3.31b}$$

$$p_\tau^{k+1} = p_\tau^k + \mathcal{T} \left( \sum d_c^k + \sum u^k \right) T_s \tag{3.31c}$$

$$0 \leq \epsilon \tag{3.32a}$$

$$0 \leq \bar{F}_p \bar{p}^k \leq p_p^{max} \tag{3.32b}$$

$$0 \leq u \leq d_p^{max} \tag{3.32c}$$

$$(p_\tau^{min} - \epsilon) \leq p_\tau^k \leq (p_\tau^{max} + \epsilon) \tag{3.32d}$$

where,

$\varrho$  is weight on minimization of the slack variable with  $\varrho \geq 0$

In the NLP program the optimization variables are now  $\mathcal{U}^k, q_C, \bar{p}, p_\tau$  and  $\epsilon$ .  $\varrho$  is kept high, so that the constraints are not violated unless its is absolutely required.

### 3.3 Nonlinear MPC implementation and simulation test results

The NMPC problem presented by equations (3.30), (3.31) and (3.32) is converted into a NLP problem using multiple shooting and implemented in CasADi [1] in MATLAB (ver. R2019b). The CasADi code defining the NMPC problem is presented in appendix A. As stated in section 3.1.1, with multiple shooting the states

along with the inputs are optimization variable, therefore in water distribution control problem the input  $u$  and the states  $q_C$ ,  $\bar{p}$ ,  $p_\tau$ , over the prediction horizon become the optimization variables. Also, when using the soft constraints the slack variable  $\epsilon$  becomes the optimization variable.

In the CasADi code all the optimization variables over the prediction horizon are defined in symbolic form and using a for-loop the objective function and the constraints are formulated. The NMPC problem is defined only once in symbolic form, and parameters such as consumer demand,  $d_c$ , the price of electricity,  $\mathcal{P}$ , and initial tank pressure,  $p_\tau^0$ , are passed to obtain optimal value of input over the prediction horizon,  $\mathcal{U}^*$ . As states are also optimization variables, the optimal values of states can also be obtained while solving the optimization problem, but in this project they are not being used.

### 3.3.1 NMPC control results

The NMPC optimization problem weight and system constraints used in the simulation test are presented below:

- Weights in the cost function

$$\mathcal{Q} = \begin{bmatrix} 5.5 \cdot 10^{10} & 0 \\ 0 & 5.5 \cdot 10^{10} \end{bmatrix} \quad (3.33)$$

$$\mathcal{R} = \begin{bmatrix} 1 & 0 \\ 0 & 1 \end{bmatrix} \quad (3.34)$$

$$\varrho = 1 \cdot 10^5 \quad (3.35)$$

- Constraints

$$0 \leq \epsilon \quad (3.36)$$

$$0 \leq \mathcal{M}_p^+ \bar{p}^k \leq 0.6 \quad (3.37)$$

$$0 \leq u \leq 0.3 \quad (3.38)$$

$$(0.0098 - \epsilon) \leq p_\tau^k \leq (0.0391 + \epsilon) \quad (3.39)$$

Figures 3.2, 3.3 and 3.4 presents simulation results for the NMPC control test. The NMPC control with aforementioned parameters is implemented on a nonlinear plant model of the water distribution network presented in section 2.4. In the simulation 1 minute is a representation of 1 hour in real life, therefore 2 days of real life is represented with 48 minute of simulation run time. In this simulation test

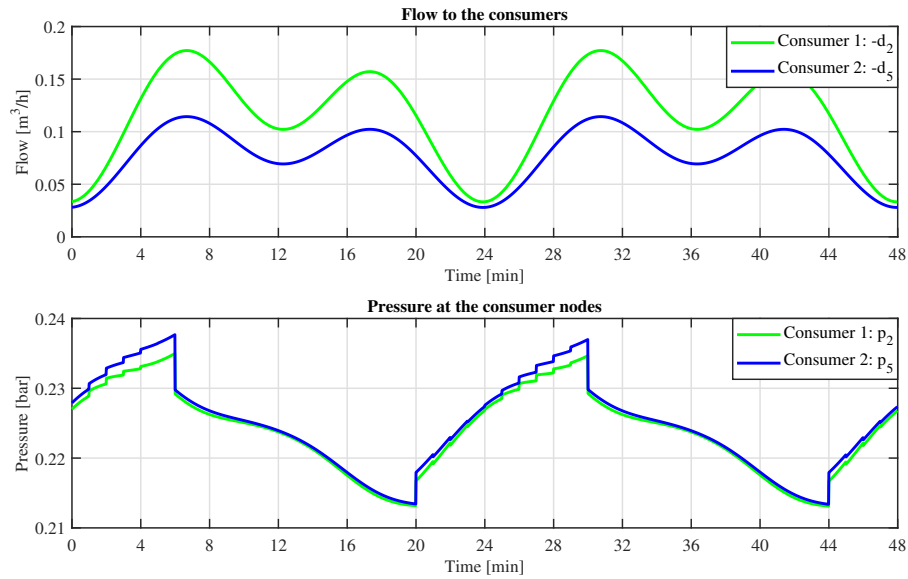


**Figure 3.2:** Consumer nodal demand flows and NMPC simulation results for pressure at consumer end

the future consumer demands are assumed to be known and provided to NMPC for solving the optimization problem.

Figure 3.2 presents the consumer demand pattern, for the two consumers, throughout the simulation period. The consumer demand is periodic over a period of 24 minute. In the simulation the consumer demand curve is chosen to reflect a real life scenario, where the consumer demands are expected to be high during morning and evening hours compared to afternoon and night hours. The figure also presents the pressure changes at the consumer ends, which is due to pump control by NMPC.

The NMPC is also provided with unit price of electricity over the simulation period. The varying electricity price in simulation is presented by figure 3.3. Again, the price curve is periodic with a period of 24 minute. The prices are low at 0.7 DKK/kW minute from 0 to 6 minute and 20 to 24 minute time instance, compared to 1.4 DKK/kW minute from 6 to 20 minute time instance, over the 24 minute period. These are again to reflect real life scenario, where the electricity prices are expected to be low during the night time compared to day time.

Figure 3.3 also presents the changes in the level of water in the tank throughout the simulation. The level is increasing when the price of electricity is low and this evident from the fact that the NMPC controls the pump to run during the time when the price of electricity is low, and this presented in figure 3.4. During these periods the pump supplies water to the consumers as well as the tank. During the

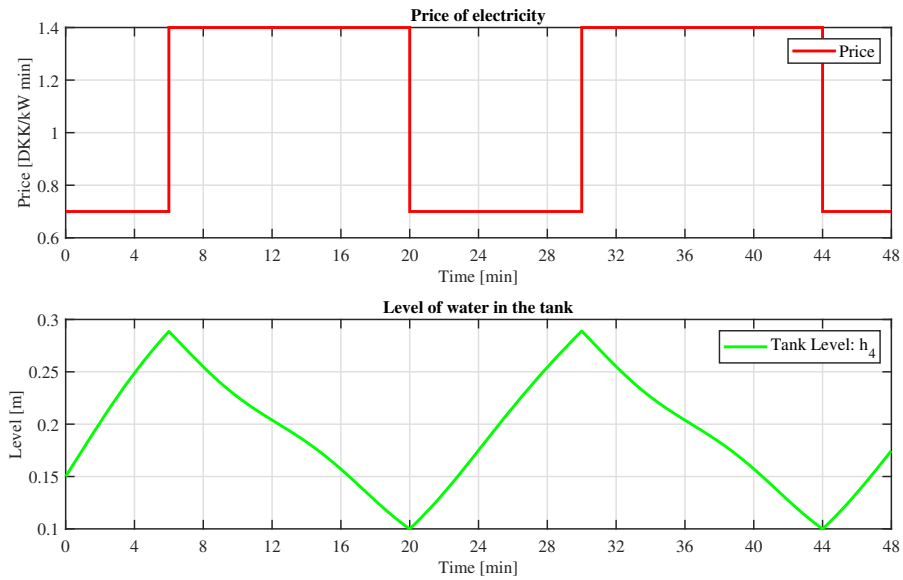


**Figure 3.3:** Varying unit price of electricity and NMPC simulation results for level of water in the tank

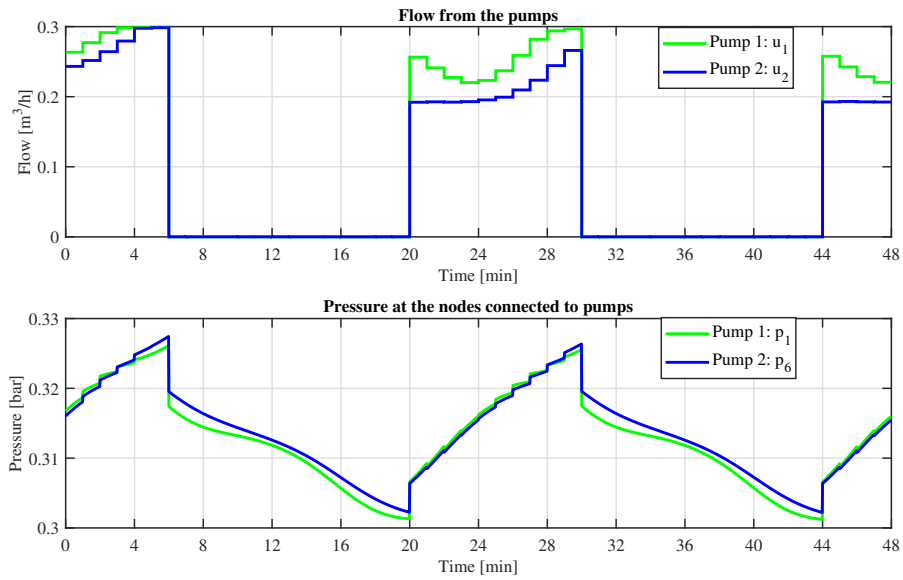


**Figure 3.4:** NMPC simulation results for flow from the pumps and the pressure at pump nodes

high electricity price period the pumps are stopped and the consumer demands are met by the tank and that can be observed as the level of water in the tank decreases when the electricity prices are high. Figure 3.4 also presents the pressure at the pump nodes, when the pumps are running the pressure is developed by the pumps and when the pumps are in stopped condition the pressure is developed due to tank pressure. Further simulation and laboratory tests are presented in chapter 6.

### 3.4 Stability analysis

The results from [22], presented a oscillatory behavior of the pump flow when controlled by the local PI controller in the laboratory setup. Figure 3.5 presents local flow control of the pumps by a PI controller in the laboratory setup(laboratory setup is presented in chapter 5). The P and I gain for the PI controller are 3 and 1.1 respectively. A constant flow set-point of  $0.3 \text{ m}^3/\text{h}$  is provided to the PI controller for 16 minute by a on/off supervisory control and the PI control aims to control the pump flows at the set-point. From the figure it can be observed that even with a constant set-point for a long duration the pump flows are oscillatory.

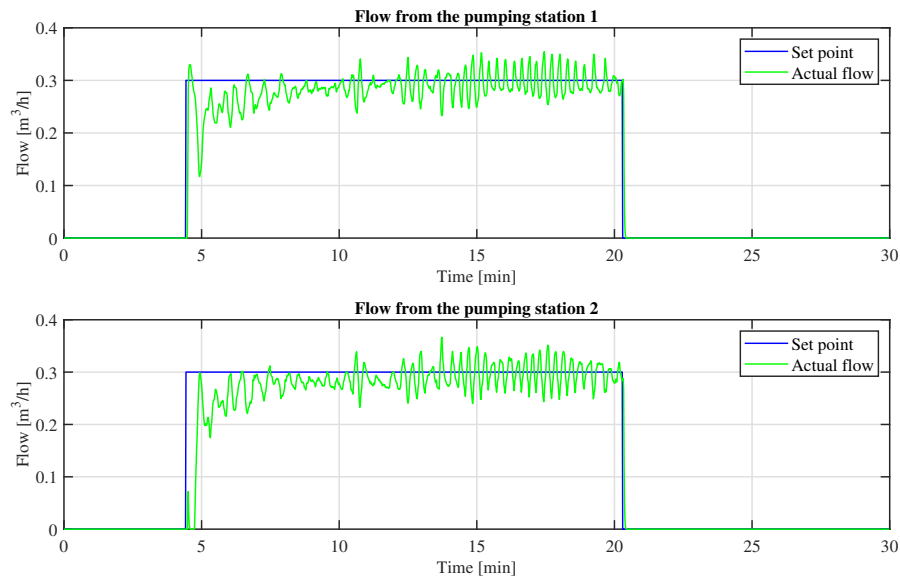


**Figure 3.5:** Local flow control of the pump flows by a PI controller

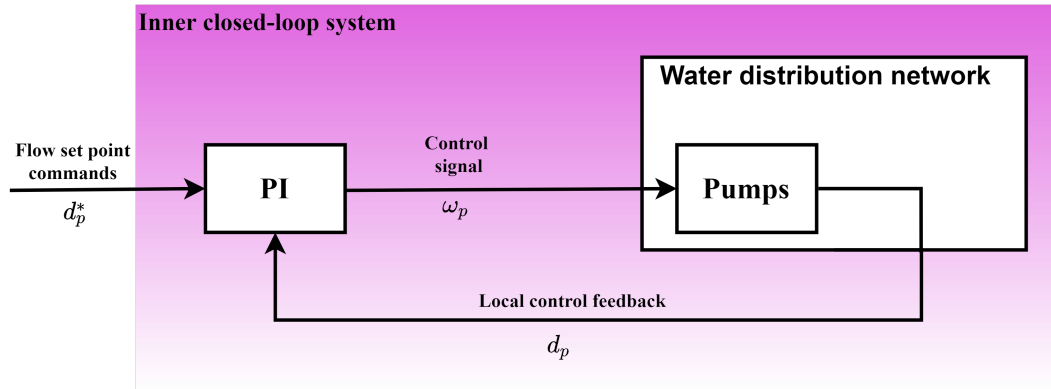


Figure 3.6: Inner closed-loop control structure

To analyse this oscillatory behavior, stability analysis of the inner closed-loop system is presented in this section. Figure 3.6 presents the inner closed-loop control structure. The inner closed-loop system consists of water distribution network with a feedback PI controller. PI controller regulate the speed of the pumps to control the flow delivered by the pumps.

First, Lyapunov stability of the nonlinear closed-loop system, with no delay, is inspected, as it allows to understand the global qualitative behaviour of the system[16]. Then, to analyse stability of the system with delay, the nonlinear water distribution network model is linearised at an equilibrium point and a closed-loop state space model is formed with PI control and output delay. To comment on the stability of the linearised system, eigenvalues of the state transition matrix are analysed.

### 3.4.1 Lyapunov stability analysis

In this section stability of a system is to be understood as stability of equilibrium points in the sense of Lyapunov. Lyapunov stability analysis allows to comment on qualitative behaviour of a system in the vicinity of an equilibrium point or in some cases global qualitative behaviour of the system [16]. To begin with, definition on stability of an equilibrium point and Lyapunov stability theorem is presented. Thereafter stability of the nonlinear closed loop system, with the water distribution network model given by eq. (2.89), is analysed.

#### Lyapunov stability theory

For a system,

$$\dot{x} = f(x) \quad (3.40)$$

where  $f : D \rightarrow R^n$  is a locally Lipschitz map from a domain  $D \subset R^n$  into  $R^n$ . A point  $\bar{x} \in D$  is an equilibrium point for (3.40) if  $f(\bar{x}) = 0$ . For a system any equilibrium point can be shifted to origin, i.e.  $\bar{x} = 0$ , with a change of variables [16]. Henceforth, without loss of generality, the stability definition and theorems are presented for equilibrium at origin.

The definition for stability of an equilibrium point, as stated in [16], is given by,

**Definition 3.4.1** *The equilibrium point  $x = 0$  of (3.40) is*

- *stable if, for each  $\varepsilon > 0$ , there is  $\delta = \delta(\varepsilon) > 0$  such that*

$$\|x\| < \delta \Rightarrow \|x\| < \varepsilon, \quad \forall t \geq 0 \quad (3.41)$$

- *unstable if it is not stable.*
- *asymptotically stable if it is stable and  $\delta$  can be chosen such that*

$$\|x(0)\| < \delta \Rightarrow \lim_{t \rightarrow \infty} x(t) = 0 \quad (3.42)$$

Now, Lyapunov's stability theorem as stated in [16] is given by,

**Theorem 3.4.1 (Lyapunov's stability theorem)** *Let  $x = 0$  be an equilibrium point for (3.40) and  $D \subset R^n$  be a domain containing  $x = 0$ . Let  $V : D \rightarrow R$  be a continuously differentiable function such that*

$$V(0) = 0 \quad \text{and} \quad V(x) > 0 \quad \text{in} \quad D - \{0\} \quad (3.43)$$

$$\dot{V}(x) \leq 0 \quad \text{in} \quad D \quad (3.44)$$

*Then,  $x = 0$  is stable. Moreover, if*

$$\dot{V}(x) < 0 \quad \text{in} \quad D - \{0\} \quad (3.45)$$

*then  $x = 0$  is asymptotically stable.*

A continuously differentiable function,  $V(x)$ , satisfying eq. (3.43) is said to be a valid Lyapunov function candidate and if it also satisfying (3.44) it is said to be a Lyapunov function[16]. Lyapunov's stability theorem's conditions are only sufficient and not necessary, that is to say failure to find a Lyapunov function does not imply that the equilibrium point is not stable[16].

Also defining definiteness of a function,  $V(x)$  with  $V(0) = 0$ , as stated in [16].

$$V(x) > 0 \quad (\text{for } x \neq 0) \rightarrow \text{positive definite}$$

$$V(x) \geq 0 \quad (\text{for } x \neq 0) \rightarrow \text{positive semi-definite}$$

$$V(x) < 0 \quad (\text{for } x \neq 0) \rightarrow \text{negative definite}$$

$$V(x) \leq 0 \quad (\text{for } x \neq 0) \rightarrow \text{negative semi-definite}$$

Furthermore, global asymptotic stability of a equilibrium point, as stated in [16] is given by,

**Theorem 3.4.2 (Barbashin-Krasovskii theorem)** *Let  $x = 0$  be an equilibrium point for (3.40). Let  $V : \mathbb{R}^n \rightarrow \mathbb{R}$  be a continuously differentiable function such that*

$$V(0) = 0 \quad \text{and} \quad V(x) > 0 \quad \forall x \neq 0 \quad (3.46)$$

$$\|x\| \rightarrow \infty \Rightarrow V(x) \rightarrow \infty \quad (3.47)$$

$$\dot{V}(x) < 0, \quad \forall x \neq 0 \quad (3.48)$$

then  $x = 0$  is globally asymptotically stable.

### Stability analysis of the nonlinear closed-loop system

As mentioned in section 3.1, a local PI control is designed to control the flow from the pumps into the water distribution network. Reference pump flow set-points are provided to the PI control by NMPC and PI control regulates the speed to the pumps to control the flows at the set-points. The equation for the PI can be given as,

$$\dot{\zeta} = -K_i(q_p - q_p^*) \quad (3.49a)$$

$$\omega_p^2 = -K_p(q_p - q_p^*) + \zeta \quad (3.49b)$$

where,

- $\zeta$  is the integral state
- $K_i$  is a positive definite diagonal matrix of integral gain
- $K_p$  is a positive definite diagonal matrix of proportional gain
- $\omega_p$  is a vector of rotational speed of the pumps in the network
- $q_p$  is a vector of flows through the pump edges of the network
- $q_p^*$  is a vector of arbitrary equilibrium flows through the pump edges of the network

Now, flow in the pump edges can be represented as,

$$q_p = Pq \quad (3.50)$$

where,

$P \in \mathbb{R}^{n_p \times m}$  is a matrix to extract  $q_p$  from  $q$  in the form  $[I_p \quad 0]$

Furthermore, substituting  $q$  from eq. (2.61),

$$q_p = PB_n^T q_n \quad (3.51)$$

$$\Rightarrow q_p = Cq_n \quad (3.52)$$

where,

$$C = PB_n^T \quad (3.53)$$

Similarly, the vector for pressure in the pump edges can be extracted from the vector of pressure in all edges, corresponding to pump model(eq. (2.19) as,

$$\alpha_p(q_p, \omega_p) = P\alpha(q, \omega) \quad (3.54)$$

From the pump model, eq. (2.19), the pressure from the pumps in vector form can be given as,

$$\alpha_p(q_p, \omega_p) = -A_{h2}|q_p| \circ q_p + A_{h0}\omega_p^2 \quad (3.55)$$

where,

$|q_p| \circ q_p$  represents Hadamard product or element wise multiplication of vectors

$A_{h2} \in \mathbb{R}^{n_p \times n_p}$  is a positive definite diagonal matrix with pump constant

$A_{h0} \in \mathbb{R}^{n_p \times n_p}$  is a positive definite diagonal matrix with pump constant

The dynamics of the tank is extremely slow compared to the flow dynamics in the network, that is to say during a small period of time where the flows would have changed the tank pressure would be near constant. Therefore, in the stability analysis only the flow dynamics have been considered and the tank pressure is assumed to be constant. The dynamic model for the flows in the network is given by eq. (2.89a), can also be presented in terms of  $q_n$  as,

$$B_n \mathcal{J} B_n^T \dot{q}_n = -B_n(\lambda(B_n^T q_n) + \mu(B_n^T q_n, OD) - \alpha(B_n^T q_n, \omega)) + \mathcal{N}(\bar{z} - \mathbb{1}z_0) + \mathcal{I}(p_\tau - \mathbb{1}p_0) \quad (3.56)$$

Furthermore, for simplification consumer valve's opening degrees are also assumed to be constant.

$$B_n \mathcal{J} B_n^T \dot{q}_n = -B_n(\lambda(B_n^T q_n) + \mu(B_n^T q_n) - \alpha(B_n^T q_n, \omega)) + \mathcal{N}(\bar{z} - \mathbb{1}z_0) + \mathcal{I}(p_\tau - \mathbb{1}p_0) \quad (3.57)$$

Equation (3.57) can also be written as,

$$\mathcal{J}_n \dot{q}_n = -f(q_n) + B_n \alpha(q_n, \omega) + \mathcal{N}(\bar{z} - \mathbb{1}z_0) + \mathcal{I}(p_\tau - \mathbb{1}p_0) \quad (3.58)$$

where,

$$\mathcal{J}_n = B_n \mathcal{J} B_n^T \quad (3.59)$$

$$f(q_n) = B_n (\lambda(B_n^T q_n) + \mu(B_n^T q_n)) \quad (3.60)$$

Furthermore, using the extraction matrix  $P$   $\alpha(\cdot)$  can be represented in terms of  $\alpha_p(\cdot)$ , eq. (3.54).

$$\mathcal{J}_n \dot{q}_n = -f(q_n) + B_n P^T \alpha_p(q_p, \omega_p) + \mathcal{N}(\bar{z} - \mathbb{1}z_0) + \mathcal{I}(p_\tau - \mathbb{1}p_0) \quad (3.61)$$

Using eq. (3.52),  $q_p$  can be represented in terms of  $q_n$ ,

$$\mathcal{J}_n \dot{q}_n = -f(q_n) + B_n P^T \alpha_p(Cq_n, \omega_p) + \mathcal{N}(\bar{z} - \mathbb{1}z_0) + \mathcal{I}(p_\tau - \mathbb{1}p_0) \quad (3.62)$$

$$\Rightarrow \mathcal{J}_n \dot{q}_n = -f(q_n) + B_n P^T \alpha_p(q_n, \omega_p) + \mathcal{N}(\bar{z} - \mathbb{1}z_0) + \mathcal{I}(p_\tau - \mathbb{1}p_0) \quad (3.63)$$

Now, the closed-loop system model of the water distribution network (eq. (3.63)) with the PI control (eq. (3.49)) can be given as,

$$\mathcal{J}_n \dot{q}_n = -f(q_n) + B_n P^T \alpha_p(q_n, -K_p(q_p - q_p^*) + \zeta) + \mathcal{N}(\bar{z} - \mathbb{1}z_0) + \mathcal{I}(p_\tau - \mathbb{1}p_0) \quad (3.64a)$$

$$\Rightarrow \mathcal{J}_n \dot{q}_n = -f(q_n) + B_n P^T \alpha_p(q_n, K_p, \zeta) + \mathcal{N}(\bar{z} - \mathbb{1}z_0) + \mathcal{I}(p_\tau - \mathbb{1}p_0) \quad (3.64b)$$

$$\dot{\zeta} = -K_i(q_p - q_p^*) \quad (3.64c)$$

Furthermore, using eq. (3.52), eq. (3.64) can be written as,

$$\mathcal{J}_n \dot{q}_n = -f(q_n) + g(q_n, K_p, \zeta) + \mathcal{N}(\bar{z} - \mathbb{1}z_0) + \mathcal{I}(p_\tau - \mathbb{1}p_0) \quad (3.65a)$$

$$\dot{\zeta} = -K_i C(q_n - q_n^*) \quad (3.65b)$$

where,

$$g(q_n, K_p, \zeta) = B_n P^T \alpha_p(q_n, K_p, \zeta) \quad (3.66)$$

The objective is to analyse closed loop system stability at an arbitrary equilibrium point but the Lyapunov's stability theorem 3.4.1 is only defined for equilibrium point at origin. The equilibrium point of the original system can be shifted to origin by change of variables and transforming the original system to an incremental system.

Consider the equilibrium point  $q_n^*$ , and at the equilibrium point,

$$\dot{q}_n = 0 \quad (3.67)$$

$$\dot{\zeta} = 0 \quad (3.68)$$

$$q_n = q_n^* \quad (3.69)$$

Therefore, eq. (3.65a) at equilibrium point is given as,

$$0 = -f(q_n^*) + g(q_n^*, K_p, \zeta^*) + \mathcal{N}(\bar{z} - \mathbb{1}z_0) + \mathcal{I}(p_\tau - \mathbb{1}p_0) \quad (3.70)$$

With the change of variables, the states and the function for incremental model can be defined as,

$$\begin{aligned} \tilde{q}_n &= q_n - q_n^* \\ \Rightarrow q_n &= \tilde{q}_n + q_n^* \end{aligned} \quad (3.71)$$

$$\begin{aligned} \tilde{\zeta} &= \zeta - \zeta^* \\ \Rightarrow \zeta &= \tilde{\zeta} + \zeta^* \end{aligned} \quad (3.72)$$

$$\begin{aligned} \tilde{f}(\tilde{q}_n) &= f(q_n) - f(q_n^*) \\ \Rightarrow f(q_n) &= \tilde{f}(\tilde{q}_n) + f(q_n^*) \end{aligned} \quad (3.73)$$

$$\begin{aligned} \tilde{g}(\tilde{q}_n, K_p, \tilde{\zeta}) &= g(q_n, K_p, \zeta) - g(q_n^*, K_p, \zeta^*) \\ \Rightarrow g(q_n, K_p, \zeta) &= \tilde{g}(\tilde{q}_n, K_p, \tilde{\zeta}) + g(q_n^*, K_p, \zeta^*) \end{aligned} \quad (3.74)$$

Substituting from equations (3.71),(3.72),(3.73) and (3.74) into the closed-loop system eq. (3.65).

$$\mathcal{J}_n \dot{\tilde{q}}_n = -\tilde{f}(\tilde{q}_n) - f(q_n^*) + \tilde{g}(\tilde{q}_n, K_p, \tilde{\zeta}) + g(q_n^*, K_p, \zeta^*) + \mathcal{N}(\bar{z} - \mathbb{1}z_0) + \mathcal{I}(p_\tau - \mathbb{1}p_0) \quad (3.75a)$$

$$\dot{\tilde{\zeta}} = -K_i C \tilde{q}_n \quad (3.75b)$$

Using the condition that at equilibrium point eq. (3.70) is zero, eq. (3.75) is reduced to,

$$\mathcal{J}_n \dot{\tilde{q}}_n = -\tilde{f}(\tilde{q}_n) + \tilde{g}(\tilde{q}_n, K_p, \tilde{\zeta}) \quad (3.76a)$$

$$\dot{\tilde{\zeta}} = -K_i C \tilde{q}_n \quad (3.76b)$$

For the incremental system the equilibrium point would always be origin, irrespective of the desired equilibrium of the original system. Now for the incremental system candidate Lyapunov function is proposed in eq. (3.77), similar to Lyapunov function proposed for a closed hydraulic network in [26].

$$V_{wn}(\tilde{q}_n, \tilde{\zeta}) = \frac{1}{2} \tilde{q}_n^T \mathcal{J}_n \tilde{q}_n + \frac{1}{2} \tilde{\zeta}^T A_{h0}^T K_i^{-1} \tilde{\zeta} \quad (3.77)$$

The proposed Lyapunov function is zero at origin and positive definite otherwise due to it's quadratic form for both the terms. Therefore condition (3.43) is satisfied and  $V_{wn}(\tilde{q}_n, \tilde{\zeta})$  is a valid Lyapunov function candidate.

$$V_{wn}(0, 0) = 0 \quad (3.78a)$$

$$V_{wn}(\tilde{q}_n, \tilde{\zeta}) = \frac{1}{2} \tilde{q}_n^T \mathcal{J}_n \tilde{q}_n + \frac{1}{2} \tilde{\zeta}^T A_{h0}^T K_i^{-1} \tilde{\zeta} > 0 \quad \forall (\tilde{q}_n, \tilde{\zeta}) \neq 0 \quad (3.78b)$$

Calculating the time derivative of the Lyapunov function candidate (3.77),

$$\dot{V}_{wn}(\tilde{q}_n, \tilde{\zeta}) = \tilde{q}_n^T \mathcal{J}_n \dot{\tilde{q}}_n + \tilde{\zeta}^T A_{h0}^T K_i^{-1} \dot{\tilde{\zeta}} \quad (3.79)$$

Substituting system dynamics from eq. (3.76),

$$\dot{V}_{wn}(\tilde{q}_n, \tilde{\zeta}) = \tilde{q}_n^T (-\tilde{f}(\tilde{q}_n) + \tilde{g}(\tilde{q}_n, K_p, \tilde{\zeta})) + \tilde{\zeta}^T A_{h0}^T K_i^{-1} (-K_i C \tilde{q}_n) \quad (3.80)$$

$$\Rightarrow \dot{V}_{wn}(\tilde{q}_n, \tilde{\zeta}) = -\underbrace{\tilde{q}_n^T \tilde{f}(\tilde{q}_n)}_{\#1} + \underbrace{\tilde{q}_n^T \tilde{g}(\tilde{q}_n, K_p, \tilde{\zeta})}_{\#2} - \underbrace{\tilde{\zeta}^T A_{h0}^T C \tilde{q}_n}_{\#3} \quad (3.81)$$

For the ease of understanding of the readers, each term in (3.81) is simplified separately. Term (#1), (#2) and (#3) are denoted by  $\dot{V}_{wn}^{(\#1)}$ ,  $\dot{V}_{wn}^{(\#2)}$  and  $\dot{V}_{wn}^{(\#3)}$  respectively. The final comments on the definiteness of  $\dot{V}_{wn}(\tilde{q}_n, \tilde{\zeta})$  is provided at the end.

Foremost, term (#2),  $\dot{V}_{wn}^{(\#2)}$  is simplified.

$$\dot{V}_{wn}^{(\#2)} = \tilde{q}_n^T \tilde{g}(\tilde{q}_n, K_p, \tilde{\zeta}) \quad (3.82)$$

Substituting from eq. (3.74) and expanding  $\tilde{g}(\cdot)$ ,

$$\dot{V}_{wn}^{(\#2)} = \tilde{q}_n^T (g(q_n, K_p, \zeta) - g(q_n^*, K_p, \zeta^*)) \quad (3.83)$$

Substituting from eq. (3.66)

$$\dot{V}_{wn}^{(\#2)} = (q_n - q_n^*)^T B_n P^T (\alpha_p(q_p, K_p, \zeta) - \alpha_p(q_p^*, K_p, \zeta^*)) \quad (3.84)$$

Substituting the pump model, (3.55), for  $\alpha_p(\cdot)$  and also using (3.51), (3.84) can be given as,

$$\begin{aligned} \dot{V}_{wn}^{(\#2)} = (q_p - q_p^*)^T & (-A_{h2}|q_p| \circ q_p + A_{h0}(-K_p(q_p - q_p^*) + \zeta) \\ & + A_{h2}|q_p^*| \circ q_p^* - A_{h0}(-K_p(q_p^* - q_p^*) + \zeta^*)) \end{aligned} \quad (3.85)$$

$$\begin{aligned} \Rightarrow \dot{V}_{wn}^{(\#2)} = (q_p - q_p^*)^T & (-A_{h2}|q_p| \circ q_p + A_{h2}|q_p^*| \circ q_p^*) \\ & + (q_p - q_p^*)^T (-A_{h0}K_p(q_p - q_p^*)) \\ & + (q_p - q_p^*)^T (A_{h0}\zeta - A_{h0}\zeta^*) \end{aligned} \quad (3.86)$$

$$\begin{aligned} \Rightarrow \dot{V}_{wn}^{(\#2)} = & - \underbrace{(q_p - q_p^*)^T A_{h2}(|q_p| \circ q_p - |q_p^*| \circ q_p^*)}_{\#a} \\ & - \underbrace{(q_p - q_p^*)^T A_{h0}K_p(q_p - q_p^*)}_{\#b} \\ & + \underbrace{(q_p - q_p^*)^T A_{h0}(\zeta - \zeta^*)}_{\#c} \end{aligned} \quad (3.87)$$

Now, simplifying term (#3),  $\dot{V}_{wn}^{(\#3)}$  from (3.81).

$$\dot{V}_{wn}^{(\#3)} = \tilde{\zeta}^T A_{h0}^T C \tilde{q}_n \quad (3.88)$$

Expanding  $\tilde{\zeta}$  and  $\tilde{q}_n$  using eq. (3.71) and (3.72) respectively.

$$\dot{V}_{wn}^{(\#3)} = (\zeta - \zeta^*)^T A_{h0}^T C (q_n - q_n^*) \quad (3.89)$$

Using eq. (3.52),  $q_p$  is extracted from  $q_n$ .

$$\dot{V}_{wn}^{(\#3)} = (\zeta - \zeta^*)^T A_{h0}^T (q_p - q_p^*) \quad (3.90)$$

Substituting  $\dot{V}_{wn}^{(\#2)}$  from (3.87) and  $\dot{V}_{wn}^{(\#3)}$  from (3.90) back into eq. (3.81).

$$\begin{aligned}
\dot{V}_{wn}(\tilde{q}_n, \tilde{\zeta}) = & -\tilde{q}_n^T \tilde{f}(\tilde{q}_n) \\
& - (q_p - q_p^*)^T A_{h2}(|q_p| \circ q_p - |q_p^*| \circ q_p^*) \\
& - (q_p - q_p^*)^T A_{h0} K_p (q_p - q_p^*) \\
& + (q_p - q_p^*)^T A_{h0} (\zeta - \zeta^*) \\
& - (\zeta - \zeta^*)^T A_{h0}^T (q_p - q_p^*) \quad (3.91)
\end{aligned}$$

$$\begin{aligned}
\Rightarrow \dot{V}_{wn}(\tilde{q}_n, \tilde{\zeta}) = & -\tilde{q}_n^T \tilde{f}(\tilde{q}_n) \\
& - (q_p - q_p^*)^T A_{h2}(|q_p| \circ q_p - |q_p^*| \circ q_p^*) \\
& - (q_p - q_p^*)^T A_{h0} K_p (q_p - q_p^*) \quad (3.92)
\end{aligned}$$

Equation (3.92) can also be written as,

$$\dot{V}_{wn}(\tilde{q}_n, \tilde{\zeta}) = -\underbrace{\tilde{q}_n^T \tilde{f}(\tilde{q}_n)}_{\#x} - \underbrace{(q_p - q_p^*)^T A_{h2}(h(q_p) - h(q_p^*))}_{\#y} - \underbrace{(q_p - q_p^*)^T A_{h0} K_p (q_p - q_p^*)}_{\#z} \quad (3.93)$$

where

$$h(q_p) = |q_p| \circ q_p \quad (3.94)$$

Equation (3.93) presents time derivative of the Lyapunov function candidate, eq. (3.81), in a simplified form.

For term (#x),  $\tilde{f}(\tilde{q}_n)$  can be expanded using eq. (3.73).

$$\tilde{q}_n^T \tilde{f}(\tilde{q}_n) = \tilde{q}_n^T (f(q_n) - f(q_n^*)) \quad (3.95)$$

Furthermore, substituting  $f(\cdot)$  from eq. (3.60),

$$\tilde{q}_n^T \tilde{f}(\tilde{q}_n) = \tilde{q}_n^T B_n (\lambda(B_n^T q_n) + \mu(B_n^T q_n) - \lambda(B_n^T q_n^*) - \mu(B_n^T q_n^*)) \quad (3.96)$$

Substituting  $\tilde{q}_n$  from eq. (3.71)

$$\tilde{q}_n^T \tilde{f}(\tilde{q}_n) = (q_n - q_n^*)^T B_n (\lambda(B_n^T q_n) + \mu(B_n^T q_n) - \lambda(B_n^T q_n^*) - \mu(B_n^T q_n^*)) \quad (3.97)$$

Using relation (2.61), (3.97) can be written as,

$$\tilde{q}_n^T \tilde{f}(\tilde{q}_n) = (q - q^*)^T (\lambda(q) + \mu(q) - \lambda(q^*) - \mu(q^*)) \quad (3.98)$$

$$\Rightarrow \quad \tilde{q}_n^T \tilde{f}(\tilde{q}_n) = (q - q^*)^T (\lambda(q) - \lambda(q^*)) + (q - q^*)^T (\mu(q) - \mu(q^*)) \quad (3.99)$$

$\lambda(\cdot)$  and  $\mu(\cdot)$  are vector form of  $\lambda_k(\cdot)$ , (2.21b), and  $\mu_k(\cdot)$ , (2.21c), which are strictly increasing functions and also zero at zero argument. Therefore,  $\tilde{q}_n^T \tilde{f}(\tilde{q}_n)$  is positive definite  $\forall \tilde{q}_n \neq 0$ .

In term (#y),  $A_{h2}$  is a positive definite diagonal matrix and function  $h(\cdot)$ , (3.94), is a strictly increasing function by definition. Therefore, term (#y) is positive definite  $\forall \tilde{q}_p \neq 0$  and with the relation (3.52) positive semi-definite  $\forall \tilde{q}_n \neq 0$ .

In the term (#z),  $A_{h0}$  and  $K_p$  are positive definite diagonal matrices, therefore because of it's quadratic form term it is positive definite  $\forall \tilde{q}_p \neq 0$  and again with the relation (3.52) positive semi-definite  $\forall \tilde{q}_n \neq 0$ .

To summarize term (#x) is positive definite, (#y) and (#z) are positive semi-definite  $\forall \tilde{q}_n \neq 0$ . Consequently,  $\dot{V}_{wn}(\tilde{q}_n, \tilde{\zeta})$  is negative definite  $\forall \tilde{q}_n \neq 0$ . But,  $\dot{V}_{wn}(\tilde{q}_n, \tilde{\zeta})$  is only negative semi-definite  $\forall (\tilde{q}_n, \tilde{\zeta}) \neq 0$ , as from eq. (3.93),  $\dot{V}_{wn}(\tilde{q}_n, \tilde{\zeta})$  is not a function of  $\tilde{\zeta}$ . Therefore, only (3.43) and (3.44) conditions are satisfied and, from this it can be concluded that  $V_{wn}(\tilde{q}_n, \tilde{\zeta})$  is a Lyapunov function for the closed-loop incremental system and the equilibrium point is just stable.

### LaSalle-Barbashin-Krasovskii theorem

As stated in [16], LaSalle-Barbashin-Krasovskii theorem can be given as,

**Theorem 3.4.3 (LaSalle-Barbashin-Krasovskii theorem)** *Let  $x = 0$  be an equilibrium point for (3.40). Let  $V : D \rightarrow R$  be a continuously differentiable positive definite function on a domain  $D$  containing the origin  $x = 0$ , such that  $\dot{V}(x) \leq 0$  in  $D$ . Let  $S = \{x \in D | \dot{V}(x) = 0\}$  and suppose that no solution can stay identically in  $S$ , other than the trivial solution  $x(t) \equiv 0$ . Then, the origin is asymptotically stable. Furthermore, if  $V$  is also radially unbounded, then the origin is globally asymptotically stable.*

From Theorem 3.4.3, if it could be proven that no solution trajectory can stay identically at points where  $\dot{V}_{wn}(\tilde{q}_n, \tilde{\zeta}) = 0$ , except  $(\tilde{q} = 0, \tilde{\zeta} = 0)$ , then the equilibrium point is stable.

The incremental closed loop system, eq. (3.76), again stated here,

$$\mathcal{J}_n \dot{\tilde{q}}_n = -\tilde{f}(\tilde{q}_n) + \tilde{g}(\tilde{q}_n, K_p, \tilde{\zeta}) \quad (3.100a)$$

$$\dot{\tilde{\zeta}} = -K_i C \tilde{q}_n \quad (3.100b)$$

Expanding  $\tilde{f}$  and  $\tilde{g}$  using eq. (3.73) and (3.74).

$$\mathcal{J}_n \dot{\tilde{q}}_n = -f(q_n) + f(q_n^*) + g(q_n, K_p, \zeta) - g(q_n^*, K_p, \zeta^*) \quad (3.101a)$$

$$\dot{\tilde{\zeta}} = -K_i C \tilde{q}_n \quad (3.101b)$$

Expanding  $g(\cdot)$  using eq. (2.78) and then expanding  $\alpha(\cdot)$  using eq. (3.55).

$$\begin{aligned} \mathcal{J}_n \dot{\tilde{q}}_n = & -f(q_n) + f(q_n^*) + B_n P^T (-A_{h2} |q_p| \circ q_p + A_{h0} (-K_p (q_p - q_p^*) + \zeta) \\ & + A_{h2} |q_p^*| \circ q_p^* - A_{h0} (-K_p (q_p^* - q_p^*) + \zeta^*)) \end{aligned} \quad (3.102a)$$

$$\dot{\tilde{\zeta}} = -K_i C \tilde{q}_n \quad (3.102b)$$

Now for  $\tilde{q} = 0$ ,  $q_n = q_n^*$ , also due to (3.52)  $q_p = q_p^*$ . With this relation and eq. (3.53), eq. (3.102) is reduced to,

$$0 = C^T A_{h0} (\zeta - \zeta^*) \quad (3.103a)$$

$$\dot{\tilde{\zeta}} = 0 \quad (3.103b)$$

$A_{h0}$  is a positive definite diagonal matrix and  $C$  is a extraction matrix, implying  $\zeta = \zeta^*$ , ( $\tilde{\zeta} = 0$ ) when  $\tilde{q} = 0$ . In conclusion  $\tilde{q} = 0$  implies  $\tilde{\zeta} = 0$  and  $\dot{\tilde{\zeta}} = 0$ , therefore from theorem 3.4.3 it can be said that the equilibrium point ( $\tilde{q} = 0, \tilde{\zeta} = 0$ ) is asymptotically stable. Also, Lyapunov function  $V_{wn}(\tilde{q}_n, \tilde{\zeta})$  is radially unbounded therefore it can be concluded that the equilibrium point ( $\tilde{q} = 0, \tilde{\zeta} = 0$ ) is globally asymptotically stable. For the system it implies that for any positive definite  $K_p$  and  $K_i$  the water network model can be stabilized at an arbitrary equilibrium point by the PI controller.

### 3.4.2 Stability analysis on the linearized model with delay and PI control

Section 3.4.1 concludes that the inner closed-loop system is globally asymptotically stable at an arbitrary equilibrium point but the results from the laboratory test, presented in figure 3.5, contradicts this. This could be due to the fact that the laboratory setup has an output delay, which was not been taken into account in the Lyapunov stability analysis.

Figure 3.7 presents the delay in the pumps in the laboratory setup. A step input of 70% pump speed is given to the pump at 5 sec time instance and in the figure it can be observed that the flow only starts to rise at 9 sec time instance, signifying a output delay of 4 sec in the water network.

To analyse stability of the closed loop network with the output delay the water network model is linearised at an equilibrium point. And as [16] points out, qualitative behaviour of a nonlinear system near an equilibrium point can be deduced from it's linearised system at that point. Again for simplification in the stability analysis of the linearised system, the consumer valve's opening degree is assumed to be constant. The nonlinear dynamic model for the water network is given by eq. (2.89), again presented here.

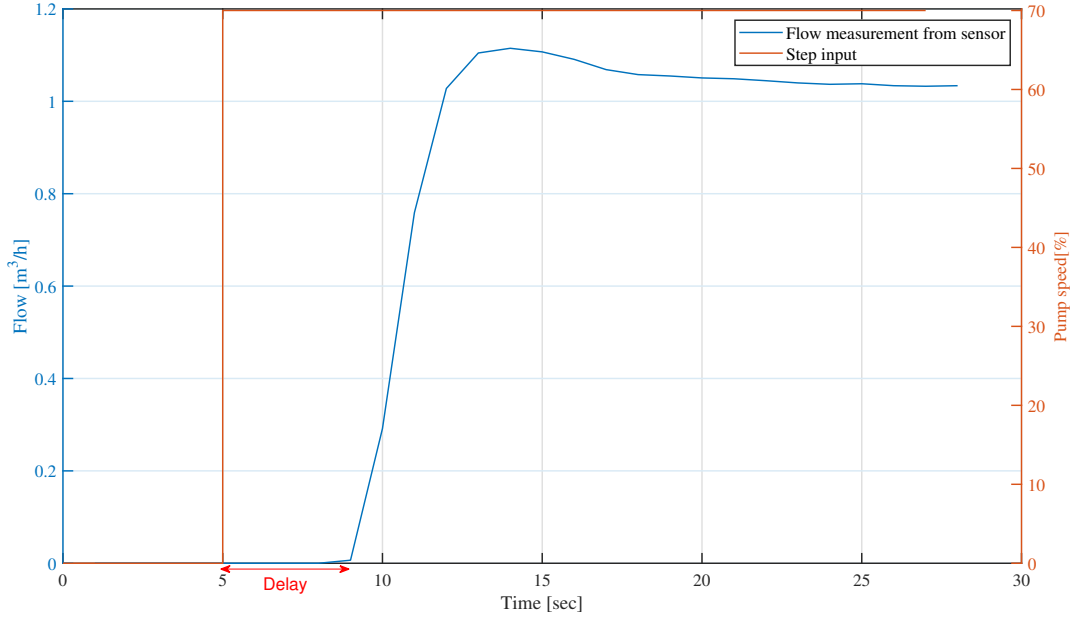


Figure 3.7: Delay in the pumps in the laboratory setup

$$B_n \mathcal{J} B_n^T \dot{q}_n = -B_n (\lambda(q_C, \bar{d}_f, \bar{d}_\tau) + \mu(q_C, \bar{d}_f, \bar{d}_\tau, OD) - \alpha(q_C, \bar{d}_f, \bar{d}_\tau, \omega)) + \mathcal{N}(\bar{z} - \mathbb{1}z_0) + \mathcal{I}(p_\tau - \mathbb{1}p_0) \quad (3.104a)$$

$$\dot{p}_\tau = -\mathcal{T}d_\tau \quad (3.104b)$$

$\omega$  can be represented in terms of  $\omega_p$  and eq. (3.104) can also be written as,

$$\dot{q}_n = (B_n \mathcal{J} B_n^T)^{-1} (-B_n (\lambda(q_n) + \mu(q_n) - \alpha(q_n, \omega_p)) + \mathcal{N}(\bar{z} - \mathbb{1}z_0) + \mathcal{I}(p_\tau - \mathbb{1}p_0)) \quad (3.105a)$$

$$\dot{p}_\tau = -\mathcal{T}d_\tau \quad (3.105b)$$

Equation (3.105) can be represented in form,

$$\dot{x} = f_c(x, \omega_p) \quad (3.106)$$

where,

$$x = \begin{bmatrix} q_n \\ p_\tau \end{bmatrix} \quad (3.107)$$

$$f_c = \begin{bmatrix} (B_n \mathcal{J} B_n^T)^{-1} (-B_n (\lambda(q_n) + \mu(q_n) - \alpha(q_n, \omega_p)) + \mathcal{N}(\bar{z} - \mathbb{1}z_0) + \mathcal{I}(p_\tau - \mathbb{1}p_0)) \\ -\mathcal{T}d_\tau \end{bmatrix} \quad (3.108)$$

The states in the model, (3.106), are  $q_n$ ,  $p_\tau$  and the input to the model is  $\omega_p$ . The nonlinear model can be linearised using Taylor series expansion at an equilibrium point,  $(x^*, \omega_p^*)$ ,

$$f_c(x, \omega_p) \approx f_c(x^*, \omega_p^*) + \left. \frac{\partial f_c}{\partial x} \right|_{(x^*, \omega_p^*)} \tilde{x} + \left. \frac{\partial f_c}{\partial \omega_p} \right|_{(x^*, \omega_p^*)} \tilde{\omega}_p \quad (3.109)$$

where,

$$\tilde{x} = x - x^* \quad (3.110a)$$

$$\tilde{\omega}_p = \omega_p - \omega_p^* \quad (3.110b)$$

For the water distribution network presented in section 2.4, an operating point for the input,  $\omega_p$ , is chosen and the equilibrium point for the system is calculated. Linearised model can be represented in a form as,

$$\dot{\tilde{x}} = A_{sys}\tilde{x} + B_{sys}\tilde{\omega}_p \quad (3.111a)$$

$$y = \tilde{q}_p = C_{sys}\tilde{x} \quad (3.111b)$$

where,

$\tilde{q}_p$  is a vector of flows through the pump edges of the network

Equilibrium point calculation and linearised model matrices are presented in appendix B.

A delay in a system in Laplace transform is given as  $e^{-T_d s}$ , which can be approximated using Padé approximant as,

$$e^{-T_d s} = \frac{1 - (T_d s/2)}{1 + (T_d s/2)} \quad (3.112)$$

where,

$T_d$  is the delay time

The transfer function for delay can be represented in state space form as,

$$\dot{x}_d = A_d x_d + B_d u_d \quad (3.113a)$$

$$y_d = \tilde{q}_{p,d} = C_d x_d + D_d u_d \quad (3.113b)$$

where,

$x_d$  is the state of the delay model  
 $u_d$  is the input to the delay model  
 $y_d$  is the output of the delay model  
 $\tilde{q}_{p,d}$  is the delayed pump flow measured by the sensors  
 $A_d, B_d, C_d$  and  $D_d$  are the state space matrices of the delay model

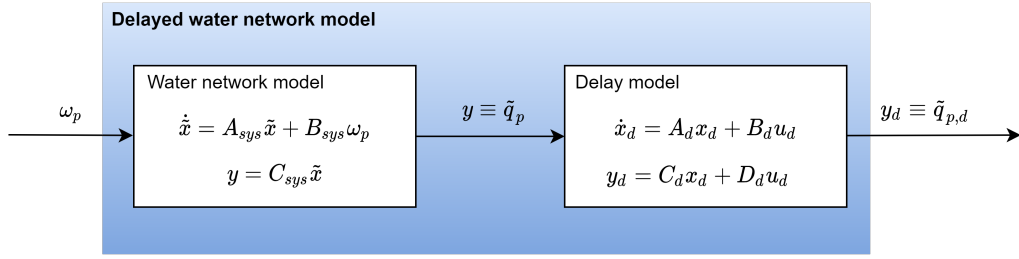


**Figure 3.8:** Complete delayed water distribution network model

Figure 3.8 presents complete delayed water distribution network model. The delayed model consist of water network model,(3.111), to which the input is  $\tilde{\omega}_p$  and the output is  $\tilde{q}_p$ , and the delay model, (3.113), to which the input is  $\tilde{q}_p$  and the output is  $\tilde{q}_{p,d}$ . Equivalent delayed water distribution network model, with input  $\tilde{\omega}_p$  and output  $\tilde{q}_{p,d}$  can be given as,

$$\dot{x}_{cd} = A_{cd}x_{cd} + B_{cd}\tilde{\omega}_p \quad (3.114a)$$

$$y_d = \tilde{q}_{p,d} = C_{cd}x_{cd} \quad (3.114b)$$

where,

$$x_{cd} = \begin{bmatrix} \tilde{x} \\ x_d \end{bmatrix} \quad (3.115a)$$

$$A_{cd} = \begin{bmatrix} A_{sys} & 0 \\ B_d C_{sys} & A_d \end{bmatrix} \quad (3.115b)$$

$$B_{cd} = \begin{bmatrix} B_{sys} \\ 0 \end{bmatrix} \quad (3.115c)$$

$$C_{cd} = [D_d C_{sys} \quad C_d] \quad (3.115d)$$

Again, values of all the system matrices are presented in appendix B. To this delayed linearised system model, (3.114), a feedback PI control is applied. The aim of the PI control is to regulate pump speeds to control pump flows at given set-point. The equation for PI control can be given as,

$$\dot{\zeta} = -K_i(\tilde{q}_{p,d} - \tilde{q}_p^*) \quad (3.116a)$$

$$\tilde{\omega}_p = -K_p(\tilde{q}_{p,d} - \tilde{q}_p^*) + \zeta \quad (3.116b)$$

where,

- $\zeta$  is the integral state
- $K_i$  is a positive definite diagonal matrix of integral gain
- $K_p$  is a positive definite diagonal matrix of proportional gain
- $\tilde{q}_p^*$  is a vector of pump flows set-point

With network model (3.114) and the PI control (3.116), the closed loop system model can be given as,

$$\dot{x}_{cl} = A_{cl}x_{cl} + B_{cl}\tilde{q}_p^* \quad (3.117a)$$

$$y_d = \tilde{q}_{p,d} = C_{cl}x_{cl} \quad (3.117b)$$

where,

$$x_{cl} = \begin{bmatrix} x_{cl} \\ \zeta \end{bmatrix} \quad (3.118a)$$

$$A_{cl} = \begin{bmatrix} A_{cd} - B_{cd}K_pC_{cd} & B_{cd} \\ -K_iC_{cd} & 0 \end{bmatrix} \quad (3.118b)$$

$$B_{cl} = \begin{bmatrix} B_{cd}K_p \\ K_i \end{bmatrix} \quad (3.118c)$$

$$C_{cl} = [C_{cd} \ 0] \quad (3.118d)$$

Qualitative behaviour of this linear closed-loop delayed system model can be determined by analysing the eigenvalues of the state transition matrix  $A_{cl}$ . From the elements of  $A_{cl}$  it can be observed that the eigenvalues, ergo the closed-loop system behaviour is dependent on the delay and the PI gains. Eigenvalues of  $A_{cl}$ , assuming a 4 sec delay and various PI gains is presented below,

- $K_p= 3, K_i= 1.1$

$$eig(A_{cl}) = \begin{bmatrix} -38.1027 \\ -23.8710 \\ -0.1893 + 0.4848j \\ -0.1893 - 0.4848j \\ -0.2176 + 0.2991j \\ -0.2176 - 0.2991j \\ -0.0001 \\ -0.2908 + 0.0236j \\ -0.2908 - 0.0236j \\ -0.3117 + 0.0209j \\ -0.3117 - 0.0209j \end{bmatrix} \quad (3.119)$$

Figure 3.9 presents the local flow control of the pumps by PI control with PI gains  $K_p= 3, K_i= 1.1$  for both the pumps. The oscillations in the flow can be accounted for the imaginary part of the eigenvalues in (3.119).

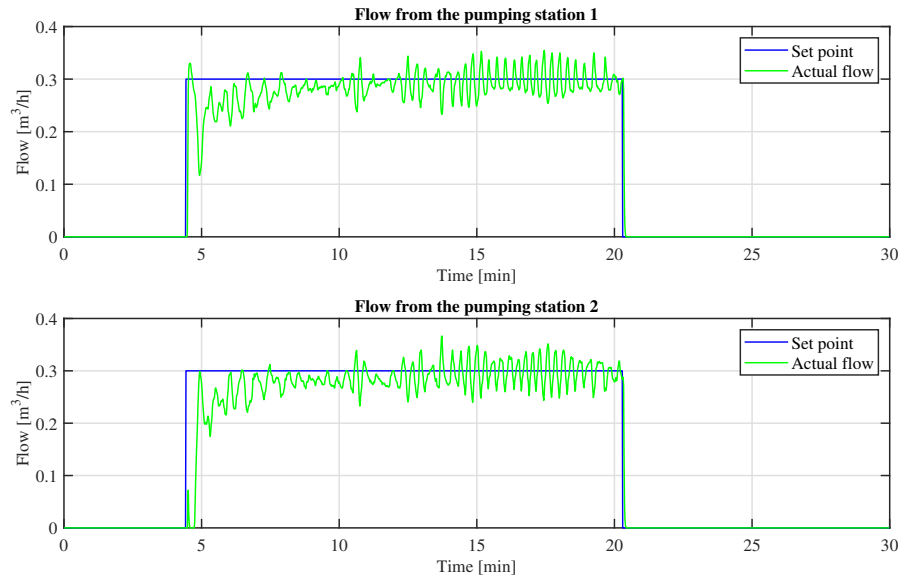


**Figure 3.9:** Local flow control of the pump flows by a PI controller with PI gains  $K_p=3$ ,  $K_i=1.1$

- $K_p=1.7$ ,  $K_i=0.7$

$$\text{eig}(A_{cl}) = \begin{bmatrix} -38.2777 \\ -23.9393 \\ -0.2825 + 0.2869j \\ -0.2825 - 0.2869j \\ -0.0001 \\ -0.2285 + 0.1222j \\ -0.2285 - 0.1222j \\ -0.3158 + 0.0583j \\ -0.3158 - 0.0583j \\ -0.3322 + 0.0303j \\ -0.3322 - 0.0303j \end{bmatrix} \quad (3.120)$$

Figure 3.10 presents the local flow control of the pumps by PI control with PI gains  $K_p=1.7$ ,  $K_i=0.7$  for both the pumps. Comparing the flow behaviour in 3.10 with 3.9, the oscillations are to a smaller extent, this is because the imaginary part of the eigenvalues in (3.120) is smaller. Also, due to small PI gain values the system behaviour is slow as it takes longer time to even reach the set-point, which is also not desirable.

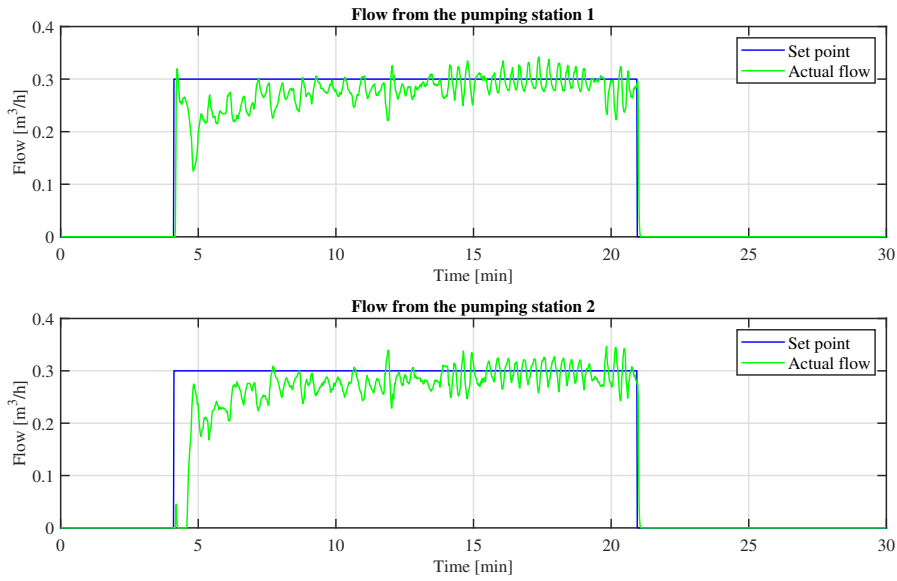


**Figure 3.10:** Local flow control of the pump flows by a PI controller with PI gains  $K_p=1.7$ ,  $K_i=0.7$

- $K_p=1.7$ ,  $K_i=0.7$  with delay of 6 sec

$$\text{eig}(A_{cl}) = \begin{bmatrix} -38.2797 \\ -23.9406 \\ -0.0001 \\ -0.1259 + 0.2462j \\ -0.1259 - 0.2462j \\ -0.1231 + 0.1667j \\ -0.1231 - 0.1667j \\ -0.4753 \\ -0.4345 \\ -0.2665 \\ -0.3073 \end{bmatrix} \quad (3.121)$$

The eigenvalues of the system with an increased delay of 6 sec and PI gains of  $K_p=1.7$ ,  $K_i=0.7$  for both the pumps are given by (3.121). It can be seen that with increased delay the imaginary part in the eigenvalues are larger, and this could result in higher oscillations in the system.

To summarize the stability analysis of the closed-loop system of the water distribution network flow control by a PI controller, it can be said that the system is globally asymptotically stable when the system does not have any delay. The oscillations observed in the laboratory test could be due to output delay in the

laboratory setup. Higher the delay in the system the oscillations are higher. Low PI gains can result in lower oscillations but they slow down the system behaviour resulting in longer time to reach the set-point. With a sampling time of 1 minute for the supervisory control a fast response is required from the inner closed-loop system, therefore for the testing of supervisory control in the laboratory setup,  $K_p=3$ ,  $K_i=1.1$ , PI gains were selected. Supervisory control test results in the laboratory setup are presented in chapter 6.

## Chapter 4

# Consumer demand prediction using Kalman filter

In this chapter a predictor for consumer demand prediction will be presented. Foremost a Fourier series model of the periodic consumer demand has been developed. Then, the developed model along with tank pressure measurements are used in a Kalman filter for estimation of the consumer demands. Furthermore, a Kalman filter based predictor is developed for prediction of future consumer nodal demands to be used along with NMPC for the control of water distribution network.

### 4.1 Fourier analysis

Any arbitrary periodic signal can be modelled as a weighted combination of sines and cosines using Fourier series as presented below[7],

$$y_F(t) = a_0 + \sum_{n=1}^N \left( a_n \cos(n\omega_0 t) + b_n \sin(n\omega_0 t) \right) \quad (4.1)$$

where,

$$\omega_0 = 2\pi f_0 \quad (4.2)$$

- $f_0$  is the fundamental frequency of the periodic signal
- $a_n$  is weight of the cosine components of the  $n^{th}$  harmonic in the periodic signal
- $b_n$  is weight of the sine components of the  $n^{th}$  harmonic in the periodic signal

Instead of representing the Fourier series in terms of fundamental frequency and it's harmonics, it can also be represented with only the  $L$  dominant frequencies

and the other frequencies can be disregarded. With this form number of terms to be used to represent the Fourier series reduces. Taking into account only the  $L$  dominant frequencies of the signal, the Fourier series in eq. (4.1) can also be presented as,

$$y_F(t) = a_0 + \sum_{l=1}^L \left( a_l \cos(\omega_l t) + b_l \sin(\omega_l t) \right) \quad (4.3)$$

The discretized Fourier series can now be presented as,

$$y_F^k = a_0 + \sum_{l=1}^L \left( a_l \cos(\omega_l k T_s) + b_l \sin(\omega_l k T_s) \right) \quad \text{for } k = 1, \dots, K \quad (4.4)$$

where,

- $K$  is the total number of data samples
- $y_F^k$  is the signal value at  $k^{\text{th}}$  instance
- $T_s$  is the sampling time

#### 4.1.1 State space representation of Fourier series model

The Fourier series model can also be represented in discrete time state space form of

$$x^{k+1} = \phi x^k + \Gamma u^k \quad (4.5a)$$

$$y_F^k = C x^k + D u^k \quad (4.5b)$$

where,

- $x^k$  is the state vector
- $u^k$  is the input vector
- $\phi$  is the state transition matrix
- $\Gamma$  is the input matrix
- $C$  is the output matrix
- $D$  is the feed-through matrix

A representation in a discrete time state space form allows predicting the values of the next state and output, based on knowledge of current state and input values assuming a perfect model. Initially, considering there is only one dominant frequency.

$$\begin{aligned} y_F^k &= a_0 + a_1 \cos(\omega_1 k T_s) + b_1 \sin(\omega_1 k T_s) \\ &= x_1^k + x_2^k \end{aligned} \quad (4.6)$$

with

$$x^k = \begin{bmatrix} a_0 \\ a_1 \cos(\omega_1 k T_s) + b_1 \sin(\omega_1 k T_s) \\ -a_1 \sin(\omega_1 k T_s) + b_1 \cos(\omega_1 k T_s) \end{bmatrix} \quad (4.7)$$

where,

$T_s$  is the sampling time

Now, the state value at time instance  $(k + 1)$  can be given in form of state value at time instance  $k$  as,

$$\begin{aligned} x_1^{k+1} &= a_0 \\ &= x_1^k \end{aligned} \quad (4.8)$$

$$\begin{aligned} x_2^{k+1} &= a_1 \cos(\omega_1 (k + 1) T_s) + b_1 \sin(\omega_1 (k + 1) T_s) \\ &= a_1 \cos(\omega_1 k T_s + \omega_1 T_s) + b_1 \sin(\omega_1 k T_s + \omega_1 T_s) \\ &= \cos(\omega_1 T_s) (a_1 \cos(\omega_1 k T_s) + b_1 \sin(\omega_1 k T_s)) + \sin(\omega_1 T_s) (-a_1 \sin(\omega_1 k T_s) + b_1 \cos(\omega_1 k T_s)) \\ &= \cos(\omega_1 T_s) x_2^k + \sin(\omega_1 T_s) x_3^k \end{aligned} \quad (4.9)$$

Similarly,

$$x_3^{k+1} = -\sin(\omega_1 T_s) x_2^k + \cos(\omega_1 T_s) x_3^k \quad (4.10)$$

With equations (4.6), (4.8), (4.9) and (4.10) state space matrices can be given as,

$$\phi = \begin{bmatrix} 1 & 0 & 0 \\ 0 & \cos(\omega_1 T_s) & \sin(\omega_1 T_s) \\ 0 & -\sin(\omega_1 T_s) & \cos(\omega_1 T_s) \end{bmatrix} \quad (4.11)$$

$$\Gamma = 0 \quad (4.12)$$

$$C = [1 \quad 1 \quad 0] \quad (4.13)$$

$$D = 0 \quad (4.14)$$

Complete state space model can be presented as,

$$x^{k+1} = \begin{bmatrix} 1 & 0 & 0 \\ 0 & \cos(\omega_1 T_s) & \sin(\omega_1 T_s) \\ 0 & -\sin(\omega_1 T_s) & \cos(\omega_1 T_s) \end{bmatrix} x^k \quad (4.15a)$$

$$y_F^k = [1 \ 1 \ 0] x^k \quad (4.15b)$$

Now considering  $L$  dominant frequencies in the signal, the output equation can be given by eq. (4.4) and the state vector can be given as,

$$x^k = \begin{bmatrix} a_0 \\ a_1 \cos(\omega_1 k T_s) + b_1 \sin(\omega_1 k T_s) \\ -a_1 \sin(\omega_1 k T_s) + b_1 \cos(\omega_1 k T_s) \\ a_2 \cos(\omega_2 k T_s) + b_2 \sin(\omega_2 k T_s) \\ -a_2 \sin(\omega_2 k T_s) + b_2 \cos(\omega_2 k T_s) \\ \vdots \\ a_L \cos(\omega_L k T_s) + b_L \sin(\omega_L k T_s) \\ -a_L \sin(\omega_L k T_s) + b_L \cos(\omega_L k T_s) \end{bmatrix} \quad (4.16)$$

With equations (4.4) and (4.16), the state space model matrices can now be given as,

$$\phi = \begin{bmatrix} 1 & 0 & 0 & \cdots & 0 \\ 0 & \phi_1 & 0 & \cdots & 0 \\ 0 & 0 & \phi_2 & \cdots & 0 \\ \vdots & \vdots & \vdots & \ddots & \vdots \\ 0 & 0 & 0 & \cdots & \phi_L \end{bmatrix} \quad (4.17)$$

$$\phi_i = \begin{bmatrix} \cos(\omega_i T_s) & \sin(\omega_i T_s) \\ -\sin(\omega_i T_s) & \cos(\omega_i T_s) \end{bmatrix} \quad (4.18)$$

$$\Gamma = 0 \quad (4.19)$$

$$C = [1 \ 1 \ 0 \ 1 \ 0 \ \cdots \ 1 \ 0]_{1 \times (2L+1)} \quad (4.20)$$

$$D = 0 \quad (4.21)$$

Complete state space model for the periodic signal considering  $L$  dominant frequencies can be given as,

$$x^{k+1} = \begin{bmatrix} 1 & 0 & 0 & \cdots & 0 \\ 0 & \phi_1 & 0 & \cdots & 0 \\ 0 & 0 & \phi_2 & \cdots & 0 \\ \vdots & \vdots & \vdots & \ddots & \vdots \\ 0 & 0 & 0 & \cdots & \phi_L \end{bmatrix} x^k \quad (4.22a)$$

$$y_F^k = [1 \ 1 \ 0 \ 1 \ 0 \ \cdots \ 1 \ 0] x^k \quad (4.22b)$$

The discrete state space model presented in (4.22) with any chosen sampling time  $T_s$ , the periodic signal can be predicted, given initial condition of the states.

Assuming consumer demand to be periodic, a consumer demand curve can also be represented as a periodic signal and in turn can be represented by the Fourier series state space model.

$$D_c^k = y_F^k \quad (4.23)$$

where,

$D_c^k$  is sum of all consumer demands in the network at  $k^{th}$  instance  $D_c^k = \sum d_c^k$   
 $y_F^k$  is the output of the Fourier series state space model

Therefore, given the initial conditions the consumer demand curve can be predicted using the Fourier series state space model. However, in reality the correct initial conditions are not known, which might result in incorrect predictions. To deal with this issue a Kalman filter is to be developed, discussed in section 4.2

## 4.2 Prediction of the consumer demand curve with Kalman filter

### 4.2.1 Kalman filter

Kalman filter is an optimal state estimator for a linear system, which can be used for prediction or filtering of state data[8]. Given a discrete time state space system as,

$$x^{k+1} = \phi x^k + \Gamma u^k + w^k \quad (4.24a)$$

$$y^k = C x^k + v^k \quad (4.24b)$$

where,

$w^k \sim \mathcal{N}(0, Q)$  is the process noise at  $k^{th}$  time instance  
 $v^k \sim \mathcal{N}(0, R)$  is the measurement noise at  $k^{th}$  time instance  
 $Q$  is the covariance matrix of the process noise  
 $R$  is the covariance matrix of the measurement noise

In a Kalman filter algorithm the process and measurement noises are assumed to be white and independent.

At  $k^{th}$  time instance given the initial state value,  $x^0$ , and the measurement,  $y^0 \dots y^k$  and  $u^0 \dots u^k$ , an optimal estimator provides an optimal estimate for  $\hat{x}^k$ . The estimate is optimal in sense that it minimizes the mean square error, i.e. minimizing  $\mathbb{E}[(x^k - \hat{x}^k)^T (x^k - \hat{x}^k)]$ . This formulation is known as linear minimum

mean square error (LMMSE) estimator and this requires prior knowledge till time instance  $k$ . Kalman filter is a recursive implementation of the LMMSE estimator, in which knowledge of state at  $(k^{th} - 1)$  time instance and current measurement is required for optimal estimation. The properties of LMMSE estimator also applies to Kalman filter and therefore Kalman filter is also an optimal and unbiased estimator fulfilling the orthogonality principle[8].

The Kalman filter algorithm comprises of a prediction steps and correction step. In the prediction steps, given the correct state information,  $\hat{x}^{k|k}$ , and the current inputs,  $u^k$ , the next state value,  $\hat{x}^{k+1|k}$ , is predicted. Also, the auto-covariance of the predicted state estimate error,  $P^{k+1|k}$  is calculated in the prediction steps. The notation  $k|k$  denotes estimate for  $k^{th}$  time instance given all the information till  $k^{th}$  time instance, whereas notation  $k+1|k$  denotes estimate for  $k^{th} + 1$  time instance given all the information till  $k^{th}$  time instance. In the correction steps, given the previously predicted state,  $\hat{x}^{k|k-1}$ , and the current measured output,  $y^k$ , the optimal state value,  $\hat{x}^{k|k}$ , is estimated. Again, auto-covariance of the corrected state estimate error,  $P^{k|k}$  is calculated in the correction steps. The complete Kalman filter algorithm as given in [9, 4] is presented below,

### Initialization

1. Set appropriate values for  $Q$  and  $R$  matrices
2. Initialize with a predicted state estimate

$$\hat{x}^0 = x^{init} \quad (4.25)$$

3. Set an initial value for auto-covariance of the predicted state estimate error

$$p^0 = p^{init} \quad (4.26)$$

### Correction Steps

4. Calculate Kalman Filter Gain,  $K$

$$K^k = P^{k|k-1} C^T [C P^{k|k-1} C^T + R]^{-1} \quad (4.27)$$

5. Calculate innovation variable,  $e$

$$e^k = y^k - C \hat{x}^{k|k-1} \quad (4.28)$$

6. Calculate the corrected state estimate,  $\hat{x}^{k|k}$

$$\hat{x}^{k|k} = \hat{x}^{k|k-1} + K^k e^k \quad (4.29)$$

7. Calculate auto-covariance of corrected state estimate error

$$P^{k|k} = [I - K^k C] P^{k|k-1} \quad (4.30)$$

### Prediction Steps

8. Predict state estimate for the next time instance

$$\hat{x}^{k+1|k} = \phi x^{k|k} + \Gamma u^k \quad (4.31)$$

9. Calculate auto-covariance of predicted state estimate error

$$P^{k+1|k} = \phi P^{k|k} \phi^T + Q \quad (4.32)$$

Repeat steps 4 to 9

## 4.2.2 Kalman filter for the estimation of the consumer demand

The discretized equation for pressure at the bottom of the elevated reservoir can be given by (2.52),

$$p_{\tau}^{k+1} = p_{\tau}^k - \mathcal{T} d_{\tau}^k T_s \quad (4.33)$$

where

$$d_{\tau}^k = - \left( \sum d_c^k + \sum u^k \right) \quad (4.34)$$

$$d_{\tau}^k = - \left( D_c^k + U^k \right) \quad (4.35)$$

where,

$\mathcal{T}$	is the tank parameter dependent on the cross sectional area	$[\text{Pa}/\text{m}^3]$
$D_c^k$	is sum of all consumer demands in the network at $k^{\text{th}}$ instance	$D_c^k = \sum d_c^k$
$U^k$	is sum of all flow from the pumps into the network at $k^{\text{th}}$ instance	$U^k = \sum u^k$

Now (4.33) can be written as,

$$p_{\tau}^{k+1} = p_{\tau}^k + \mathcal{T} T_s D_c^k + \mathcal{T} T_s U^k \quad (4.36)$$

With the consumer demand curve presented as a Fourier series state space model, in (4.22) and (4.23), the difference equation for pressure at the bottom of the elevated reservoir can be represented in state space model form, with state vector being,

$$x^k = \begin{bmatrix} a_0 \\ a_1 \cos(\omega_1 k T_s) + b_1 \sin(\omega_1 k T_s) \\ \vdots \\ -a_L \sin(\omega_L k T_s) + b_L \cos(\omega_L k T_s) \\ p_\tau^k \end{bmatrix} \quad (4.37)$$

The input to the model is the flow from the pumps, and only measurement available from the sensor is the pressure at the bottom of the elevated reservoir, and therefore the input and the output vectors can now defined as,

$$u^k = U^k \quad (4.38)$$

$$y^k = p_\tau^k \quad (4.39)$$

With equations (4.37), (4.38) and (4.39), the state space model matrices can now be given as,

$$\phi = \begin{bmatrix} 1 & 0 & 0 & 0 & 0 & \cdots & 0 & 0 & 0 \\ 0 & \phi_1 & 0 & 0 & 0 & \cdots & 0 & 0 & 0 \\ 0 & 0 & \phi_2 & 0 & 0 & \cdots & 0 & 0 & 0 \\ 0 & 0 & 0 & \phi_3 & 0 & \cdots & 0 & 0 & 0 \\ 0 & 0 & 0 & 0 & \phi_4 & \cdots & 0 & 0 & 0 \\ \vdots & \vdots & \vdots & \vdots & \vdots & \ddots & \vdots & \vdots & \vdots \\ 0 & 0 & 0 & 0 & 0 & \cdots & \phi_L & 0 & 0 \\ \mathcal{T}T_s & \mathcal{T}T_s & 0 & \mathcal{T}T_s & 0 & \cdots & \mathcal{T}T_s & 0 & 1 \end{bmatrix} \quad (4.40)$$

$$\Gamma = \begin{bmatrix} 0 \\ 0 \\ 0 \\ 0 \\ 0 \\ \vdots \\ 0 \\ \mathcal{T}T_s \end{bmatrix} \quad (4.41)$$

$$C = [0 \quad \cdots \quad 0 \quad 1] \quad (4.42)$$

$$D = 0 \quad (4.43)$$

The complete state space model can be presented as,

$$x^{k+1} = \begin{bmatrix} 1 & 0 & 0 & 0 & 0 & \cdots & 0 & 0 & 0 \\ 0 & \phi_1 & 0 & 0 & 0 & \cdots & 0 & 0 & 0 \\ 0 & 0 & \phi_2 & 0 & 0 & \cdots & 0 & 0 & 0 \\ 0 & 0 & 0 & \phi_3 & 0 & \cdots & 0 & 0 & 0 \\ 0 & 0 & 0 & 0 & \phi_4 & \cdots & 0 & 0 & 0 \\ \vdots & \vdots & \vdots & \vdots & \vdots & \ddots & \vdots & \vdots & \vdots \\ 0 & 0 & 0 & 0 & 0 & \cdots & \phi_L & 0 & 0 \\ \mathcal{T}T_s & \mathcal{T}T_s & 0 & \mathcal{T}T_s & 0 & \cdots & \mathcal{T}T_s & 0 & 1 \end{bmatrix} x^k + \begin{bmatrix} 0 \\ 0 \\ 0 \\ 0 \\ 0 \\ \vdots \\ 0 \\ \mathcal{T}T_s \end{bmatrix} U^k \quad (4.44a)$$

$$y^k = [0 \ \cdots \ 0 \ 1] x^k \quad (4.44b)$$

Using the state space model, presented in eq. (4.44), in Kalman filter along with tank pressure measurements and pumps flows, all the states can be estimated. From the estimated states, the consumer demand can be estimated as,

$$\hat{D}_c^k = [1 \ 1 \ 0 \ 1 \ 0 \ \cdots \ 1 \ 0 \ 0] \hat{x}^k \quad (4.45)$$

where,

$\hat{D}_c^k$  is the estimated consumer demand at  $k^{th}$  instance  
 $\hat{x}^k$  is the estimated state vector at  $k^{th}$  instance from Kalman filter

The tank pressure measurements from the sensor will also consist of sensor noise. This sensor noise is also filtered in the Kalman filter and the estimate of the tank pressure can be given as,

$$\hat{p}_\tau^k = [0 \ \cdots \ 0 \ 1] \hat{x}^k \quad (4.46)$$

where,

$\hat{p}_\tau^k$  is the estimated pressure of the tank at  $k^{th}$  instance

### 4.3 Predictor simulation test results

Figure 4.1 presents a simulated consumer demand pattern for the network presented in section 2.4. The time scale is of 24 minute, to signify 24 hrs of a day, with a sampling time of 1 sec. The consumer demand presented is the total consumer demand of the network, i.e. sum of the two consumer demands. For presentation the consumer demand plotted is negative of the actual consumer demand. The consumer demand is simulated with a periodic signal function composed of 0.0007 and 0.0014 Hz frequency components. These values were chosen as with these values the simulated consumer demand represents actual demand pattern in

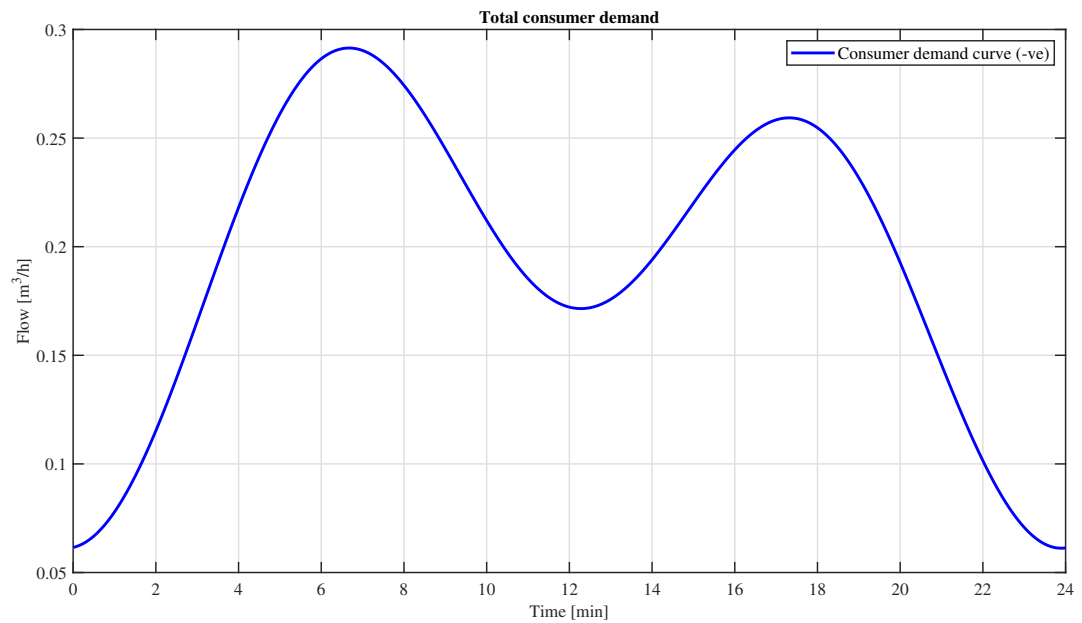


Figure 4.1: Simulated total consumer demand curve of the network

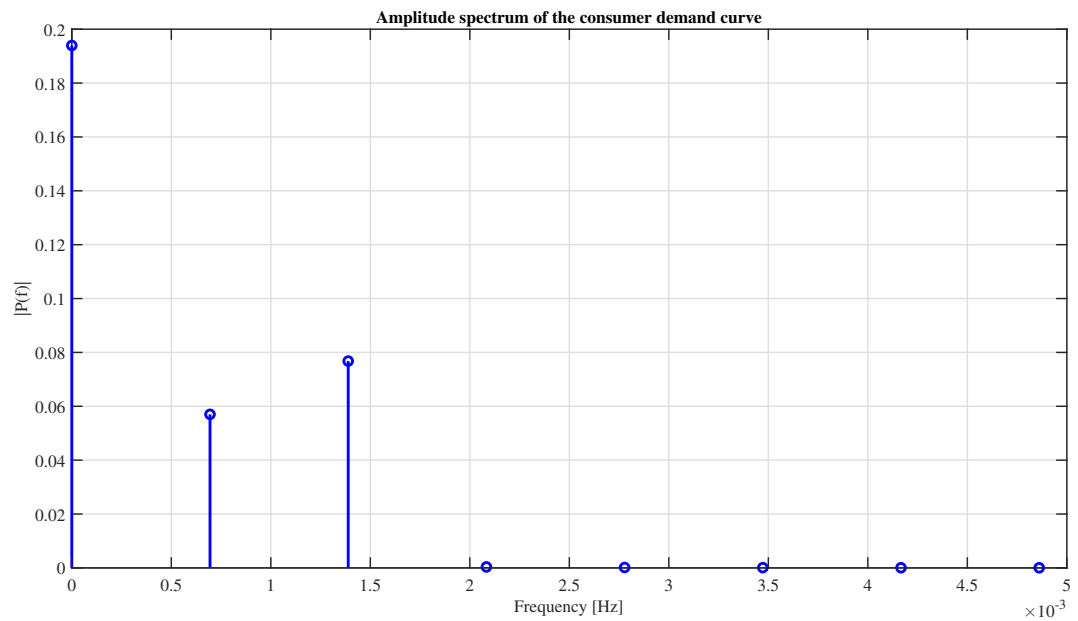


Figure 4.2: Amplitude spectrum of the consumer demand curve presented in fig 4.1

a water network, that is demands are high during morning and evening hours and low during afternoon and night hours.

Using the data from the simulated consumer demand curve, figure 4.1, the power distribution of various frequency component is calculated using fast Fourier transform. From the power distribution amplitude spectrum of the consumer demand curve can be plotted, presented in figure 4.2. Amplitude spectrum is square root of power spectrum, which again represents power distribution of different frequency components in a signal. From an amplitude spectrum plot dominant frequencies of signal can be found, i.e. by defining a threshold power and if for a frequency the power is higher than the threshold it can be considered as a dominant frequency. From the amplitude spectrum plot of the consumer demand curve, it is observed that the consumer demand curve is composed of two dominant frequency components, i.e  $L = 2$ .

$$\omega_1 = 2\pi f_1 = 2\pi(0.0007) = 0.0044 \quad (4.47a)$$

$$\omega_2 = 2\pi f_2 = 2\pi(0.0014) = 0.0087 \quad (4.47b)$$

This finding matches with the foreknowledge, as the consumer demand curve is simulated by the periodic signal function with the same frequencies. This is a method proposed to fixed dominant frequencies for any given periodic signal and the results, (4.47), show that the proposed method produces correct results.

From the frequencies given in eq. (4.47) with sampling time  $T_s = 60$  sec, the state space matrices for the consumer demand curve presented in figure 4.1 can be given as,

$$\phi = \begin{bmatrix} 1 & 0 & 0 & 0 & 0 \\ 0 & 0.9659 & 0.2588 & 0 & 0 \\ 0 & -0.2588 & 0.9659 & 0 & 0 \\ 0 & 0 & 0 & 0.8660 & 0.5000 \\ 0 & 0 & 0 & -0.5000 & 0.8660 \end{bmatrix} \quad (4.48a)$$

$$\Gamma = 0 \quad (4.48b)$$

$$C = [1 \ 1 \ 0 \ 1 \ 0] \quad (4.48c)$$

$$D = 0 \quad (4.48d)$$

The state space model developed for the consumer demand curve, in eq. (4.48), can be validated by running an open loop simulation with state space model and comparing it with the actual consumer demand curve. Figure 4.3 presents comparison of the actual and the predicted consumer demand curve using a state space model. The initial state values are provided to be same as the actual consumer

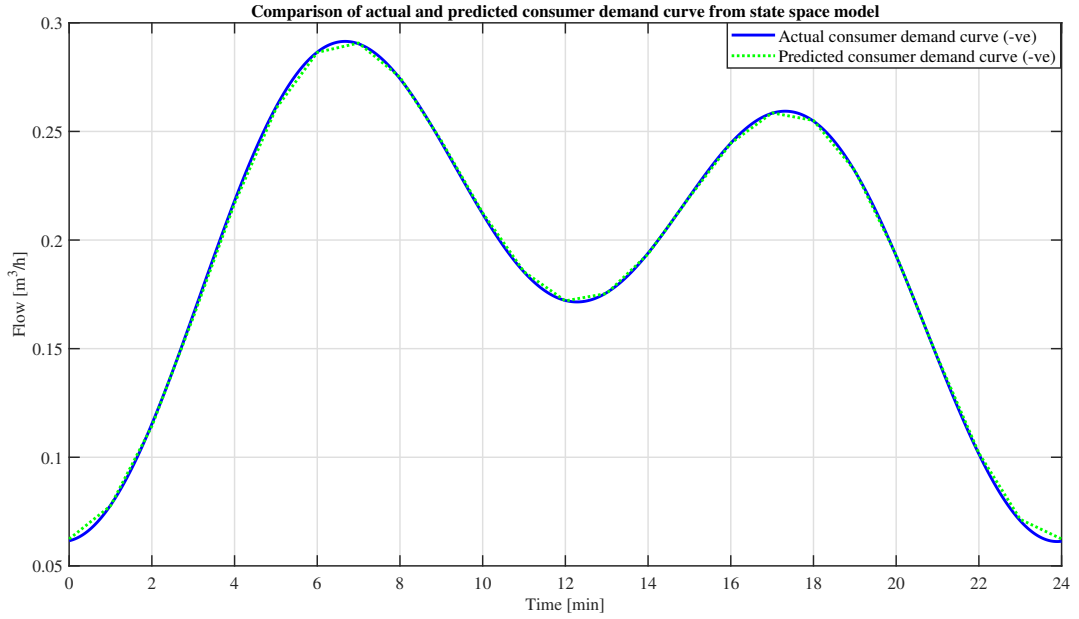


**Figure 4.3:** Comparison of actual and predicted consumer demand curve from state space model

demand curve, and the state space model, in eq. (4.48), is used for prediction of the consumer demand curve over 24 minute time period. From the figure 4.3 it can be seen that given correct initial conditions the state space model developed is capable of predicting the consumer demand curve and this validates the developed state space Fourier series model for the consumer demand curve.

However, as discussed before the initial state conditions are not known, therefore the state space model for the consumer demand curve, in eq. (4.48), along with the parameters of the water distribution network presented in section 2.4, the state space model matrices for the model in eq. (4.44) can be given as,

$$\phi = \begin{bmatrix} 1 & 0 & 0 & 0 & 0 & 0 \\ 0 & 0.9659 & 0.2588 & 0 & 0 & 0 \\ 0 & -0.2588 & 0.9659 & 0 & 0 & 0 \\ 0 & 0 & 0 & 0.8660 & 0.5000 & 0 \\ 0 & 0 & 0 & -0.5000 & 0.8660 & 0 \\ 0.0058 & 0.0058 & 0 & 0.0058 & 0 & 1 \end{bmatrix} \quad (4.49a)$$

$$\Gamma = \begin{bmatrix} 0 \\ 0 \\ 0 \\ 0 \\ 0.0058 \end{bmatrix} \quad (4.49b)$$

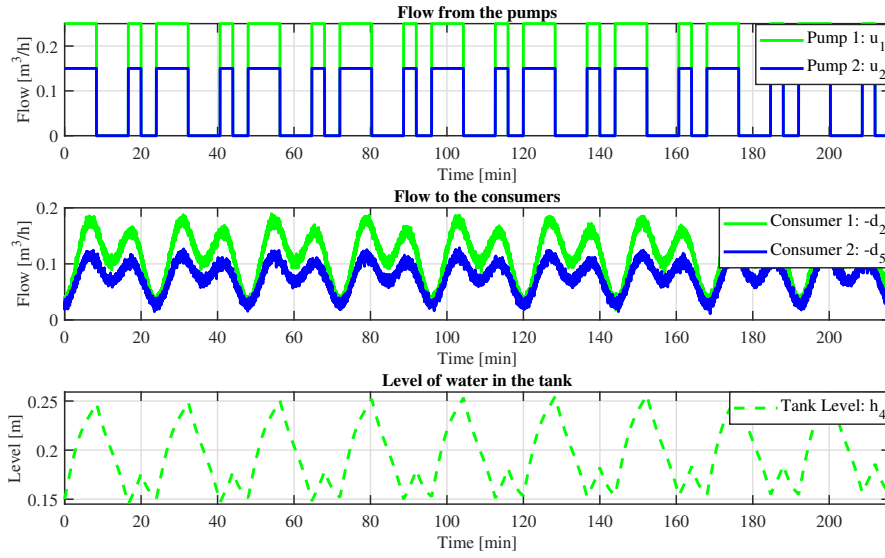


**Figure 4.4:** Open loop simulation test data: Flow from the pumps, consumer demand curve and level of water in the tank

$$C = [0 \ 0 \ 0 \ 0 \ 0 \ 1] \quad (4.49c)$$

$$D = 0 \quad (4.49d)$$

The Kalman filter is tested with an open loop simulation test data for the network presented in section 2.4. Figure 4.4 presents open loop simulation test data over a period of 216 minutes. The pump flows and the consumer demand curves are periodic over a period of 24 minutes. Over this 24-minute period, the pumps are running intermittently, from 0 to 10 minutes and 15 to 20 minutes in each period. When the pumps are running, pump 1 provides a flow of  $0.25 \text{ m}^3/\text{h}$  and pump 2 provides a flow of  $0.15 \text{ m}^3/\text{h}$ . When the pumps are running, the consumer demands are met by the pumps and also the water flows into the tank, and the level of the tank can be seen to be increasing. When the pumps stop, the consumer demands are met by the tank and the level of the tank can be seen to be decreasing.

The measurement data, i.e. pressure at the bottom of the tank, and the input data, i.e. flow from the pumps, is given to the Kalman filter. Gaussian white noise with 0 mean and covariance of  $2.5 \cdot 10^{-7}$  is added to the measurement data to simulate measurement noise in the data. The Kalman filter parameters are presented below:

- Initial state estimate

$$x^{init} = [0 \ 0 \ 0 \ 0 \ 0 \ 0] \quad (4.50)$$

- Initial covariance matrix of the predicted state estimate error

$$p^{init} = \begin{bmatrix} 100 & 0 & 0 & 0 & 0 & 0 \\ 0 & 100 & 0 & 0 & 0 & 0 \\ 0 & 0 & 100 & 0 & 0 & 0 \\ 0 & 0 & 0 & 100 & 0 & 0 \\ 0 & 0 & 0 & 0 & 100 & 0 \\ 0 & 0 & 0 & 0 & 0 & 100 \end{bmatrix} \quad (4.51)$$

- Covariance matrix of process noise

$$Q = 10^{-4} \begin{bmatrix} 0.5 & 0 & 0 & 0 & 0 & 0 \\ 0 & 0.5 & 0 & 0 & 0 & 0 \\ 0 & 0 & 0.5 & 0 & 0 & 0 \\ 0 & 0 & 0 & 0.5 & 0 & 0 \\ 0 & 0 & 0 & 0 & 0.5 & 0 \\ 0 & 0 & 0 & 0 & 0 & 1.7 \cdot 10^{-5} \end{bmatrix} \quad (4.52)$$

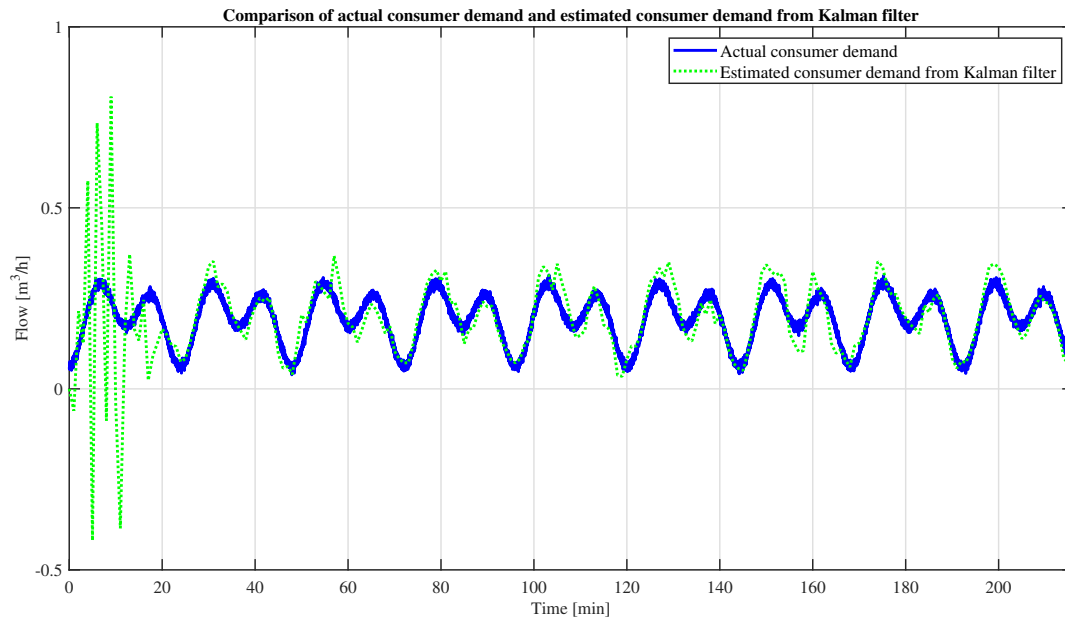
- Covariance of measurement noise

$$R = 2.5 \cdot 10^{-7} \quad (4.53)$$

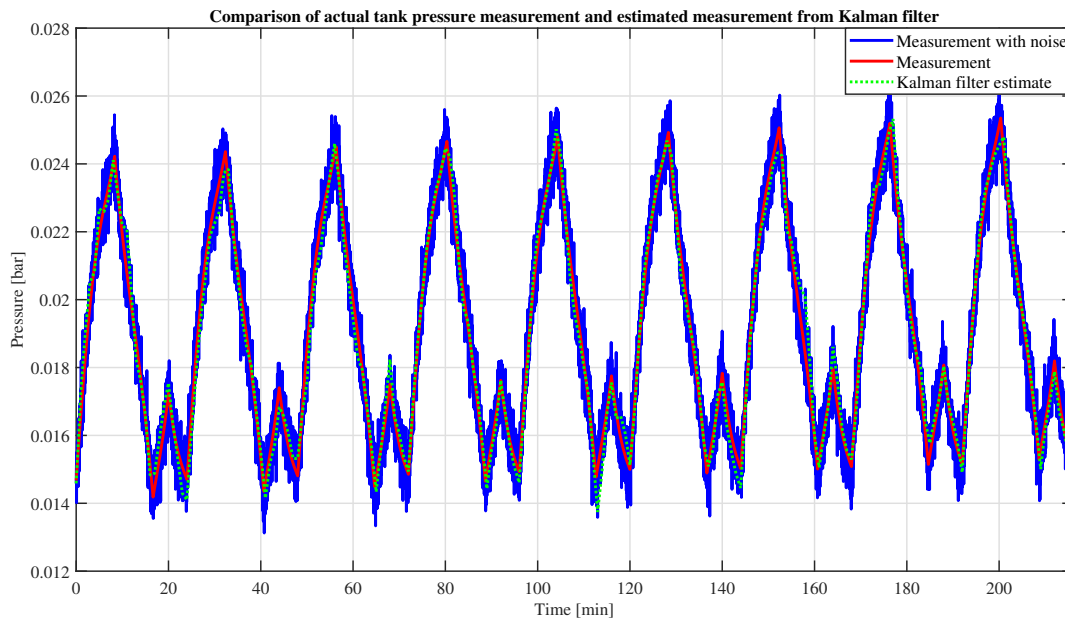
The Kalman filter aims to estimate total consumer demand in the network. Figure 4.5 presents a comparison between the actual consumer demand and the estimated consumer demand. It is to be noted that consumer demand presented here is the sum of both the consumer demands in the network. The initial estimate value is 0 and it can be observed that after a period of 25 minute the estimated consumer demand converges to the actual consumer demand, and later follows it closely throughout the simulation period.

Figure 4.6 presents a comparison between actual pressure measurements (with noise) at the bottom of the tank and the Kalman filter estimated pressure. As mentioned before the Kalman filter is presented with noisy measurements and the Kalman filter aims to filter the noise. The figure also presents the pressure measurements without noise and it can be observed that the Kalman filter is successful in estimating the pressure measurements.

From these results it can be concluded that Kalman filter developed could be used for the prediction of the consumer demand curve.



**Figure 4.5:** Comparison of actual consumer demand and the estimated consumer demand from the Kalman filter



**Figure 4.6:** Comparison of tank pressure measurement from the sensor with sensor noise, pressure measurement without sensor noise and the estimated pressure from the Kalman filter

### 4.3.1 Kalman filter based consumer demand predictor

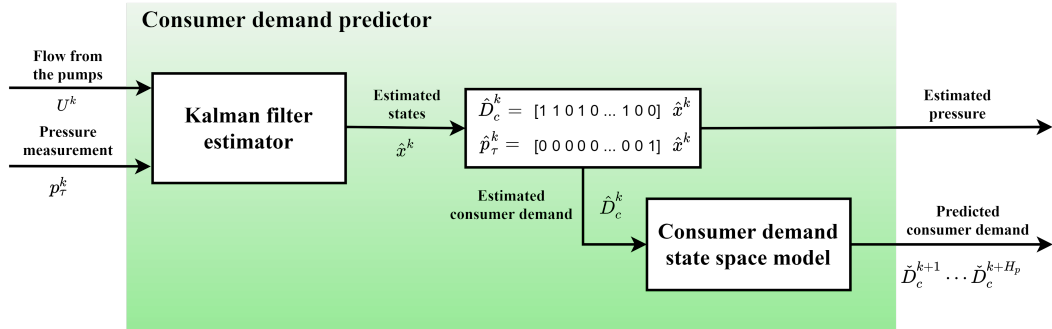
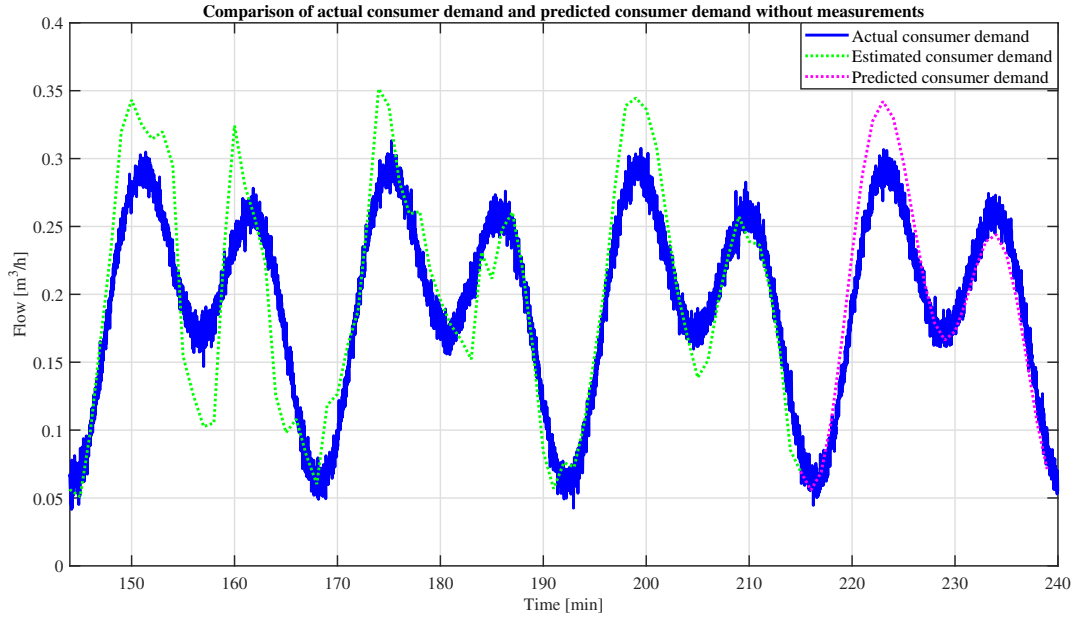


Figure 4.7: The structure of consumer demand predictor

Section 4.2.2 presented Kalman filter that can be used for estimation of the consumer demand based on the measurement signals of the pressure in the tank, whereas the NMPC requires the future prediction of the consumer demand to solve the optimization problem. The structure of the consumer demand predictor is presented in figure 4.7. The consumer demand predictor consists of the Kalman filter estimator, the one presented in section 4.2.2, which takes value of the flow from the pumps and the tank pressure measurements as an input, and provides estimate of the states as an output. From the estimated states, the estimates of the consumer demand and the tank pressure can be calculated using eq. (4.45) and (4.46). Once the consumer demand at the  $k^{\text{th}}$  instance is estimated the future consumer demand till the prediction horizon ( $k + H_p$ ) can be predicted by using Fourier series state space model of the consumer demand curve given by eq. (4.48). At the next time instance ( $k + 1$ ), with the new measurement signal available, the estimate of consumer demand is updated and again future consumer demand over the prediction horizon is predicted.

Figure 4.8 is an extension of the simulation test results presented by figure 4.5 and 4.6, which presents a comparison between actual consumer demand and the predicted consumer demand. At time instance 215 minute the consumer demand is estimated using the Kalman filter, and using this value as the initial state in the consumer demand curve state space model, eq. (4.48), the future consumer demand is predicted over the prediction horizon till 239 minute time instance. From the figure it can be observed that even without the measurement signals the predicted consumer demand curve closely follows the actual consumer demand curve.



**Figure 4.8:** Comparison of the actual consumer demand and the predicted consumer demand from the consumer demand predictor

The predicted consumer demand from the predictor is sum of all the consumer demands in the network, whereas the optimization problem in NMPC requires prediction of individual consumer demands of each consumer. Individual consumer demands of the consumer nodes can be represented as,

$$d_c = vD_c \quad (4.54)$$

where,

- $d_c$  is a vector of consumer nodal demand flows in the network
- $D_c$  is sum of all consumer demand flows in the network
- $v$  is distribution vector of total consumer demand among the individual consumers.  $\sum_i v_i = 1$  and  $v_i \in [0, 1]$

In this project, the distribution vector,  $v$ , is assumed to be constant and based on the prior knowledge of the consumer demand pattern. Also,  $v$  can be assumed to be known as in a real life scenario it can be approximated using consumer billing data. For the network simulation test presented by figure 4.4, the distribution vector is found to be,

$$v = \begin{bmatrix} 0.5939 \\ 0.4061 \end{bmatrix} \quad (4.55)$$

Figure 4.9 presents a comparison between actual consumer demand and the predicted consumer demand for each node individually. From the prediction of

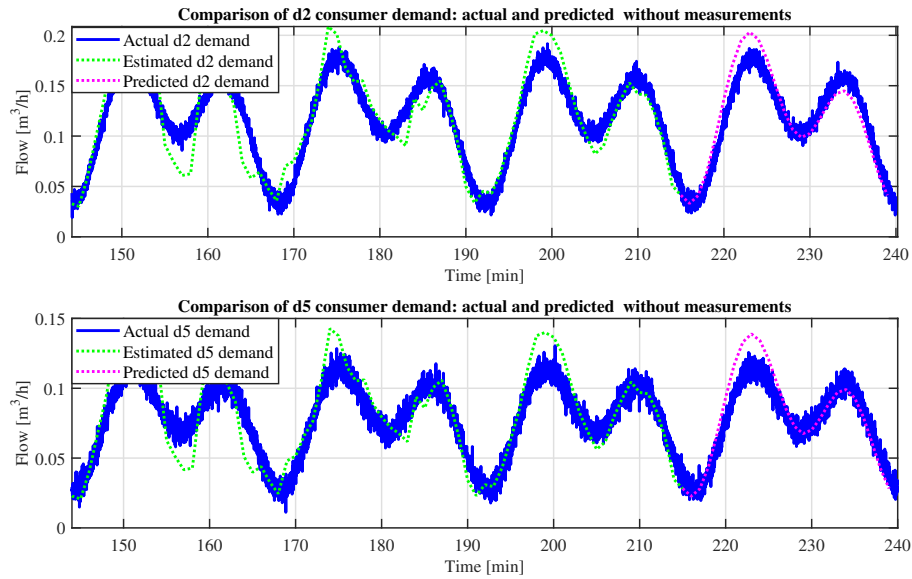


**Figure 4.9:** Comparison of the individual actual consumer demand and the predicted consumer demand

the total consumer demand, from figure 4.8, using the distribution vector, from eq. (4.55), individual consumer demands for node  $d_2$  and  $d_5$  is calculated. Again, it can be observed that the predicted individual consumer nodal demands closely follows the actual consumer nodal demands. With the results from this section it can be concluded that the Kalman filter based predictor developed can be used for prediction of consumer nodal demands, further to be used in solving NMPC optimization problem.

Figure 4.10 presents an updated control structure with the consumer demand predictor. The consumer demand predictor takes in the actual flow from the pumps to the network and the tank pressure measurements from the sensor as an input.

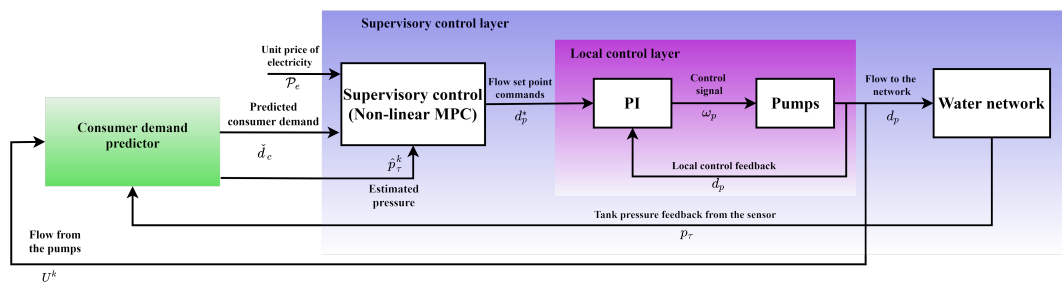


**Figure 4.10:** The updated control structure along with the Kalman filter based consumer demand predictor

The output from the predictor is the future prediction of the consumer demands, which is provided to the NMPC. During the initial period when the predictions are not correct, a upper and lower saturation limits are applied over prediction based on the knowledge that at any given point the consumer demand would not be more than a certain value and consumers won't be supplying water to the network. The consumer demand predictor also estimates the tank pressure value, which is also provided to the NMPC for solving the optimization problem. And again the NMPC and the consumer demand predictor operates at a sampling time of 60 sec, whereas the PI control operates at a sampling time of 1 sec.

Using the control structure, figure 4.10, simulation and laboratory tests were carried out and the results are presented in chapter 6.



## Chapter 5

# Laboratory Setup

This chapter presents the water distribution network setup in the laboratory. First the modular structure and various modules of the smart water laboratory are presented. Then the communication network in the laboratory is presented. Then the network built in the laboratory is presented. Finally, the implementation of the control structure in a Simulink program for testing of the controller in the laboratory is presented.

### 5.1 Smart water laboratory

The water network presented in section 2.4 is emulated in a smart water laboratory. The laboratory is a modular type consisting different modules, such as pumping station module, pipe module, consumer station module, to emulate different parts of a water distribution network. These modules can be connected to each other by means of external pipes to form a desired water network.

Figure 5.1 presents a 3-dimensional representation of a one the smart water laboratory module. The module presented in the figure is a consumer station module which can be used to emulate a consumer or an elevated reservoir. Each module is equipped with some actuators and sensor for control and monitoring of the network. Each module has hand operated exterior valves, to which external pipes are connected to form a desired water network.

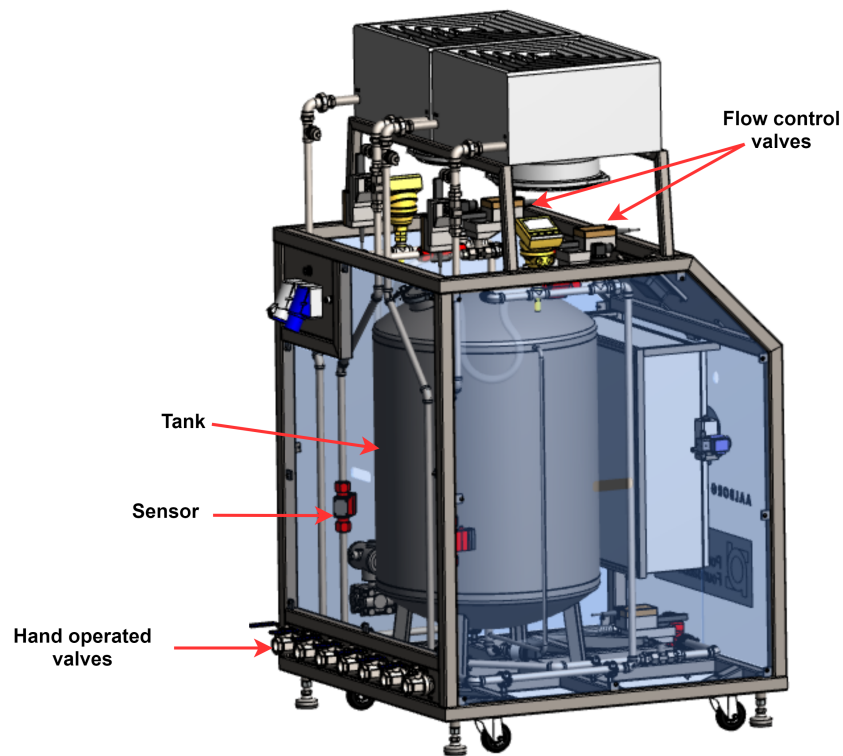


**Figure 5.1:** 3-dimensional representation of a smart water laboratory module created by Poul Due Jensen Foundation, Grundfos

### 5.1.1 Smart water laboratory modules

#### Pumping station module

Figure 5.2 presents as schematic representation of the pumping station module. As the name suggests the pumping station module is used to emulate a pumping station of a water distribution network. The pumping station modules consists a reservoir tank, which can be considered as a water production facility or an infinite reservoir in a water network. The tank's bottom valve is connected to a set of pumps, running in parallel, these pumps are denoted as the primary pumps,  $p_{pri}$ . In this project only one pump from the set has been employed. The outlet of the pump connects to one of the hand operated exterior valves, which is further connected to the water network. The primary pump in the modules is to be considered as the pumping unit in a water distribution network, and therefore the function of this pump is to supply water to the network.

The tank in the pumping station is assumed to be infinite source of water and to ensure water availability in the supply reservoir another set of pumps in the pumping module are operated, these pumps are connected in parallel and denoted

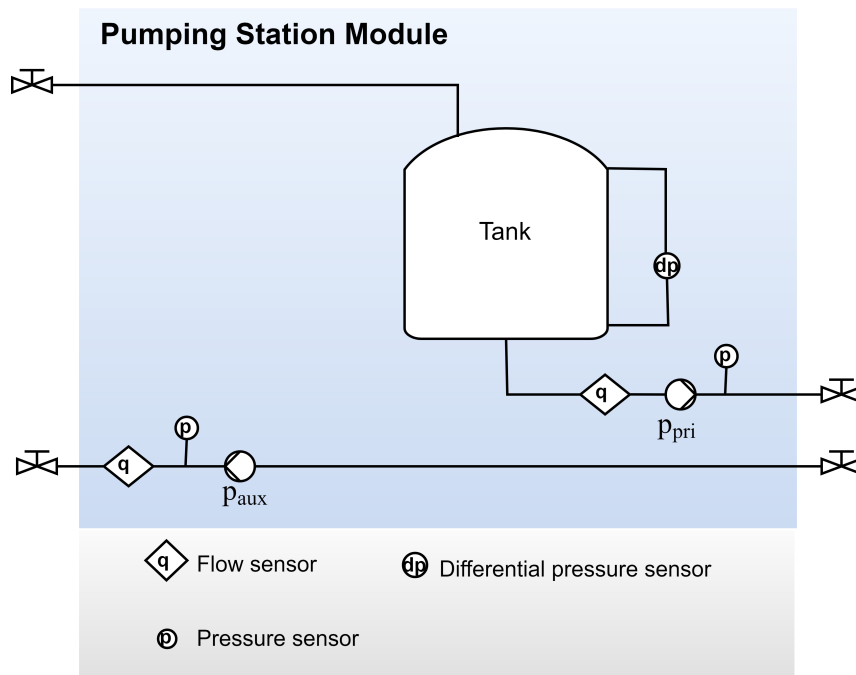


Figure 5.2: Schematic representation of the pumping station module in the smart water lab[22]

as auxiliary pumps,  $p_{aux}$ . The auxiliary pumps can be connected to the top valve of the tank. The purpose of the auxiliary pumps is to transport water from the consumer station tanks to the pumping station tanks. These pumps are not part of the water distribution network, they are not modelled and there are merely for re-circulation of water in the laboratory setup network.

Apart from the pumps, the pumping station module is equipped with flow sensors to measure the flow by pumps and pressure sensors to measure pressure supplied by the pumps.

### Pipe module

The pipe module is to emulate pipes in a water distribution network. The modules consist of 4 set of pipes connected to hand operated exterior valves at both ends, in the figure 5.3 only one such set is presented. Each set is further made of smaller pipe segments. Each set can be used to form a 3 way connection in a water distribution network. There are on/off valves,  $V_1$ ,  $V_2$ ,  $V_3$ , inside the module to select the pipe segments to be included in the laboratory water network setup. The module is equipped to measure the flow and pressure sensors.

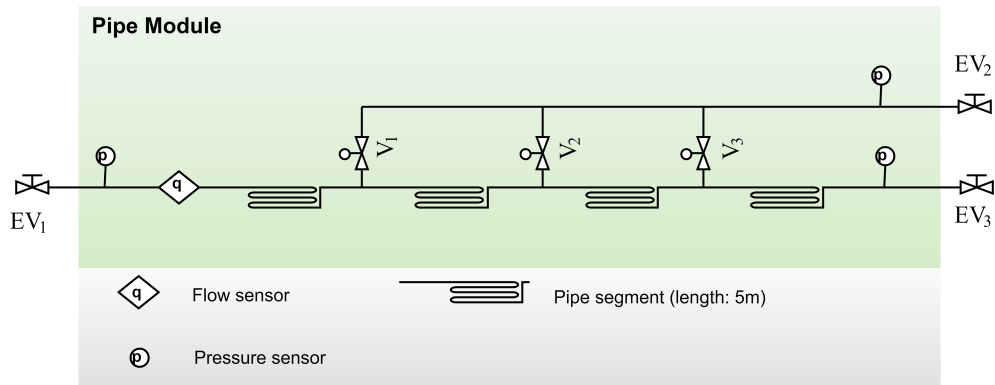


Figure 5.3: Schematic representation of the pipe module in the smart water lab[22]

### Consumer station/ Elevated reservoir module

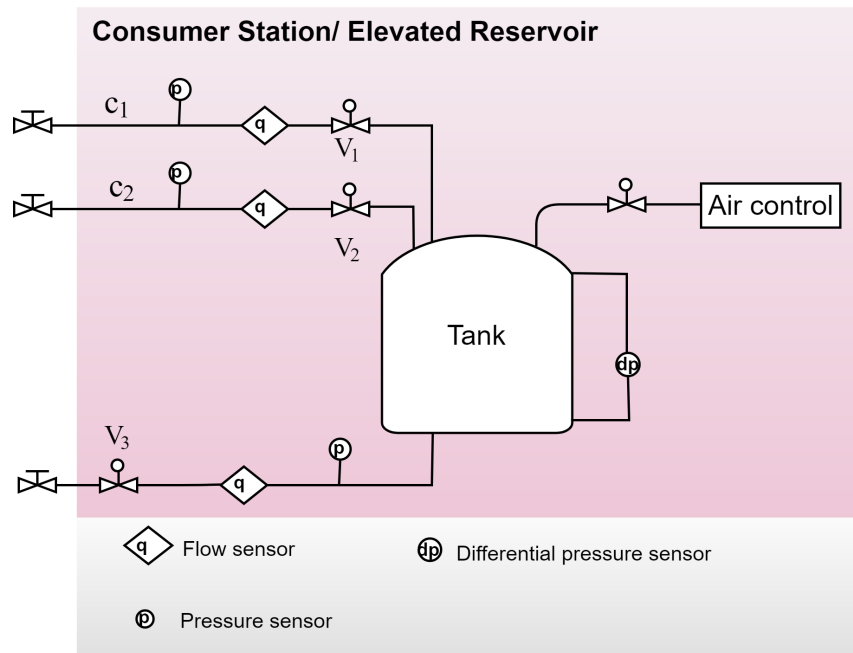


Figure 5.4: Schematic representation of the consumer station/ elevated reservoir module in the smart water lab[22]

Figure 5.4 presents schematic representation of module which has two functionality, it can either be used to emulate consumers or an elevated reservoir in the water network. 3-dimensional representation of this module was presented in figure 5.1. This module consist a tank to which controllable valves are connected at the bottom and top. When the module is to be used to emulated consumers the top flow

control,  $V_1$ ,  $V_2$ , valves come into play, the two valves can be considered to be as two consumers of the water network. The valve opening degree can be regulated to emulate variable consumer demand. The bottom valve,  $V_3$ , is from where the tank can be emptied, this valve is connected to the auxiliary pump in the pumping station module, and as mentioned before the water is re-circulated in the network.

When the module is to be used as an elevated reservoir, top valves are closed and the bottom valve is connected to the network through the hand operated exterior valve. The flow of water in the module is through bottom valve only. The module also has an air control unit with which the tank can be pressurised to emulate elevation. With the air control unit elevation for both the consumers and the reservoir can be emulated. A maximum of 5m of elevation can be emulated in the module with pressurized air. The module is also equipped with flow, pressure and differential pressure sensors.

### 5.1.2 Smart water laboratory communication network

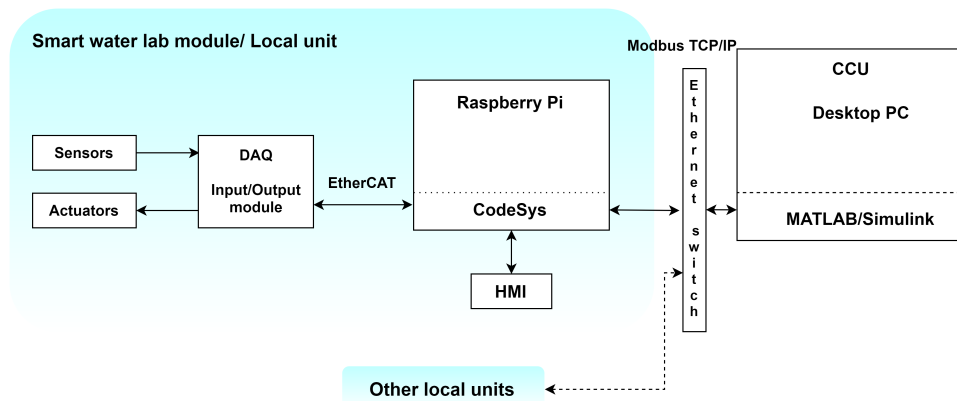


Figure 5.5: Smart water laboratory communication network setup[22]

Figure 5.5 presents the smart water laboratory communication network. On the laboratory modules the sensors and the actuators are connected to data acquisition (DAQ) input/output modules through field wire, where the communication is analog. The I/O module converts the analog signal to digital signal. The I/O modules are further connected to a Raspberry Pi, which is again present on the laboratory module, and the communication between the two is via EtherCAT. On the Raspberry Pi a CodeSys run-time system continuously runs in the back-end, converting the Raspberry Pi into a soft PLC. A HMI screen is also mounted on the Raspberry Pi, this allows local control of the laboratory module.

All the Raspberry Pi from the laboratory modules are connected to a common Ethernet switch, to which a Central Control Unit (CCU) is also connected and the communication is Modbus TCP/IP. The CCU is a desktop PC, from which the

laboratory modules can be controlled remotely. On the CCU a MATLAB/Simulink program can be used to implement a controller for the water distribution network setup.

## 5.2 Water distribution network setup in the laboratory

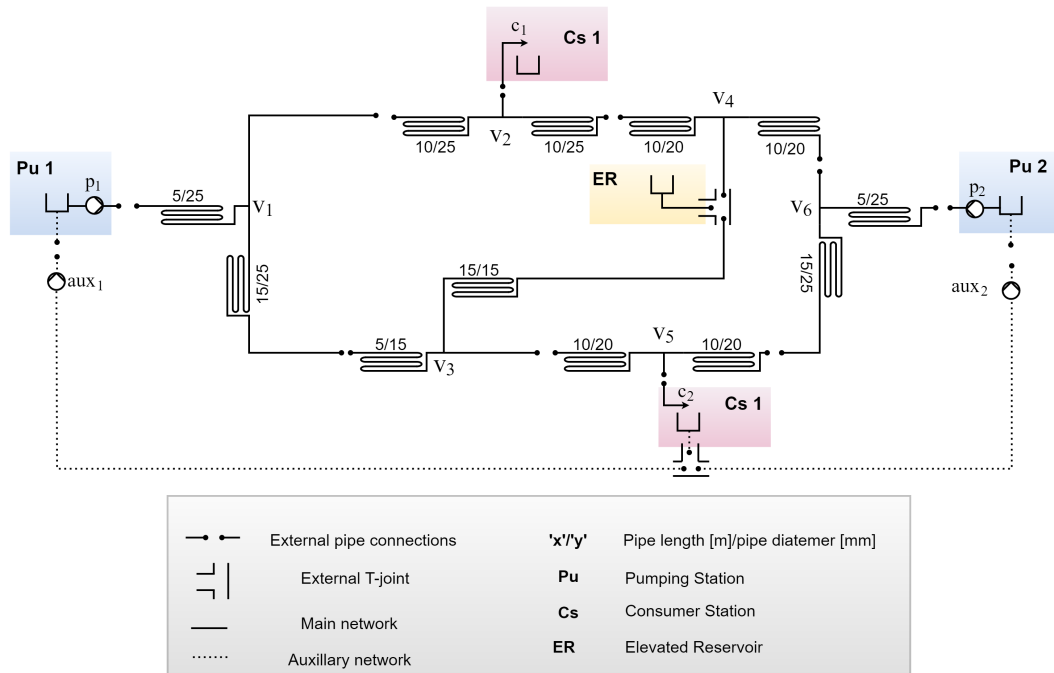


Figure 5.6: Representation of laboratory water distribution network setup[22]

Figure 5.6 presents the water distribution network setup in the smart water laboratory. This setup is to emulate the water distribution network presented in section 2.4. The water network is setup by connecting different modules, presented in section 5.1.1, by means of external pipes which is represented by broken connections in the figure.

The pipe module is used to emulate the pipes in the water distribution network and these pipes will generate pressure drop in the network. The pipe lengths and diameter are mentioned in the figure in the form  $x/y$ , where  $x$  is the length of the pipe in meters and  $y$  is the diameter of the pipe in millimeters. The network consists of two pumping station modules,  $Pu1$  and  $Pu2$ , both having primary pumps to supply water into the network. The pumping stations also have auxiliary pumps, re-circulating the water in the network, and as mentioned before these are not part of the main water network therefore it is represented with a dotted line. The water network also has an elevated reservoir, which is with the pressurized air elevated

to 3 m. There are two consumers in the water network, which are both on the same consumer station module, as consumer station modules has two flow control valves on the top to represent two consumers.

### 5.3 Control structure implementation for the laboratory setup

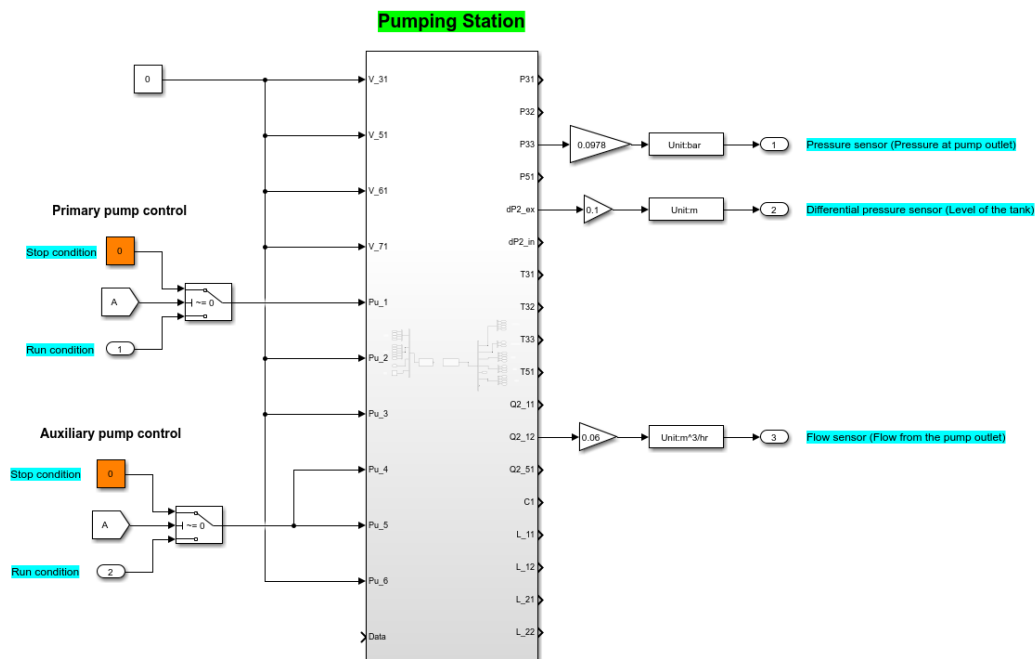
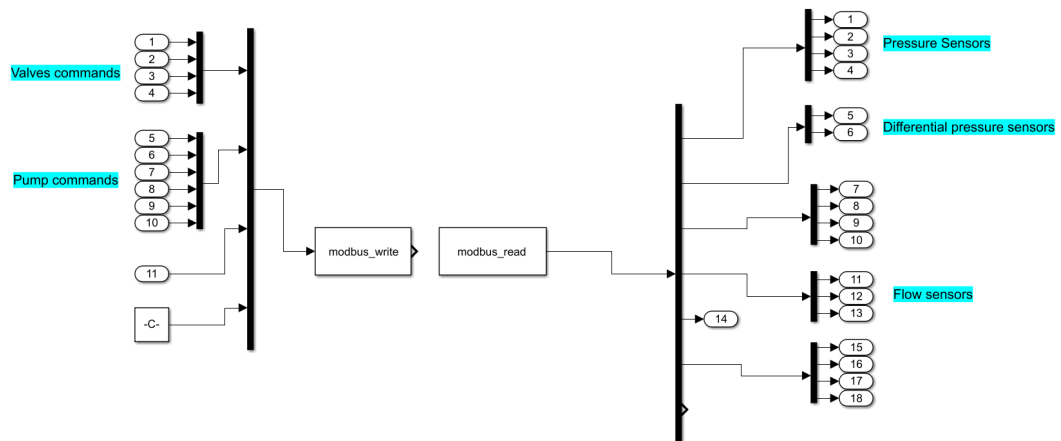


Figure 5.7: Pump block subsystem in the Simulink program[22]

The control of the water network in the laboratory from CCU is through a MATLAB/Simulink program. In the Simulink program there are subsystem blocks for each module. One of such block is presented in figure 5.7, which is a pumping station block. Inside the subsystem block there is 'modbus\_read' and 'modbus\_write' S-function to communicate with the Raspberry Pi, this is presented in figure 5.8. Programming of these blocks are not part of the project and were already available in the smart water laboratory.

The IP address of the module are provided to these S-function blocks. Different ports for different components in the module are defined. The command to be given to the module is given to 'modbus\_write' block, for example to run the primary pump, in pumping station module, at a particular speed the command in percentage will be given to the 'modbus\_write' block at the port designate for the



**Figure 5.8:** S-function blocks, 'modbus\_read' and 'modbus\_write', inside the pumping station subsystem in the Simulink program[22]

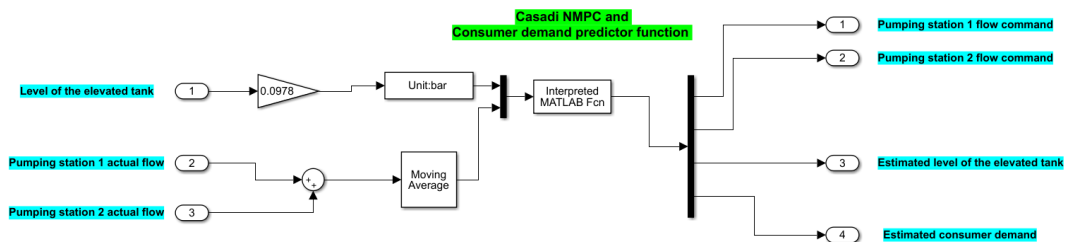


**Figure 5.9:** NMPC and consumer demand predictor implementation using Interpreted MATLAB function

primary pump. Similarly, to get a sensor reading from the module, the Simulink program reads from the 'modbus\_read' block.

Figure 5.9 presents implementation of NMPC and consumer demand predictor using Interpreted MATLAB function. Whenever the Interpreted function is called a .m file is called from Simulink in which the NMPC problem is defined and solved using CasADi [1]. The CasADi problem is defined into an optimization object variable, to which parameters are passed to obtain optimal solutions. The code for defining the NMPC problem is presented in appendix A. The consumer demand predictor is also implemented in the same .m file. The predictions of the consumer demand is used by the NMPC for calculation of optimal flow commands. The sampling time for the Interpreted function is 60 sec, which is the sampling time for the NMPC and the predictor. The Interpreted function takes level of the tank and average of the actual flow from the pumps over 60 sec as an input, and gives out optimal flow commands from the pumps and the estimates for tank level and consumer demand.

The optimal flow commands are sent to the PI controllers of each pump, which

then regulate the pump speed between 0 to 100% to control the flow at desired set-point by sending commands (between 0 to 100%) to the respective 'modbus\_write' S-function blocks. Apart from flow control of the pumps, another PI control is implemented for control of consumer demand. The consumer demand PI controller regulates the consumer valve opening degree (between 0 to 100%) to control the consumer flow to a predefined consumer demand curve.

The test results of the implemented control structure on the laboratory water distribution network are presented in section 6.3.



# Chapter 6

## Results

The test results of the NMPC along with the consumer demand predictor are presented in this chapter. First, the test details and the parameters for the NMPC and the predictor are presented. Then the test results of the control on a simulated nonlinear network model is presented. Finally, the test results on the water network setup in the laboratory is presented.

### 6.1 Test details, NMPC and predictor parameters

The control structure with the consumer demand predictor, presented in section 4.3.1, is implemented in MATLAB/Simulink and first tested on the simulated nonlinear plant model of the water network presented in section 2.4. Then the control is test on the water network setup in the laboratory, which was presented in section 5.2. The test details, and the parameters for the NMPC and the consumer demand predictor are presented below. Some of the test details and the NMPC parameters are same as used in [22].

- **Run time:** 144 minute (representation of 144 hrs(or 6 days) in real life)
- **Consumer demand pattern:** Periodic at an interval of 24 minute. 24 minute are representation of 24 hrs of day in real life, where the consumer demands are higher during morning and evening hours compared to afternoon and night hours.
- **Plant:** For simulation test, nonlinear model for the network presented in section 2.4 and for the laboratory test, the water distribution network presented in section 5.2.
- **Control structure:** Control structure presented by figure 4.10. The control structure consists of the NMPC control with optimization problem, presented

in section 3.2.2, implemented in CasADi. The control structure also consists of the consumer demand predictor presented in section 4.3.1.

- Network parameters and constants used in the test
  - Efficiency of pumps: 0.6
  - Efficiency of motors: 0.9
  - Density of water: 997 kg/m<sup>3</sup>
  - Gravitational constant: 9.81 m/s<sup>2</sup>
- Noise in consumer demand(for simulation test):  $w \sim \mathcal{N}(0, 0.01)$
- Noise in tank pressure measurement(for simulation test):  $v \sim \mathcal{N}(0, 0.0005)$
- Sampling time for the plant: 1 sec
- Sampling time for NMPC: 60 sec
- Sampling time for consumer demand predictor: 60 sec
- NMPC parameters

- Prediction horizon: 24
- Weight for minimization of operational cost:

$$Q = \begin{bmatrix} 5.5 \cdot 10^{10} & 0 \\ 0 & 5.5 \cdot 10^{10} \end{bmatrix} \quad (6.1)$$

- Weight for minimization of pressure variations at consumer nodes:

$$R = \begin{bmatrix} 1 & 0 \\ 0 & 1 \end{bmatrix} \quad (6.2)$$

- Weight for minimization of slack variable:

$$\varrho = 10^5 \quad (6.3)$$

- Minimum pressure of tank: 0.0098 bar
- Maximum pressure of tank: 0.0391 bar
- Maximum flow from the pumps: 0.3 m<sup>3</sup>/h
- Maximum pressure from the pumps: 0.6 bar
- Predictor parameters

## – System model used in the Kalman filter

$$\phi = \begin{bmatrix} 1 & 0 & 0 & 0 & 0 & 0 \\ 0 & 0.9659 & 0.2588 & 0 & 0 & 0 \\ 0 & -0.2588 & 0.9659 & 0 & 0 & 0 \\ 0 & 0 & 0 & 0.8660 & 0.5000 & 0 \\ 0 & 0 & 0 & -0.5000 & 0.8660 & 0 \\ 0.0058 & 0.0058 & 0 & 0.0058 & 0 & 1 \end{bmatrix} \quad (6.4a)$$

$$\Gamma = \begin{bmatrix} 0 \\ 0 \\ 0 \\ 0 \\ 0.0058 \end{bmatrix} \quad (6.4b)$$

$$C = [0 \ 0 \ 0 \ 0 \ 0 \ 1] \quad (6.4c)$$

$$D = 0 \quad (6.4d)$$

## – Initial state estimate

$$x^{init} = [0 \ 0 \ 0 \ 0 \ 0 \ 0] \quad (6.5)$$

## – Initial covariance matrix of the predicted state estimate error

$$P^{init} = \begin{bmatrix} 100 & 0 & 0 & 0 & 0 & 0 \\ 0 & 100 & 0 & 0 & 0 & 0 \\ 0 & 0 & 100 & 0 & 0 & 0 \\ 0 & 0 & 0 & 100 & 0 & 0 \\ 0 & 0 & 0 & 0 & 100 & 0 \\ 0 & 0 & 0 & 0 & 0 & 100 \end{bmatrix} \quad (6.6)$$

## – Covariance matrix of process noise(for simulation test)

$$Q = 10^{-4} \begin{bmatrix} 0.5 & 0 & 0 & 0 & 0 & 0 \\ 0 & 0.5 & 0 & 0 & 0 & 0 \\ 0 & 0 & 0.5 & 0 & 0 & 0 \\ 0 & 0 & 0 & 0.5 & 0 & 0 \\ 0 & 0 & 0 & 0 & 0.5 & 0 \\ 0 & 0 & 0 & 0 & 0 & 1.7 \cdot 10^{-5} \end{bmatrix} \quad (6.7)$$

- Covariance matrix of process noise(for laboratory test)

$$Q = 10^{-2} \begin{bmatrix} 0.12 & 0 & 0 & 0 & 0 & 0 \\ 0 & 0.12 & 0 & 0 & 0 & 0 \\ 0 & 0 & 0.12 & 0 & 0 & 0 \\ 0 & 0 & 0 & 0.12 & 0 & 0 \\ 0 & 0 & 0 & 0 & 0.12 & 0 \\ 0 & 0 & 0 & 0 & 0 & 4.0 \cdot 10^{-6} \end{bmatrix} \quad (6.8)$$

- Covariance of measurement noise(for simulation test)

$$R = 2.5 \cdot 10^{-7} \quad (6.9)$$

- Covariance of measurement noise(for laboratory test)

$$R = 2.5 \cdot 10^{-9} \quad (6.10)$$

- Upper saturation limit on predicted consumer demand:  $0 \text{ m}^3/\text{h}$
- Lower saturation limit on predicted consumer demand:  $-0.45 \text{ m}^3/\text{h}$

Note: Some of the parameters of the predictor are different for simulation test and the laboratory test, this due to the difference in noise that is added in the simulation test and the actual noise observed in the laboratory setup.

## 6.2 Simulation test results

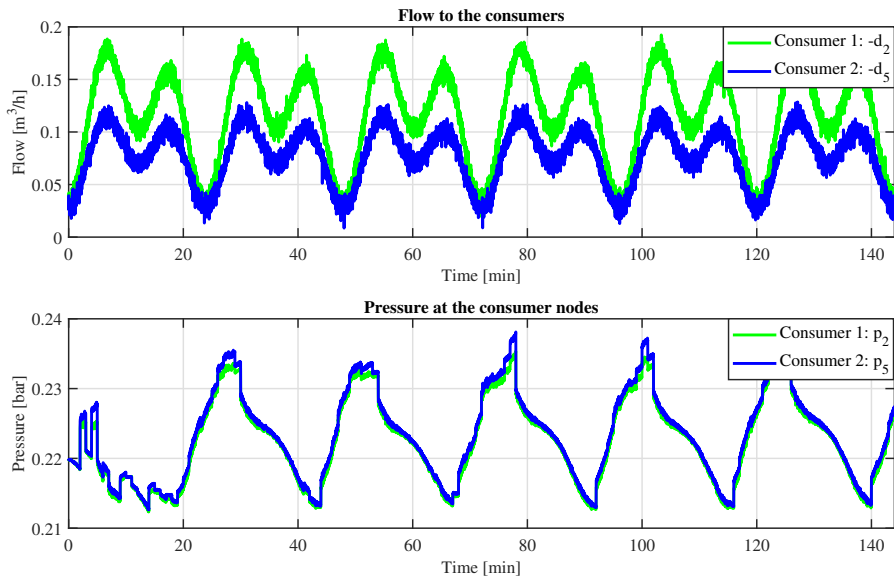
### 6.2.1 NMPC with consumer demand predictor simulation test results

Section 6.2.1 presents result of implementation of NMPC control with consumer demand predictor on a simulated nonlinear water network model.

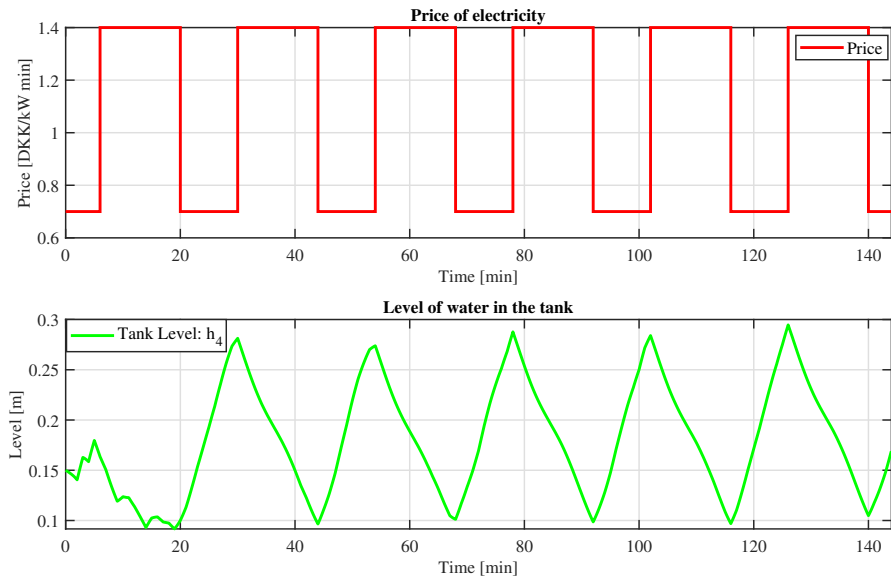
Figure 6.1 presents the varying consumer demand for both the consumers over the period of 144 minute. It also presents the pressure at the consumer nodes resulting from pump operation by NMPC control.

Figure 6.2 presents the varying price of electricity. The price curve is periodic over a period of 24 minute, the prices are higher during day hours compared to night hours. Over the 24 minute period, the prices during the day hours (6 to 20 minute) are 1.4 DKK/kW minute and during night hours (0 to 6 minute and 20 to 24 minute) are 0.7 DKK/kW minute. The figure also presents the varying tank level over the simulation period. The water flows into the tank when the pumps are running and the consequently the tank level rises. Similarly, when the pumps are stopped the tank level decreases.

Figure 6.3 presents the pump operation control by NMPC. During the initial period of 20 minute the pumps seems to be running without any pattern. After



**Figure 6.1:** Consumer nodal demand flows and NMPC simulation results for pressure at consumer end



**Figure 6.2:** Varying unit price of electricity and NMPC simulation results for level of water in the tank

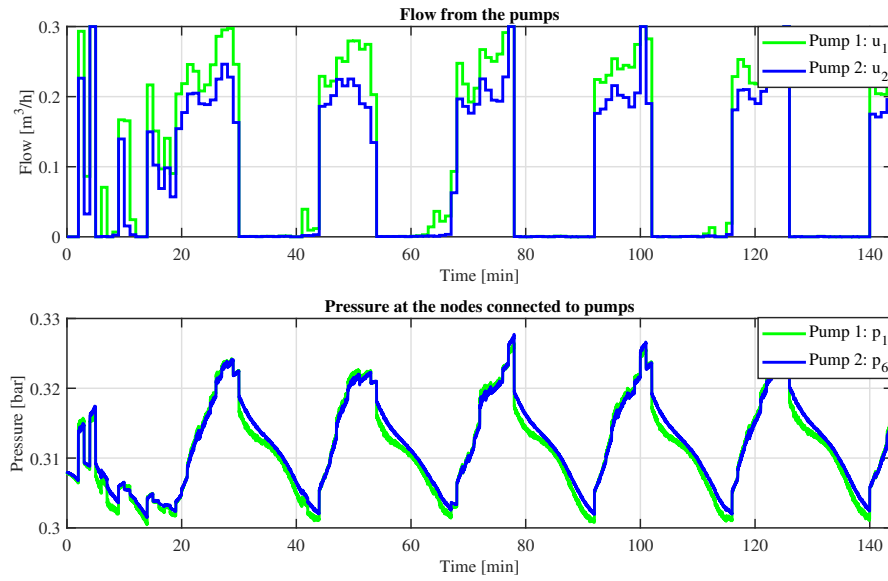


**Figure 6.3:** NMPC simulation results for flow from the pumps and the pressure at pump nodes

the 20 minute period the pumps mostly only run during the period when the price of electricity is low, this behavior is discussed in section 7.1.

Figure 6.4 presents a comparison between tank pressure measurement from the sensor with sensor noise, pressure measurement without sensor noise and the estimated pressure from the Kalman filter predictor. From the figure it can be observed that the Kalman filter effectively filters the measurement noise and the estimate closely follows the pressure measurement without sensor noise.

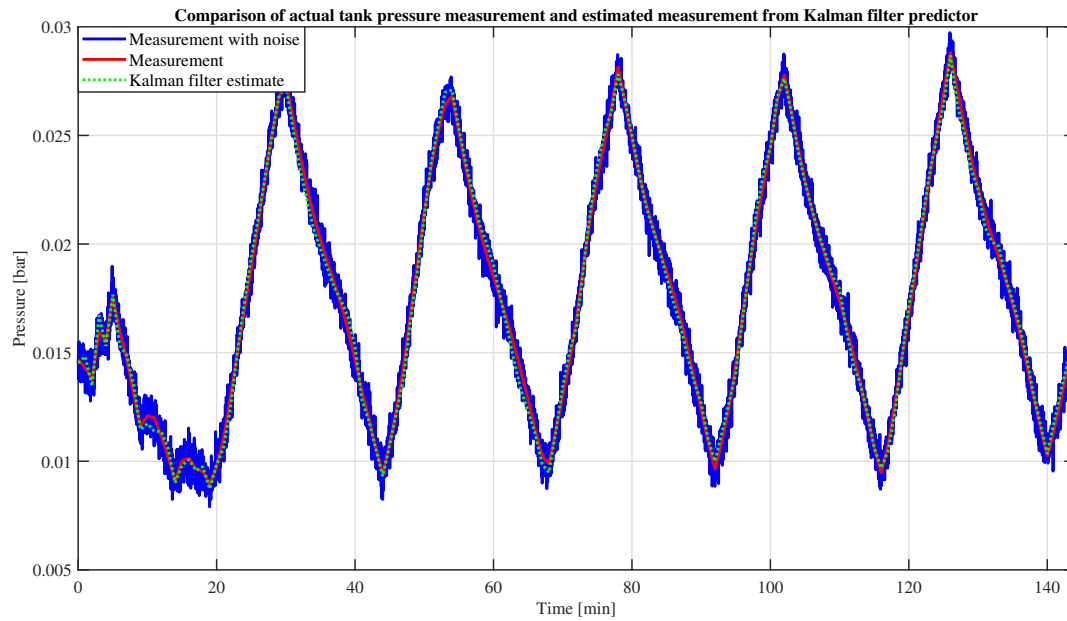


**Figure 6.4:** Comparison of tank pressure measurement from the sensor with sensor noise, pressure measurement without sensor noise and the estimated pressure from the Kalman filter predictor

Figure 6.5 and 6.6 both presents a comparison between actual consumer demand and the estimated consumer demand from the Kalman filter predictor. Figure 6.5 presents comparison for the total consumer demand in the network, whereas figure 6.6 presents comparison for demands of individual consumers which is calculated using predefined demand distribution vector. It can be observed that the consumer demand estimation is off during the initial period till 20 minute, but after 20 minute the estimation closely follows the actual demand. From the estimated demand, future consumer demands are predicted to be utilized for solving NMPC optimization problem.

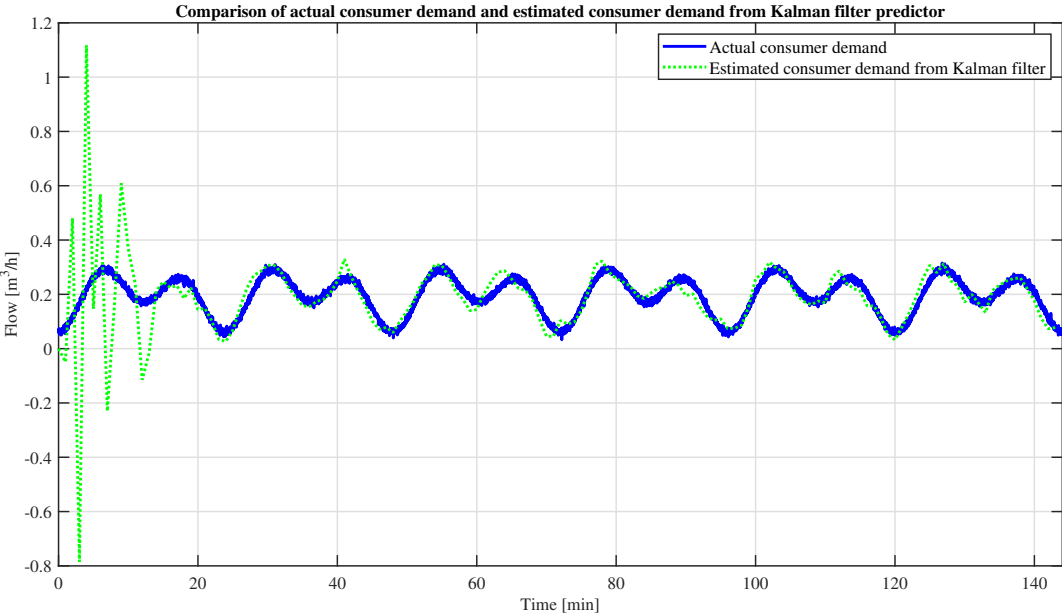


Figure 6.5: Comparison of actual consumer demand and the estimated consumer demand from the Kalman filter predictor

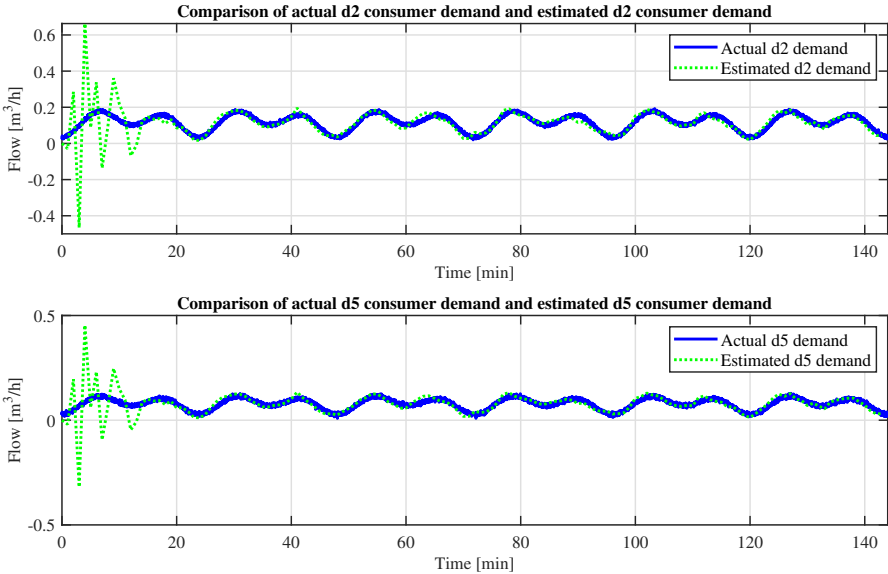
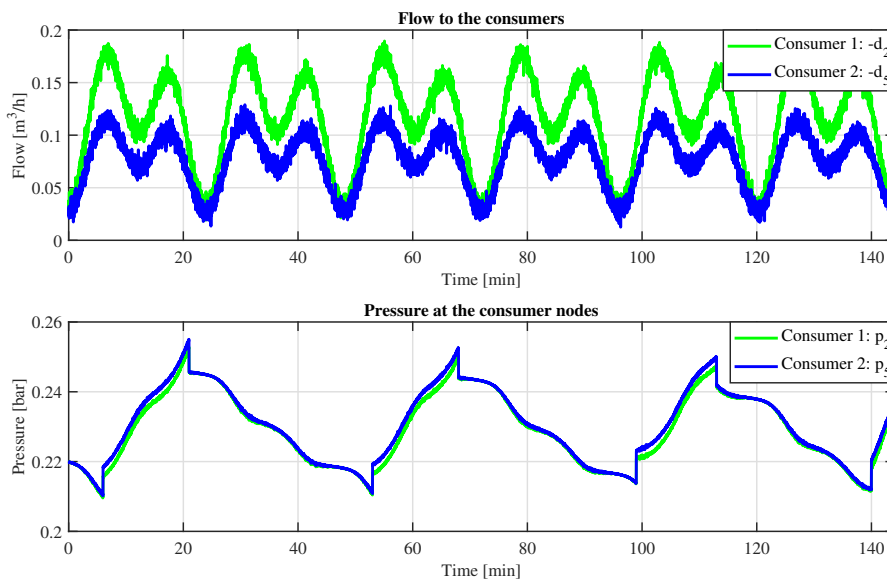


Figure 6.6: Comparison of the individual actual consumer demand and the predicted consumer demand from the Kalman filter predictor

### 6.2.2 On/off control simulation test results

For comparison of NMPC control results, an on/off control is implemented on the same water network model. The on/off control is designed to run the pumps when the level of water in tank goes below 0.1 m and stop the pumps when the level goes above 0.4 m.

Figures 6.7, 6.8 and 6.9 presents the on/off control simulation results. The consumer demand pattern is same as the one used in NMPC control simulation test presented in figure 6.7.



**Figure 6.7:** Consumer nodal demand flows and on/off simulation results for pressure at consumer end

The electricity price curve is also the same with higher prices during the day compared to night, presented in figure 6.8. Initially the pumps are in stopped condition, when the tank level reaches below 0.1 m at 6 time instance, the pumps starts to run. At 21 time instance when the tank level goes above 0.4 m the pumps are again stopped. This cycle repeats throughout the simulation period and presented in figure 6.9.

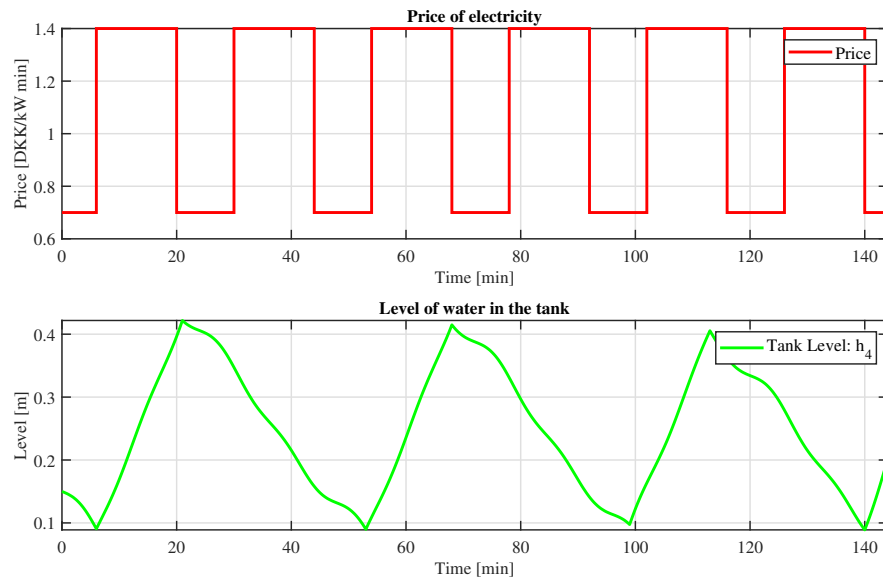


**Figure 6.8:** Varying unit price of electricity and on/off simulation results for level of water in the tank

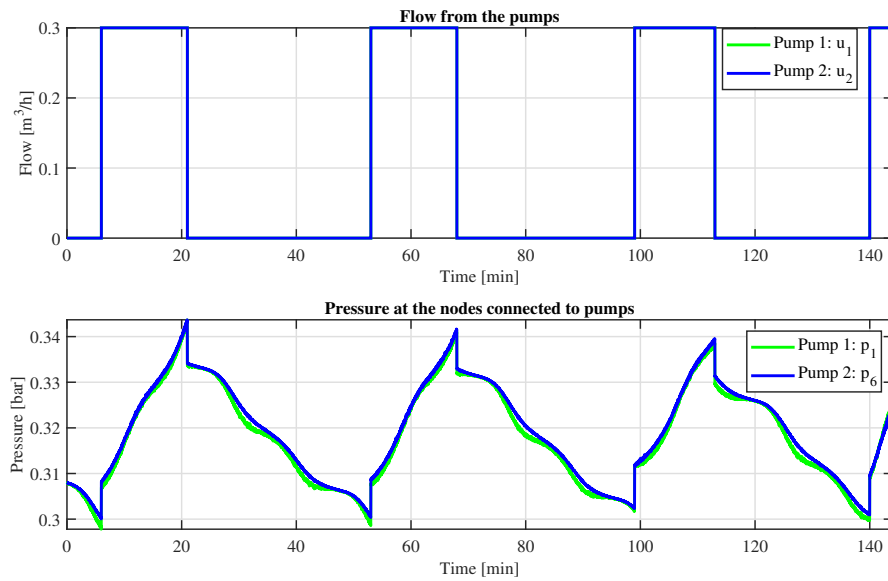


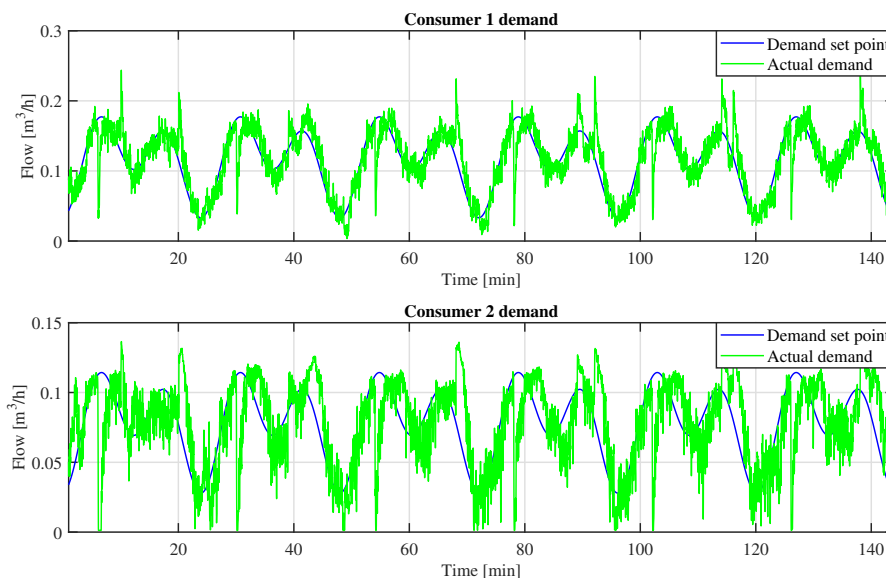
**Figure 6.9:** On/off simulation results for flow from the pumps and the pressure at pump nodes

## 6.3 Laboratory test results

### 6.3.1 NMPC with consumer demand predictor laboratory test results

Similar to simulation tests, NMPC with consumer demand predictor was also tested on the laboratory setup. The results for the laboratory test are presented by figures 6.10, 6.11, 6.12, 6.13, 6.14 and 6.15.

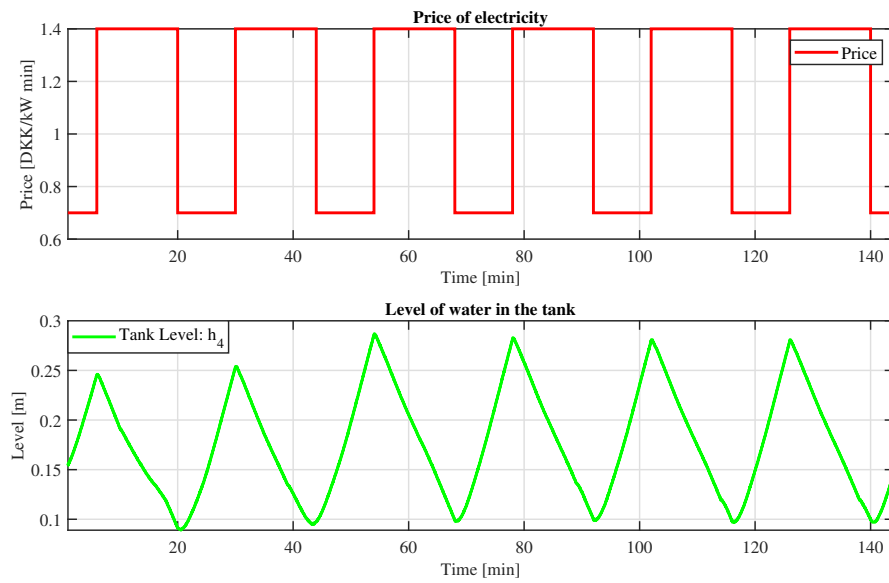
The desired consumer demand pattern is same as in the simulation tests. The desired consumer demand is given to a PI controller, the PI controller regulates the consumer valve's opening degree to control the consumer demand flow at the set-point. The PI controller is tuned manually by trial and error. The consumer demand set-point and the actual demand controlled by PI controller is presented in figure 6.10.



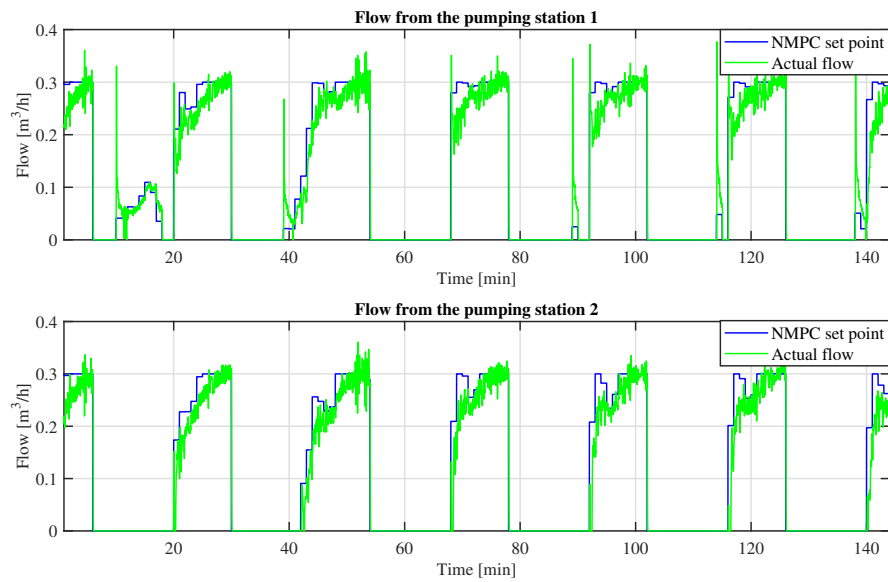
**Figure 6.10:** Consumer nodal demand set-point and the actual demand flow controlled by a PI controller in the laboratory setup

Figure 6.11 presents the varying price of electricity which is same as in the simulation tests. The figure also presents changing level of the tank over the test period. The level of the tank increases when the pumps are running and when the pumps are not running the tank supplies water to the network and level of the tank decreases.

Figure 6.12 presents the optimal pump flow set-points provided by NMPC controller and the actual pump flow controlled by a PI controller. As mentioned before, the PI controller regulates the speed of the pump to control the flow. Again, the



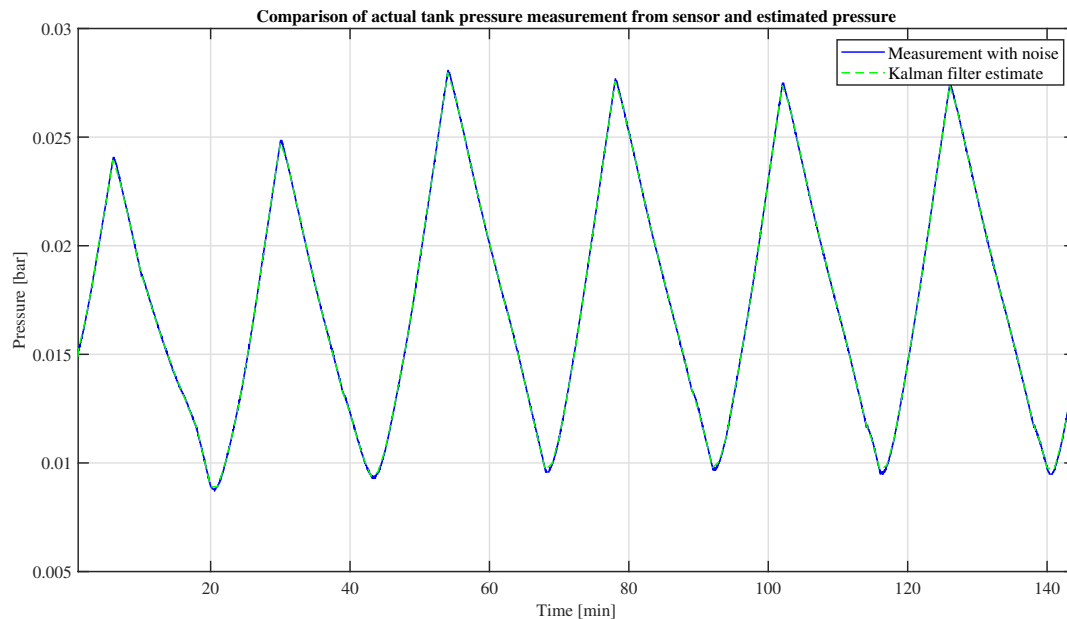
**Figure 6.11:** Varying unit price of electricity and NMPC results for level of water in the tank measured by sensor in the laboratory setup



**Figure 6.12:** Pump flow set-point by NMPC and the actual pump flows controlled by a PI controller in the laboratory setup

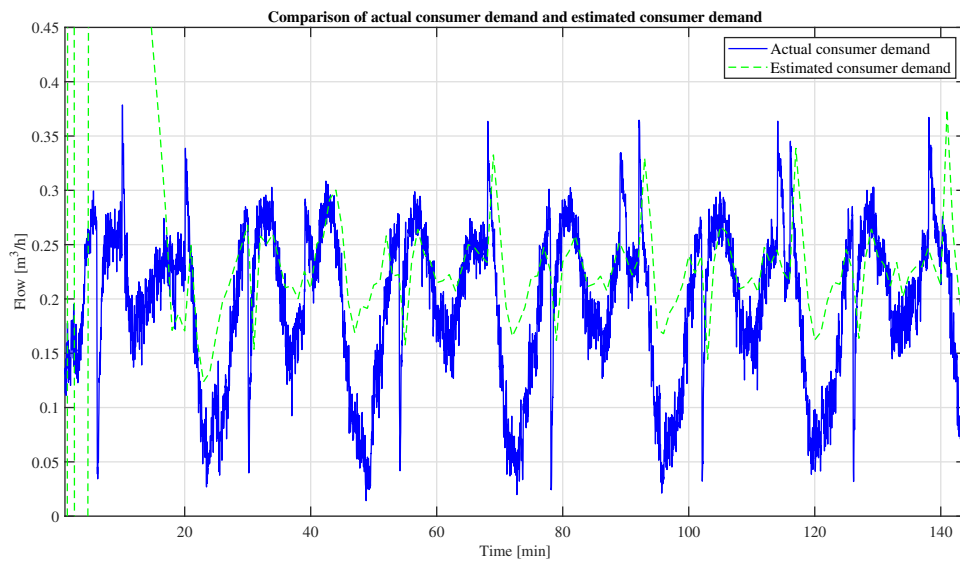
PI controller is tuned manually. The PI control implementation is presented in appendix D. As discussed in section 3.4, oscillations can be observed in the actual flow from the pumps.

Figure 6.13 presents a comparison between the the tank pressure measurement from the sensor and the estimated pressure from the Kalman filter predictor. There is not much sensor noise and it can be observed that the estimate is exactly follows the measured tank pressure.



**Figure 6.13:** Comparison of tank pressure measurement from the sensor with sensor noise and the estimated pressure from the Kalman filter predictor in the laboratory setup

Figure 6.14 and 6.15 presents a comparison between the actual consumer demand and the estimated consumer demand from the Kalman filter predictor. The predicted consumer demand is put through a saturation limit, from the prior knowledge of the network it is known that the consumer demand would not be more than  $0.45 \text{ m}^3/\text{h}$  and consumers won't be supplying water to the network. From figure 6.14, which presents estimation of the total consumer demand in the network, it can be observed that the estimated consumer demand simply follows the pattern of the actual consumer demand and not exactly estimates it. The poor performance of the predictor in the laboratory test, as compared to simulation test, is discussed in section 7.2. Similarly, from figure 6.15, which presents estimate of demands for individual consumer calculates using predefined distribution vector, it can be observed that the estimated demands follow the pattern of the actual demands.



**Figure 6.14:** Comparison of actual consumer demand and the estimated consumer demand from the Kalman filter predictor in the laboratory setup

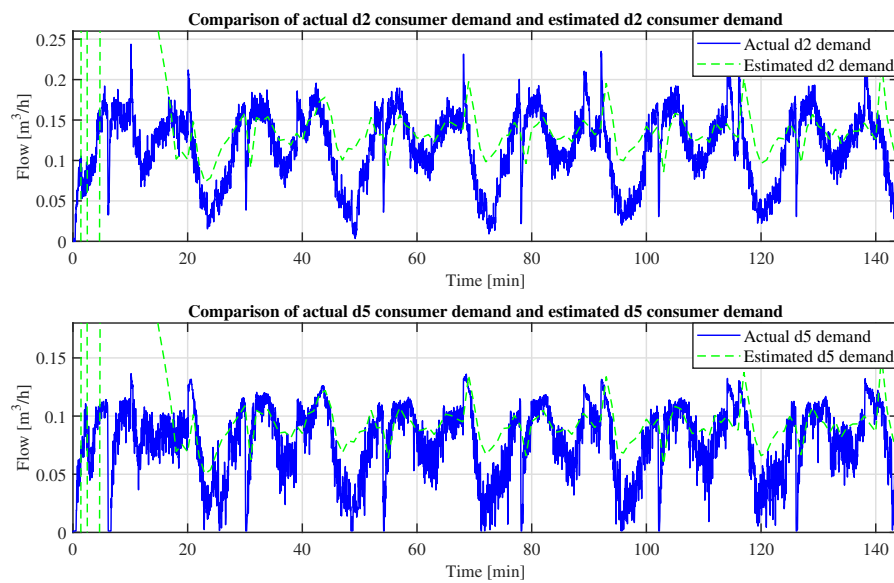


**Figure 6.15:** Comparison of the individual actual consumer demand and the predicted consumer demand from the Kalman filter predictor in the laboratory setup

### 6.3.2 On/off control laboratory test results

For comparison of the NMPC results on the laboratory setup, an on/off control is also implemented on the same laboratory setup. The on/off is designed to given

flow set-point of  $0.3 \text{ m}^3/\text{h}$  to pump PI controllers when the tank level goes below  $0.1 \text{ m}$  and stop the pumps when the tank level goes above  $0.4 \text{ m}$ . The results of the on/off implementation are presented in figures 6.16, 6.17 and 6.18.

Same as in the NMPC laboratory implementation, the consumer demand pattern is provided to the consumer PI controllers, which regulate the valve's opening degree to control the consumer demand flow. The consumer demand set-point and the actual demand flow in the test is presented in figure 6.16.

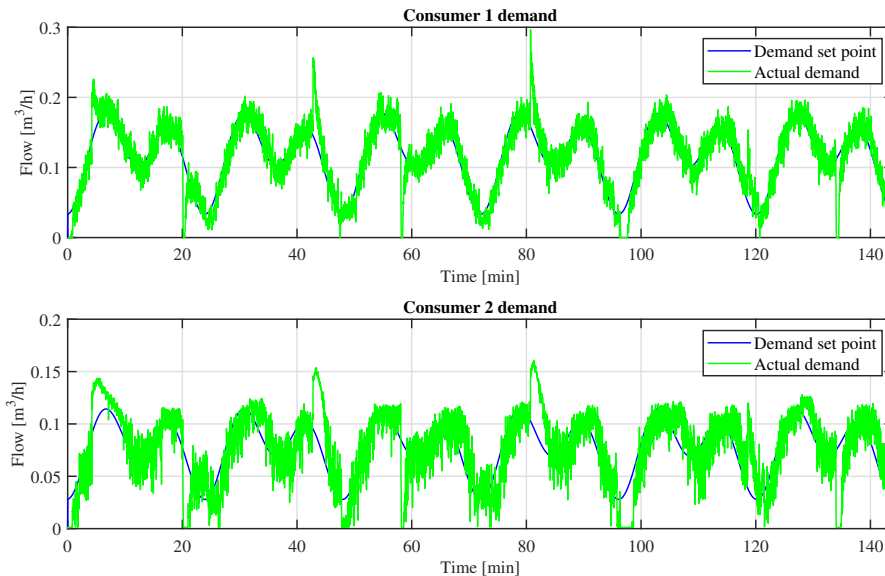


**Figure 6.16:** Consumer nodal demand set-point and the actual demand flow controlled by a PI controller in the laboratory setup

The electricity price pattern is again same as the previous tests and presented in figure 6.8. Figure 6.8 also presents the changing level of the tank, at 4 minute time instance the reaches the lower limit of  $0.1 \text{ m}$ , then the pumps starts and the level starts to increase. At 20 minute the tank level reaches it upper limit of  $0.4 \text{ m}$ , at that point the pumps stop, and this cycle repeats throughout the simulation.

Figure 6.18 presents the pump flow set-points provided by the on/off controller and the actual pump flow controller by the PI controllers. At 4 minute time instance when the tank level reaches  $0.1 \text{ m}$ , the on/off controller gives as set-point of  $0.3 \text{ m}^3/\text{h}$  to both the pump PI controllers. And again it can be observed that the actual flow from the pumps is oscillatory.

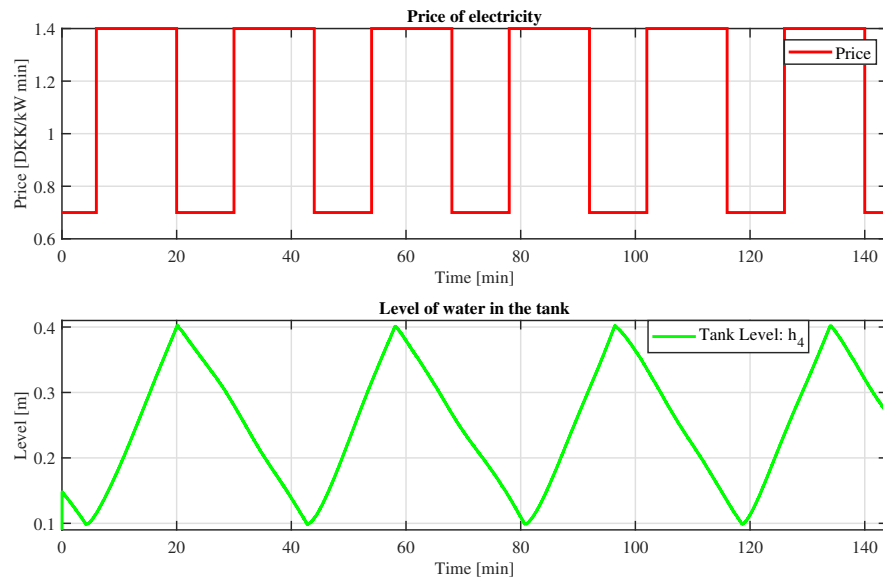


**Figure 6.17:** Varying unit price of electricity and on/off control results for level of water in the tank measured by sensor in the laboratory setup

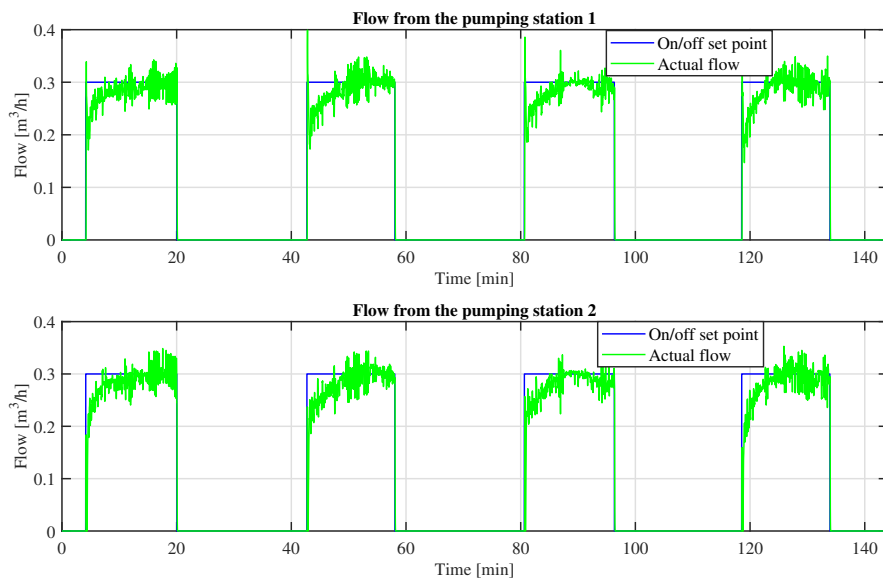


**Figure 6.18:** Pump flow set-point by on/off control and the actual pump flows controlled by a PI controller in the laboratory setup

The results of the simulation test and the laboratory test from this chapter are discussed in chapter 7.

# Chapter 7

## Discussion

In this chapter the simulation and the laboratory test results are discussed. The stability analysis of the inner closed-loop system is also discussed.

### 7.1 Discussion on simulation test results

- Simulation test results show that during the initial period till 20 minute the estimate of total consumer demand from the predictor is way-off from the actual demand. But after this period the estimate closely follows the actual consumer demand. This close estimate of the consumer demand is reasonably good and is used for prediction of future consumer demand. This predicted consumer demand is provided NMPC for solving the optimization problem.
- Estimate of demands for individual consumers is calculated using a distribution vector, as presented in (4.54). This distribution is assumed to be known and is calculated based on the prior knowledge of the distribution of consumer demand. From the simulation results it can be observed that the estimate of the individual consumer demands also closely follows the actual demand, but this was expected as the distribution vector is calculated from the actual consumer demand used in the simulation test. In a real life scenario have knowledge of the distribution vector is a fair assumption as well, as it can be calculated from yearly billing data of the consumers, giving a good approximation of the distribution vector.
- During the initial period when the estimate of the consumer demand is incorrect, it can be observed that the pump operation by the NMPC control is not as desired. During this period the pumps are not operated effectively when the price of electricity is low, resulting in running pumps when the prices are high. The pumps are running to avoid crossing the lower limit constraint of the tank level. But this behavior was expected as the incorrect estimation of

the consumer demand would result in incorrect predictions which are being used for solving the optimization problem. After the initial period when the estimates are reasonably correct, it can be observed that the NMPC mostly only operates the pumps when the prices are low.

- After the initial period when the consumer demand estimates are correct, it can be observed that the tank level rises during the low electricity price period and drop when the prices are high. The NMPC, based on the predicted consumer demand, calculates the tank level required at the end of a low price period to meet the consumer demands when the prices are high without operating the pumps. Even during the low price period when the pumps are operated, they are operated at optimal flow to fill the tank only up to the required level.
- From the results it can be observed that the NMPC sometimes operates the pump during the high price period at a low flow. NMPC does that to avoid crossing the lower limit constraint on the tank level, and the pump flow is only to meet the consumer demands and not fill the tank. This happens due to slight imprecision in the estimation of the consumer demand. Even when the tank level goes below the lower limit, the NMPC is able to handle this violation as it is developed with soft constraints.
- Comparison of NMPC with the on/off controller.

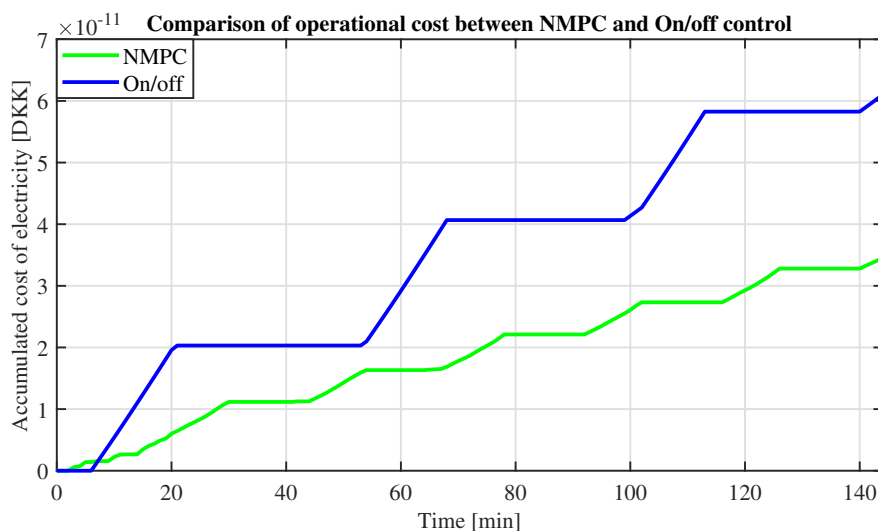


**Figure 7.1:** Comparison of accumulated cost of operation over 144 minute between the NMPC and the on/off controller in simulation test

Figure 7.1 presents a comparison of accumulated cost of operation between

the NMPC and the on/off controller after water network operation of 144 minute (representing 6 days). From the figure it can be observed that the cost of operation is less in NMPC compared to on/off controller. After 144 minute of operation, there is 43.34% saving with NMPC compared to the on/off controller.

- Comparison of NMPC with MPC results from [22]

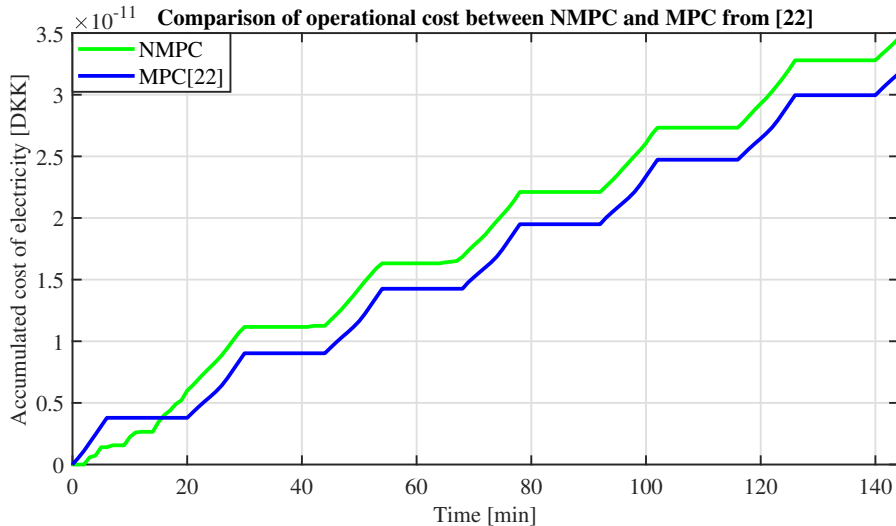


**Figure 7.2:** Comparison of accumulated cost of operation over 144 minute between the NMPC and the MPC from [22] in simulation test

From the figure 7.2 it can be observed that the MPC performance from [22] is slightly better than NMPC performance from this work, but this can be accounted to the imprecision in the consumer demand predictor. In [22], the future consumer demands were assumed to be known and provided to the MPC, which would not be the case in real life scenario. Considering the imprecision of the predictor, the performance of the NMPC and the MPC are fairly equal. MPC results of [22] are presented in appendix C.

## 7.2 Discussion on laboratory test results

- The laboratory test yields similar results to the simulation test. During the initial period the estimated consumer demand is way-off the actual consumer demand. After this period the estimation follows the pattern of the actual demand, which in this case is acceptable considering the performance of NMPC. The reason for the predictor not able to estimate the actual demand closely could be the oscillations in the actual demand.

- The NMPC implemented for the laboratory setup provides optimal pump flow commands to the local PI controllers. The PI controllers regulate the speed of the pumps to control the flows. From the results it can be observed that the flow is oscillating, comments on this oscillatory behaviour is given in section 7.3.
- After the initial period when the consumer demand estimates are incorrect, it can be observed that the NMPC gives command to operate the pumps mostly only during the low electricity price period. And similar to the simulation results, when the pumps are operated in the high electricity price period, it is to avoid crossing the lower limit constraint on the tank level.
- The actual consumer demand flow is also controlled by PI controllers. A predefined consumer demand curve is given to the PI controllers as set-point and the PI controllers regulate the opening degree of valves to control the flow. The consumer demand flow can also be observed to oscillate, this could be due to oscillating flow from the pumps and delay in the system.
- Even with the oscillating flow from the pumps and consumers, the behavior in the tank level is as expected. The tank level is observed to be rising when the price of electricity are low and when the prices are high the tank level decreases, supplying water to the water network and meeting consumer demands.
- Comparison of NMPC with the on/off controller.

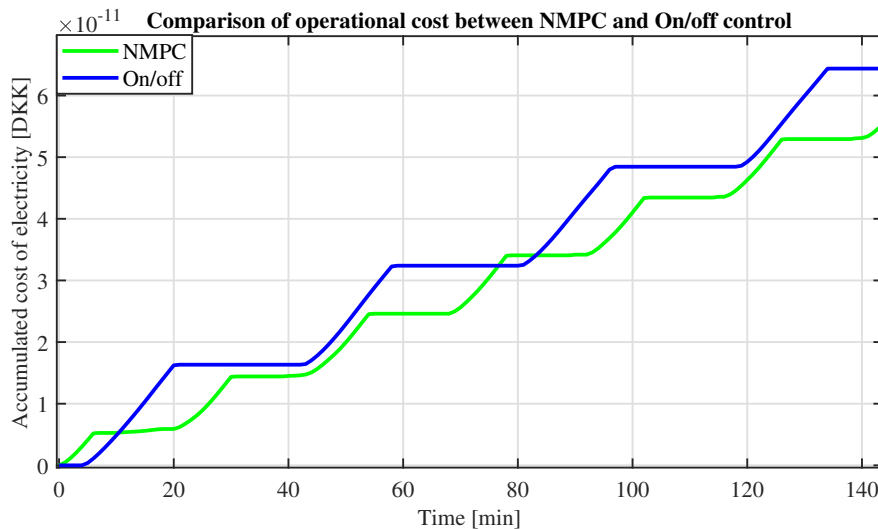


**Figure 7.3:** Comparison of accumulated cost of operation over 144 minute between the NMPC and the on/off controller in laboratory test

From figure 7.3, it can be observed that the performance of the NMPC is better than the on/off controller in terms of operational cost. The figure presents accumulated cost of operation over a period of 144 minute for both the controllers. There is 13.53% saving in NMPC operation compared to on/off control operation.

### **7.3 Discussion on stability analysis of the inner closed-loop system**

- The Lyapunov stability analysis demonstrates that the inner closed-loop system, of water network with the PI controller, is globally asymptotically stable. Global asymptotic stability implies that irrespective of the initial conditions the solution will tend towards the equilibrium point as time tends to infinity. In this case, global asymptotic stability implies that for any value of PI gain, the flow set-point can be reached and the system would be asymptotically stable.
- The Lyapunov stability analysis does not take into account the output delay in the system. The output delay in the pumps is a possible cause of oscillations in the pump flow.
- Stability analysis on the linearised system presents that with higher PI gain values the imaginary part in the eigenvalues of the closed loop system increases, implying higher oscillations. But with lower PI gain values the system response becomes slower which is also not desirable. Therefore for the NMPC test in the laboratory lower PI gain values were not chosen.



## Chapter 8

# Conclusion

This project was an extension of work presented in [22], where a MPC control was designed and implemented on the water distributed network also considered in this project. The three objectives of this project presented in chapter 1 were,

- Design and development of an nonlinear optimal control system and to compare the performance with the linear optimal control in [22].
- Design and development of a consumer demand predictor for a water distribution network, to be implemented with the nonlinear optimal control system.
- Stability analysis of closed-loop system of water distribution network pump flow control by a PI controller.

To achieve these objectives a water distribution network with an elevated tank is selected. A simplified and another detailed nonlinear model of the water network are developed. A control structure was developed with nonlinear model predictive control (NMPC) as a supervisory controller giving optimal pump flow commands to a PI controller, controlling the flow of the pumps. The simplified model was used to design this NMPC control. The objectives of the NMPC optimization problem were defined to be minimizing the operational cost and the pressure variations at the consumer node. The constraints on the optimization problem were the physical operational constraints of the pumps and the operational constraints for the tank. For the solving the optimization problem knowledge of the future consumer demand is required, therefore a Kalman filter based consumer demand predictor was also developed. The predictor was designed to take tank pressure measurements as input and estimate the consumer demand, and based on that predict the future consumer demands.

The NMPC designed was implemented in CasADi in MATLAB. Then the NMPC along with the consumer demand predictor was tested on a nonlinear simulated

network model. The simulation results show a good performance of the predictor and the NMPC. Comparing the performance of the NMPC with an on/off controller presented a saving of 43.34% in accumulated operational cost after 144 minute of operation. Also, comparing the results with the MPC results from [22], reveal the performance of NMPC and MPC are fairly equal, although the implementation of NMPC is computationally expensive compared to MPC. A water distribution network was also setup in the smart water laboratory for laboratory test of the nonlinear optimal control system. The laboratory test presented oscillatory behavior of pump flows controlled by PI controllers. The Lyapunov stability analysis revealed that the delay-free inner closed-loop system was globally asymptotically stable and implying a possible cause of oscillation could be output delay in the pump flows. Apart from the oscillations the NMPC performance in the laboratory test was satisfactory and when comparing to an on/off controller, the NMPC had a saving of 13.53% after 144 minute of operation.

## Chapter 9

# Future work

Possible improvements in the project and potential future work to this project are listed below.

- This project included NMPC implementation with the consumer demand predictor and work in [22] included MPC implementation but without consumer demand predictor. MPC implementation with the consumer demand predictor could be tested in the further work.
- Lyapunov stability analysis suggests that the delay-free inner closed-loop system is globally asymptotically stable and the possible cause of the oscillations could be delay in the system. Therefore, potential future work in the project could be design and development of local controller which mitigates the effect of delay in the system
- In this project, the objectives of the NMPC were minimizing the operational cost and the pressure variations at the consumer node. An important indicator for water quality is water retention time, which could be included as an objective of the NMPC in future work
- In this project, weights are assigned manually for the trade-off between the objectives in the optimization problem. Potential future work could include implementing some method to quantify this trade-off between the objectives.



# Bibliography

- [1] Joel A E Andersson et al. “CasADi – A software framework for nonlinear optimization and optimal control”. In: *Mathematical Programming Computation* 11.1 (2019), pp. 1–36. doi: 10.1007/s12532-018-0139-4.
- [2] K. M. Balla et al. “Model Predictive Control using linearized Radial Basis Function Neural Models for Water Distribution Networks”. In: *2019 IEEE Conference on Control Technology and Applications (CCTA)*. 2019, pp. 368–373. doi: 10.1109/CCTA.2019.8920627.
- [3] Krisztian M. Balla. “Model Predictive Control for Water Supply Networks with Storages”. MA thesis. Frederik Bajers Vej 7 9220 Aalborg Ø Tlf.: 9940 9730 Telefax: 9940 9725 <http://www.es.aau.dk>: Aalborg University The Faculty of Engineering, Science School of Information, and Communication Technology, 2018.
- [4] Rasmus Vedel Nonboe Kobborg Christian Andersen Ivik Niels Riishøj and Saruch Rathore. *Estimation of the hidden states and parameters in a reefer cargo hold*. Tech. rep. Frederik Bajers Vej 7 9220 Aalborg Ø Tel.: 9940 9730 Fax: 9940 9725 <http://www.es.aau.dk>: Aalborg University, School of Information and Communication Technology, Department of Electronic Systems, 2019.
- [5] European Commission. “Report from the Commission to the European Parliament, the Council, the European Economic and Social Committee and the Committee of the Regions”. In: *Energy prices and costs in Europe* (2018). URL: [https://ec.europa.eu/energy/sites/ener/files/epc\\_report\\_final\\_1.pdf](https://ec.europa.eu/energy/sites/ener/files/epc_report_final_1.pdf).
- [6] N. Deo. *Graph Theory with Applications to Engineering and Computer Science*. Dover Publications, 2017. ISBN: 9780486820811. URL: <https://books.google.dk/books?id=DSBMDgAAQBAJ>.
- [7] Phil PG Dyke. *An introduction to Laplace transforms and Fourier series*. Springer, 2014.
- [8] M.S. Grewal and A.P. Andrews. *Kalman Filtering: Theory and Practice with MATLAB*. Wiley - IEEE. Wiley, 2015. ISBN: 9781118984963. URL: <https://books.google.dk/books?id=Sgx9BgAAQBAJ>.

- [9] F. Haugen. "Kompendium for Kyb. 2, ved Høgskolen i Oslo, Telemark University College, Department of Electrical Engineering". In: *Information Technology and Cybernetics*. 2015.
- [10] Tom Nørgaard Jensen. "Modelling of open hydraulic networks". Lecture notes in course 'Modeling of Mechanical and Thermal Systems' at Aalborg University. 2019.
- [11] Kang Jing and Zou Zhi-Hong. "Time Prediction Model for Pipeline Leakage Based on Grey Relational Analysis". In: *Physics Procedia* 25 (2012). International Conference on Solid State Devices and Materials Science, April 1-2, 2012, Macao, pp. 2019 –2024. ISSN: 1875-3892. DOI: <https://doi.org/10.1016/j.phpro.2012.03.344>. URL: <http://www.sciencedirect.com/science/article/pii/S1875389212007602>.
- [12] Carsten Skovmose Kallesøe. *Fault detection and isolation in centrifugal pumps*. Carsten Skovmose Kallesøe, 2005.
- [13] C. S. Kallesøe, T. N. Jensen, and R. Wisniewski. "Adaptive reference control for pressure management in water networks". In: *2015 European Control Conference (ECC)*. 2015, pp. 3268–3273. DOI: 10.1109/ECC.2015.7331038.
- [14] Carsten Skovmose Kallesøe, Tom Nørgaard Jensen, and Jan Dimon Bendtsen. "Plug-and-Play Model Predictive Control for Water Supply Networks with Storage". In: *IFAC-PapersOnLine* 50.1 (2017). 20th IFAC World Congress, pp. 6582 –6587. ISSN: 2405-8963. DOI: <https://doi.org/10.1016/j.ifacol.2017.08.616>. URL: <http://www.sciencedirect.com/science/article/pii/S2405896317309953>.
- [15] Kristian Rune Poulsen Karsten Capion Morten Stryg. *Electricity Price Outlook 2018*. Tech. rep. DANSK ENERGI, 2018.
- [16] Hassan K Khalil and Jessy W Grizzle. *Nonlinear systems*. Vol. 3. Prentice hall Upper Saddle River, NJ, 2002.
- [17] J.M. Maciejowski. *Predictive Control with Constraints*. England.: Prentice Hall, 2002.
- [18] Bjarni Geir Pétursson Mathias Mølgaard. "Energy Optimization of Water Distribution Networks". MA thesis. Frederik Bajers Vej 7 9220 Aalborg Ø Tlf.: 9940 9730 Telefax: 9940 9725 <http://www.es.aau.dk>: Aalborg University The Faculty of Engineering, Science School of Information, and Communication Technology, 2015.
- [19] S McKinsey. *Charting our water future: Economic framework to inform decision-making*. 2030 Water Resources Group. 2009. URL: [https://www.mckinsey.com/~media/mckinsey/dotcom/client\\_service/sustainability/pdfs/charting%20our%20water%20future/charting\\_our\\_water\\_future\\_full\\_report\\_.ashx](https://www.mckinsey.com/~media/mckinsey/dotcom/client_service/sustainability/pdfs/charting%20our%20water%20future/charting_our_water_future_full_report_.ashx).

- [20] UNESCO World Water Assessment Programme. *The United Nations world water development report 2020: water and climate change*. ISBN:978-92-3-100371-4. UNESCO, 2020.
- [21] V. Puig et al. *Real-time Monitoring and Operational Control of Drinking-Water Systems*. Advances in Industrial Control. Springer International Publishing, 2017. ISBN: 9783319507514. URL: <https://books.google.dk/books?id=12UkDwAAQBAJ>.
- [22] Saruch Satishkumar Rathore. "Optimal control in water distribution network". 3rd semester project report. Aalborg University, School of Information and Communication Technology, Department of Electronic Systems, Dec. 18, 2019. URL: [https://projekter.aau.dk/projekter/files/320436349/Report\\_930\\_Optimal\\_control\\_in\\_water\\_distribution.pdf](https://projekter.aau.dk/projekter/files/320436349/Report_930_Optimal_control_in_water_distribution.pdf) (visited on 04/10/2020).
- [23] S. E. Shafiei, J. Stoustrup, and H. Rasmussen. "A supervisory control approach in economic MPC design for refrigeration systems". In: *2013 European Control Conference (ECC)*. 2013, pp. 1565–1570. DOI: 10.23919/ECC.2013.6669413.
- [24] P.K. Swamee and A.K. Sharma. *Design of Water Supply Pipe Networks*. Wiley, 2008. ISBN: 9780470225042. URL: <https://books.google.dk/books?id=F5dz28bt5RkC>.
- [25] K. Thulasiraman and M.N.S. Swamy. *Graphs: Theory and Algorithms*. A Wiley interscience publication. Wiley, 1992. ISBN: 9780471513568. URL: <https://books.google.dk/books?id=4kHN6uSinQoC>.
- [26] J Val. "Control of District Heating system with input-dependent state delays". PhD thesis. Master thesis, Aalborg University, 2016.
- [27] WWAP. *Water in a changing world: the United Nations world water development report 3*. ISBN 978-92-3-104095-5 978-1-84407-840-0 978-89-8225-791-9 (set, kor). London : Earthscan, 2009, 2009.



## Appendix A

# NMPC problem defined using multiple shooting in CasADi (MATLAB code)

The NMPC problem is converted to a NLP problem using multiple shooting method and defined in CasADi. The CasADi is defined in a CasADi object function to which parameters and initial condition can be passed to obtain optimal solution. The MATLAB code for the NMPC problem is presented below.

```
1
2 opti = casadi.Opti(); % Initializing CasADi
3
4 %% Constant and constraint values
5
6 eta_p=0.6; % Efficiency of pumps
7 eta_m=0.9; % Efficiency of motors
8 k_eta=1/(eta_p*eta_m*1e3*1e5*3600); % Constant based on efficiency
9
10 % Limits on different variables
11 h0_min=0.1; % [m] Minimum level in tank
12 h0_max=0.4; % [m] Max level in tank
13 p0_min=h0_min*rho_fluid*g/1e5;
14 p0_max=h0_max*rho_fluid*g/1e5;
15 u_min=[0;0];
16 u_max=[0.3;0.3]; % [m^3/h] Max flow from pumping ...
    station
17 p_p_min=[0;0];
18 p_p_max=[0.6;0.6]; % [bar] Max pressure from ...
    pumping station
19
20 %% NMPC weights
21
```

```

22 Q_weight=5.5e10*diag([1 1]);
23 R_weight=1*diag([1 1]);
24 Rho_weight=1e5;
25
26 %% Casadi variables
27
28 % Variables in the NLP problem
29 u_var=opti.variable(2, Hp);
30
31 qC_var=opti.variable(2, Hp);
32 p_bar_var=opti.variable(5, Hp);
33 p_0_var=opti.variable(1, Hp+1);
34
35 eps_var=opti.variable(1, Hp);
36
37 % Parameters in the NLP problem
38
39 p_0_par=opti.parameter(1, 1);
40
41 dc_par=opti.parameter(2, Hp);
42 C_par=opti.parameter(1, Hp);
43
44 obj=0;
45
46 for k=1:Hp
47
48     % Objective function for NMPC
49
50     C_val=diag([C_par(:,k) C_par(:,k)]); % Diagonal matrix for ...
51     p_p_val=F_p_bar*p_bar_var(:,k); % Extracting pump pressure
52
53
54     obj=obj+u_var(:,k)'*Q_weight*C_val*p_p_val*k_eta*Ts;
55     obj=obj+(F_c_bar*(p_bar_var(:,k)-mean(p_bar_var(:,k))))'...
56     *R_weight*(F_c_bar*(p_bar_var(:,k)-mean(p_bar_var(:,k))));
57     obj=obj+Rho_weight*eps_var(:,k);
58
59     % System constraints for NMPC
60
61     d_tau_val=-(sum(dc_par(:,k))+sum(u_var(:,k)));
62
63     qT_val=-inv(H_T_bar)*H_C_bar*qC_var(:,k)+inv(H_T_bar)*F_p_bar'...
64     *u_var(:,k)+inv(H_T_bar)*F_c_bar'*dc_par(:,k)+inv(H_T_bar)...
65     *F_tau_bar'*d_tau_val;
66
67     q_val=[qC_var(1,k);qT_val(1:2,1);qC_var(2,k);qT_val(3:5,1)];
68
69     lambda_q_val=lambda.*abs(q_val).*q_val;
70
71     st_l=B*lambda_q_val;

```

```

72     st_2=inv(H_T_bar')*lambda_q_val(edge_tree)-(h_bar-h_0)...
73     +ones(n_H-1,1)*p_0_var(:,k);
74     st_3=p_0_var(:,k)-tau*d_tau_val*60;
75
76     opti.subject_to(st_1==0);
77     opti.subject_to(p_bar_var(:,k)==st_2);
78     opti.subject_to(p_0_var(:,k+1)==st_3);
79
80     % Inequality constraints
81
82     opti.subject_to(u_min<=u_var(:,k));
83     opti.subject_to(u_var(:,k)<=u_max);
84
85     opti.subject_to(p_p_min<=p_p_val);
86     opti.subject_to(p_p_val<=p_p_max);
87
88     opti.subject_to((p0_min-eps_var(:,k))<=p_0_var(:,k+1));
89     opti.subject_to(p_0_var(:,k+1)<=(p0_max+eps_var(:,k)));
90
91     opti.subject_to(0<=eps_var(:,k));
92
93 end
94
95 % Constraint on the initial condition
96
97 opti.subject_to(p_0_var(:,1)==p_0_par);
98
99 % Defining options for the solver
100 opts=struct;
101 opts.ipopt.print_level=0;
102 opti.solver('ipopt',opts);
103
104 % Creating a CasADi object function for the NMPC problem
105 opti.minimize(obj);

```

The parameters and the initial condition are passed through this object function to obtain optimal values of the NLP problem variables. The NLP problem variables include the optimal pump flow command.

```

1
2 % Set value for the parameters
3     opti.set_value(p_0_par,p_esti);
4     opti.set_value(dc_par,dc_Hp);
5     opti.set_value(C_par,C_Hp);
6
7
8     sol = opti.solve();      % Solving the optimization problem with ...
9     u_all= sol.value(u_var); % Obtain optimal pump flow commands

```



## Appendix B

# Equilibrium point calculation and system matrices in the stability analysis of the linearised model

The nonlinear model of the water distribution network, presented in section 2.4, is linearised at an equilibrium point. In the network model node 10 is chosen as the reference node. The operating point for the speed of the pumps is chosen to be,

$$\omega_p^* = \begin{bmatrix} 67 \\ 67 \end{bmatrix} \quad (\text{B.1})$$

Using this operating point for the input, the state dynamics are set to zero to obtain the equilibrium point for the states. The calculated equilibrium point for the states are given below.

$$q_C^* = \begin{bmatrix} 0.214 \\ -0.025 \end{bmatrix} \quad (\text{B.2a})$$

$$\bar{d}_f^* = \begin{bmatrix} 0.320 \\ -0.290 \\ -0.291 \end{bmatrix} \quad (\text{B.2b})$$

$$\bar{d}_\tau^* = 0 \quad (\text{B.2c})$$

$$p_\tau^* = 0.031 \quad (\text{B.2d})$$

Based on the operating point state space matrices for the linearised model is

calculated to be,

$$A_{sys} = \begin{bmatrix} -0.4146 & 0 & -0.4169 & 28.6393 & 0 & 0 & 0 \\ 0 & -0.2409 & -0.0219 & 0 & -3.9529 & 0 & -3.6672 \\ -0.1943 & 0.0050 & -0.7858 & 28.6393 & 8.2352 & 0 & -1.2224 \\ 0.1206 & 0 & 0.4169 & -38.0979 & 0 & 0 & -5.6719 \\ 0.0806 & 0.0619 & -0.0968 & -0.1361 & -24.0953 & -0.1361 & -2.4448 \\ -0.0918 & -0.1517 & -0.1958 & 8.8483 & 3.7352 & -0.6104 & 20.6828 \\ 0 & 0 & 0 & 0 & 0 & -0.0001 & 0 \end{bmatrix} \quad (B.3a)$$

$$B_{sys} = \begin{bmatrix} 0.1742 & 0.0000 \\ 0.0120 & 0.0000 \\ 0.2363 & 0.0000 \\ -0.1742 & 0 \\ -0.0501 & -0.0697 \\ -0.0120 & -0.1115 \\ 0 & 0 \end{bmatrix} \quad (B.3b)$$

$$C_{sys} = \begin{bmatrix} 0 & 0 & 1 & 0 & 0 & 0 & 0 \\ 0 & 0 & -1 & -1 & -1 & -1 & 0 \end{bmatrix} \quad (B.3c)$$

The system has an output delay of 4 sec in pumps, considering this the updated state space matrices with the delay model is calculated to be,

$$A_{cd} = \begin{bmatrix} -0.4146 & 0 & -0.4169 & 28.6393 & 0 & 0 & 0 & 0 & 0 \\ 0 & -0.2409 & -0.0219 & 0 & -3.9529 & 0 & -3.6672 & 0 & 0 \\ -0.1943 & 0.0050 & -0.7858 & 28.6393 & 8.2352 & 0 & -1.2224 & 0 & 0 \\ 0.1206 & 0 & 0.4169 & -38.0979 & 0 & 0 & -5.6719 & 0 & 0 \\ 0.0806 & 0.0619 & -0.0968 & -0.1361 & -24.0953 & -0.1361 & -2.4448 & 0 & 0 \\ -0.0918 & -0.1517 & -0.1958 & 8.8483 & 3.7352 & -0.6104 & 20.6828 & 0 & 0 \\ 0 & 0 & 0 & 0 & 0 & -0.0001 & 0 & 0 & 0 \\ 0 & 0 & 1 & 0 & 0 & 0 & 0 & -0.5 & 0 \\ 0 & 0 & -1 & -1 & -1 & -1 & 0 & 0 & -0.5 \end{bmatrix} \quad (B.4a)$$

$$B_{cd} = \begin{bmatrix} 0.1742 & 0.0000 \\ 0.0120 & 0.0000 \\ 0.2363 & 0.0000 \\ -0.1742 & 0 \\ -0.0501 & -0.0697 \\ -0.0120 & -0.1115 \\ 0 & 0 \\ 0 & 0 \\ 0 & 0 \end{bmatrix} \quad (B.4b)$$

$$C_{cd} = \begin{bmatrix} 1 & 0 & 0 & 0 & 1 & 0 & 0 & 0 & 0 \\ 0 & 1 & 0 & 0 & -1 & -1 & -1 & -1 & 0 \end{bmatrix} \quad (\text{B.4c})$$



## Appendix C

# MPC simulation test results from [22]

Figures C.1, C.2 and C.2 presents MPC simulation test results from [22]. The test conditions and MPC weights are same as in this project. These results are just for comparison with results obtained in this project.

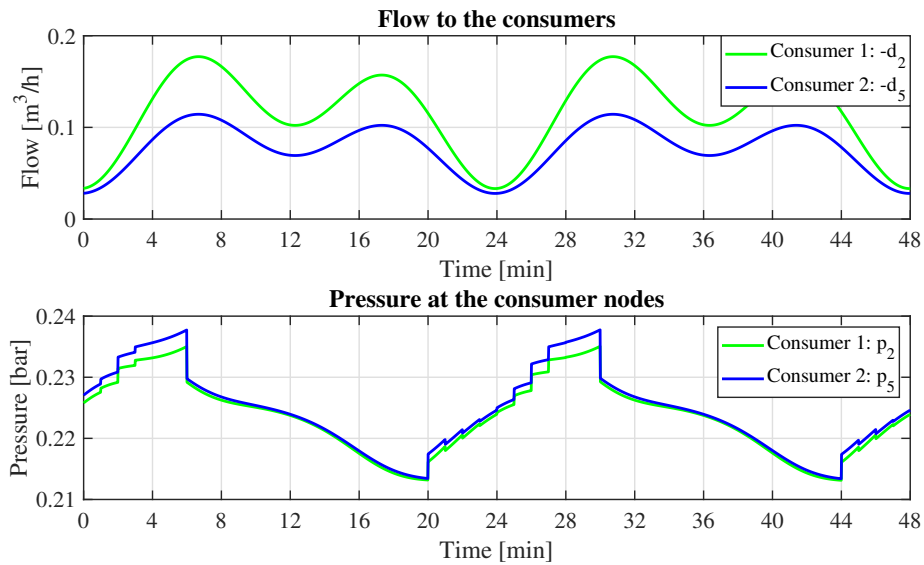


**Figure C.1:** Flow demand from the consumers and the MPC simulation results for the pressure at consumer end, for varying price of electricity[22]

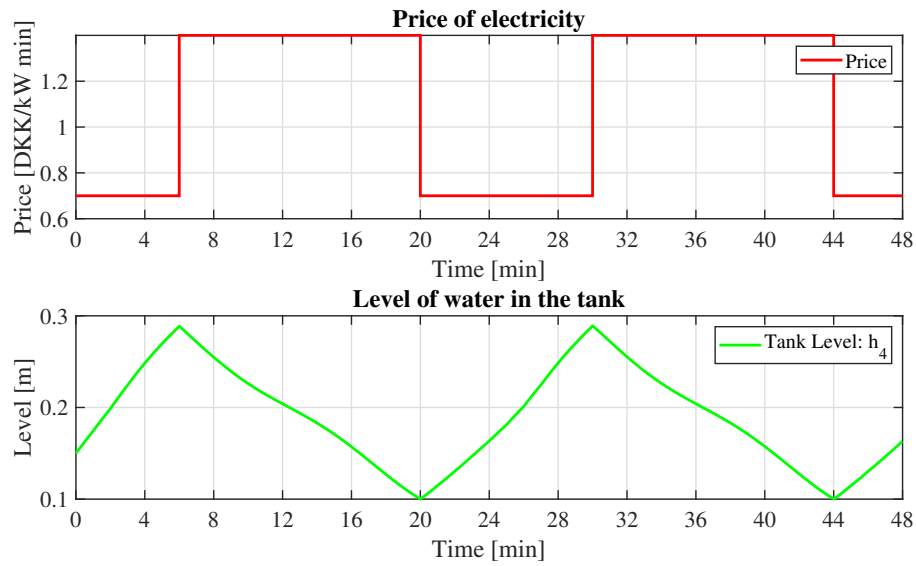


**Figure C.2:** Varying price of electricity and the MPC simulation results for the tank level[22]

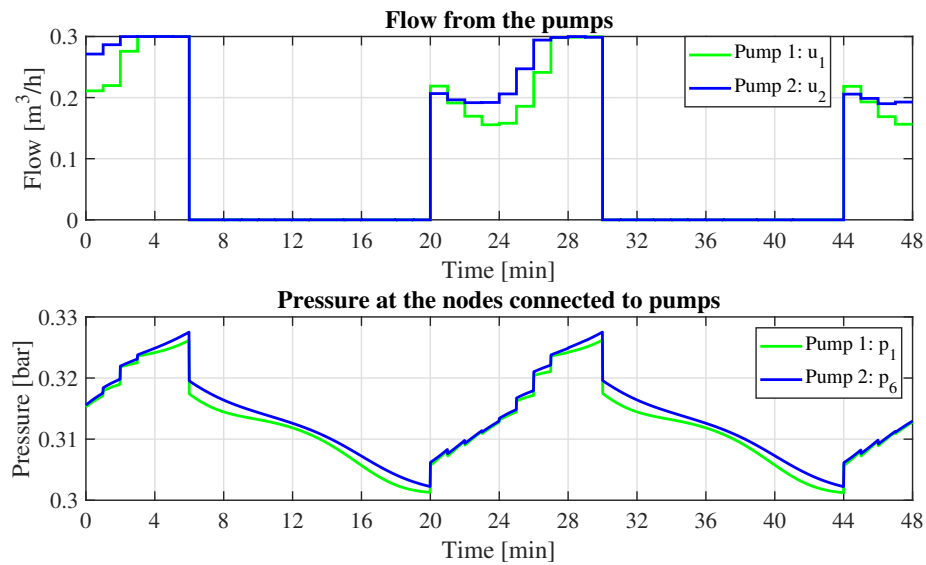


**Figure C.3:** MPC simulation results for the flow and pressure at nodes connected to the pumps, for varying price of electricity[22]

## Appendix D

# PI control implementation for the laboratory setup

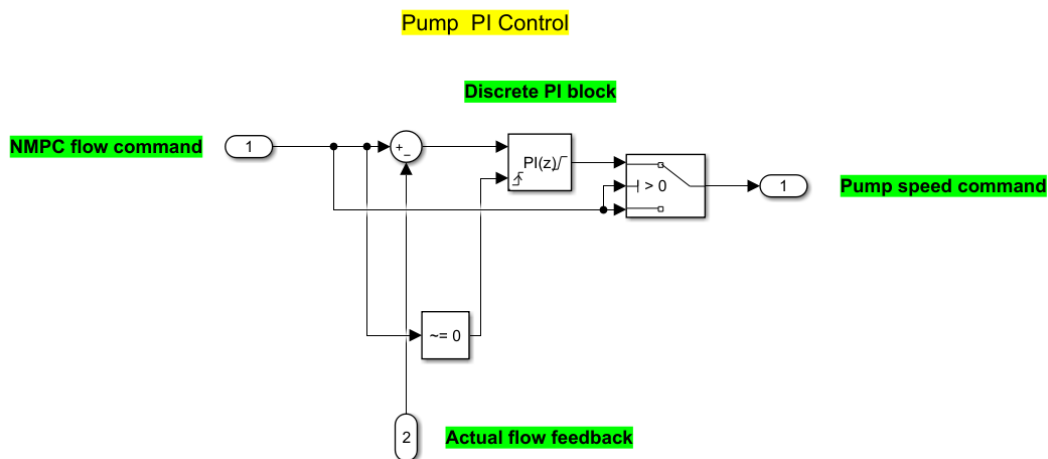


Figure D.1: PI control for the pump implemented for the laboratory setup

Figure D.1 presents the implementation of the PI control for the pumps in the laboratory setup. The PI implementation in Simulink is the same as used in [22]. PI control is implemented using predefined discrete PI block in Simulink. Saturation limits on the PI is 40 to 95, also anti-windup is enabled. When the NMPC flow command is zero, the PI block is bypassed and zero speed command is directly sent to the pumps, this is to avoid pumps running at low speed when the required flow is zero. Bypassing the PI would lead to overshoot in the flow at the instances when the PI block is again taken into line, to avoid this the PI is reset whenever the NMPC flow command goes from zero to non-zero value.



## Appendix E

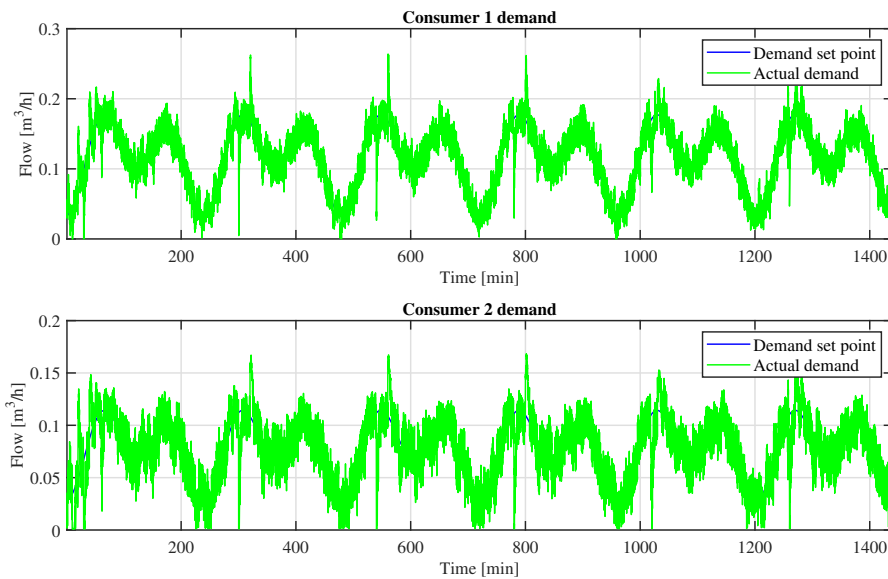
# Laboratory test results with 240 minutes representing 1 day

Another laboratory test of the NMPC was conducted with now 240 minutes representing 1 day in real life. The sampling time for the NMPC and the predictor was set to 10 minutes. This test was conducted to provide more time to the PI controller to stabilize at a given set-point before the set-point is changed.

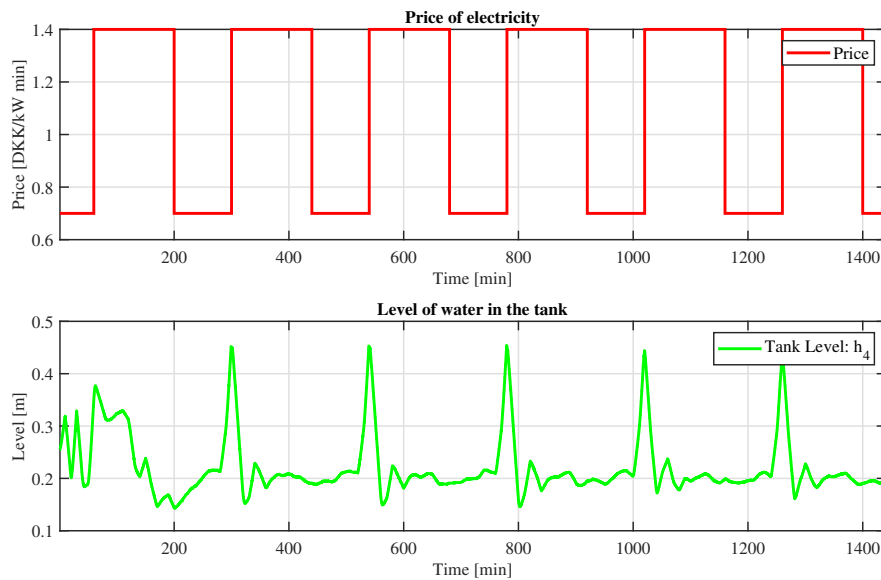
The constraint of the tank level for this test were changed to 0.2-0.5m from 0.1-0.4m. The tank's safety valve closes if the level of the water goes below 0.05m, and due to oscillation in the pump flow and with the lower limit constraint of 0.1m, the level would often go below 0.05m and the test needed to be stopped.

Figure E.2 presents the changing price of electricity and the tank level. Considering the upper limit of constraint on the tank level, the NMPC only fills the tank just before the prices are about to go high. The NMPC does this considering that the tank can be filled in that short period of time and by doing so the pumps could be operated at a lower pressure before that.

Figure E.3 presents the flow control of the pumps. As mentioned before the NMPC does not fill the tank for a longer period of time in the test and only meets the consumer demands. Due to this the pumps operate at low flows. As the PI control was manually tuned for the system to operate at a high flow, running the pumps at lower low causes much more oscillations.



**Figure E.1:** Consumer nodal demand set-point and the actual demand flow controlled by a PI controller in the laboratory setup, where 240 minutes represents 1 day



**Figure E.2:** Varying unit price of electricity and NMPC results for level of water in the tank measured by sensor in the laboratory setup, where 240 minutes represents 1 day

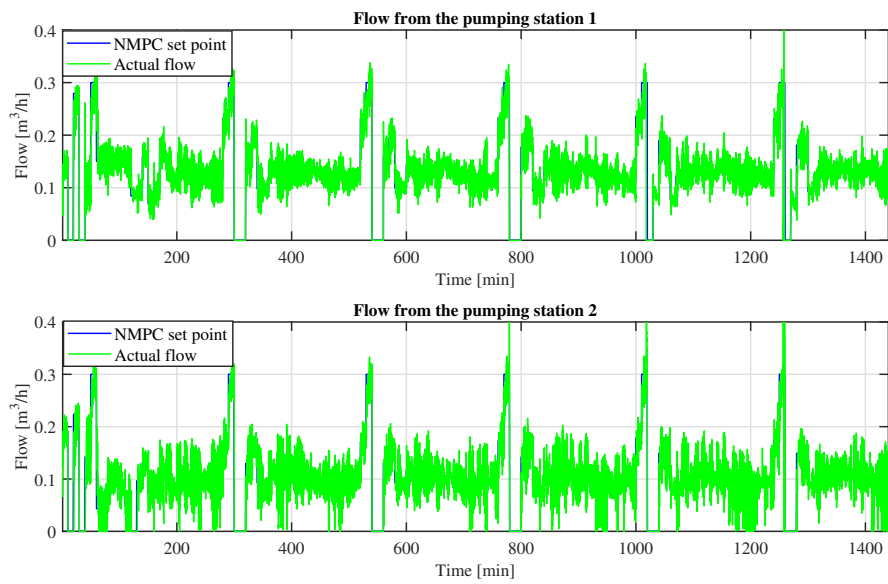


**Figure E.3:** Pump flow set-point by NMPC and the actual pump flows controlled by a PI controller in the laboratory setup, where 240 minutes represents 1 day